AN ABSTRACT OF THE DISSERTATION OF

Hsiao-Yen Ma for the degree of Doctor of Philosophy in Pharmacy presented on October 16, 2013

Title: Gene Networks During Cardiogenesis And Skeletal Myogenesis

Abstract approved:

Chrissa Kioussi

Organismal development requires a precisely orchestrated transcriptional program to correctly deploy genetic information into the genome. This process requires sophisticated gene regulatory networks at multiple spatial and temporal levels from early embryonic development to adult physiological conditions. Molecular differences that define cell types are set up during the pattern formation phase of development. Selective gene expression provides molecular markers such as sequence specific DNA-binding transcription factors (SSTFs) to define cell types. Homeodomain transcription factors are essential for embryonic pattern formation and cell specification and therefore can affect several mechanistically distinct aspects of organ development. The Pitx2 homeobox gene is expressed in the lateral plate mesoderm and it is involved in cardiac and skeletal muscle development. Mutations of Pitx2 are associated with the human Axenfeld-Rieger syndrome. Pitx2 null mice die at embryonic day 13.5 and exhibit un-septated atria and outflow tract that leads to deformed valves and arrythmias. Pitx2 promotes the proliferation of the branchial arch mesoderm-derived cells and their remodeling process, the

epithelial-mesenchymal transition, to form the outflow tract cushions by influencing the expression of SSTFs in the cardiac mesoderm. Pitx2 is expressed in skeletal muscle cells from their time as progenitors until they form mature muscle groups. In Pitx2 null mutant mice the skeletal muscles have been specified, the muscles were formed but their higher order assembly was disrupted. Pitx2 was a key player of the embryonic muscle progenitors as they transition to the fetal state. Embryonic muscle progenitors were able to delaminate from the dermomyotome and migrate to the forelimb pre-patterned anlagen but were not fast to transition to the fetal state, as their G1 phase was arrested and their motility was disrupted. We have developed a Pitx2 conditional genetic system that eliminates the early cause of death and allows us to investigate the role Pitx2 at later stages. The molecular mechanisms of muscle regeneration in adults share many characteristics with the myogenic programs that generate skeletal muscle during development. These studies will enhance the molecular understanding of myogenic development and generate muscle-impaired mouse lines for drug and regeneration studies.

Gene Networks During Cardiogenesis And Skeletal Myogenesis

by
Hsiao-Yen Ma

A DISSERTATION

submitted to

Oregon State University

in partial fulfillment of
the requirements for the
degree of

Doctor of Philosophy

Presented October 16, 2013
Commencement June 2014

Doctor of Philosophy dissertation of Hsiao-Yen Ma presented on October 16, 2013.

APPROVED:

Major Professor, representing Pharmacy

Dean of the College of Pharmacy

Dean of the Graduate School

I understand that my dissertation will become part of the permanent collection of Oregon State University libraries. My signature below authorizes the release of my dissertation to any reader upon request.

Hsiao-Yen Ma, Author

ACKNOWLEDGEMENTS

Dr. Chrissa Kioussi – Major Advisor

Dr. Michael K. Gross – Committee Member

Dr. Theresa Filtz – Committee Member

Dr. Lin Jing – Committee Member

Dr. Victor L. Hsu – Graduate Council Representative

The Kioussi Lab

The College of Pharmacy

The CGRB Core Labs

My parents Deming Ma and Lanping Shi

My husband Jun Xu

My two lovely kids Chris Xu and Ethan Xu

CONTRIBUTION OF AUTHORS

Chrissa Kioussi designed research, contributed to data analysis, writing, editing, and contributed reagents; Hsiao-Yen Ma designed research, performed research, data analysis, and writing; Michael K. Gross contributed reagents, data analysis, and analytic tools; Jun Xu, Diana Eng, Adam Campbell contributed to data.

TABLE OF CONTENTS

TABLES OF CONTENTS (CONTINUED)

LIST OF FIGURES

LIST OF TABLES

Gene Networks During Cardiogenesis And Skeletal Myogenesis

Chapter 1

Cardiogenesis and Myogenesis

Hsiao-Yen Ma and Chrissa Kioussi

Spatiotemporal expression of DNA sequence specific transcription factors (SSTFs) plays a central role in cell differentiation, organ development and embryogenesis. Combinatorial activity of SSTFs is essential for lineage specification, embryonic polarity, tissue patterning and morphogenetic movements. Homeodomain proteins are a class of SSTFs that share the “homeodomain” a 60 amino acid motif encoded by 180 bp homeobox sequences originally recognized in three Drosophila homeotic and segmentation proteins (McGinnis et al., 1984). Homeodomain proteins function as transcriptional regulators during development. Almost 200 out of the 2,000 murine SSTFs are homeobox genes. The Hox gene family includes 39 members in mammals, that patterns the body trunk and regulates the limb formation (Krumlauf, 1994). The Pax family is mostly involved in neural tube, eye and limb formation (Relaix et al., 2004; Suga et al., 2010). The Six family is essential for the formation and function of thymus and skeletal muscles (Grifone et al., 2005). The Pitx gene family is essential for neuronal, muscular and cardiac development, (Gage et al., 1999a; L'Honore et al., 2007). Pitx gene family has three members including Pitx1, Pitx2 and Pitx3. *Pitx* genes encode highly homologous proteins, identical within their homeodomains and varying mainly in the N-terminal region. Pitx1 is involved in development of a number of tissues including 1st branchial arch, body wall and hind limb musculature (Gage et al., 1999a). Conditional overexpression of Pitx1 in mice causes skeletal muscle dystrophy (Pandey et al., 2012). Pitx2 is fundamental to brain, pituitary, facial, heart and skeletal muscle development. Pitx2 knockout mice exhibit axial malformations, open body wall, cardiac malformations, lung asymmetry, and organ arrest (Kioussi et al., 2002; Kitamura et al., 1999; Lin et al., 1999; Gage et al., 1999a). Pitx3 is central to eye and dopaminergic neuron development (Qiu et al., 2008; Smidt et al., 2004) and is also implicated in developmental myogenesis (L'Honore et al., 2007). *PITX* mutations are related

to development disorders in human, with *PITX1* associated with Facioscapulohumeral muscular dystrophy (Dixit et al., 2007), *PITX2* mutations mutations associated with the Axenfeld-Rieger syndrome (Semina et al., 1996) and *PITX3* mutations associates with the Anterior Segment Mesenchymal Dysgenesis and congenital cataracts (Semina et al., 1998).

CARDIOGENESIS

The mammalian heart is the first organ to form and is vital for distribution of nutrients and oxygen though the entire embryo. Cells that contribute to the formation of the cardiac tube and later the four chamber pump follow series of critical morphogenetic events (Liu et al., 1996). Heart develops from cells of four embryonic origins; (1) the cardiac crescent, or first heart lineage, (2) the branchial arch (BA)-derived mesoderm or second heart lineage, (3) the cardiac neural crest (cNC) cells and (4) the epicardium (Kelly, 2005). The 1st lineage appears shortly after gastrulation as a population of mesodermal cells that undergo differentiation to form a tubular structure with an outer myocardium and an inner endocardium separated by an extracellular (Harvey, 2002). The linear heart tube connects with the artery at the anterior pole, which forms the outflow tract (OT), and with a vein at the venous pole, which forms the inflow tract. The 2nd lineage is a population of cardiac progenitor cells located in BA mesoderm that contributes to growth of the embryonic heart tube by adding cells at arterial and venous pole during heart looping morphogenesis. As the linear heart tube forms, second heart lineage progenitors start forming the dorsal wall of the pericardial cavity where they are characterized by continued proliferation and delayed differentiation. At E8.5, the linear heart undergoes rightward looping with subsequent formation of four chambers, right (RV) and left (LV) ventricles and right (RA) and left (LA) atria. After chamber formation

the highly regulated cell proliferation results in a process called ballooning morphogenesis. Cushions in the atrioventricular (AV) and outflow (OT) regions start to form while cells follow an epithelial to mesenchymal transition (EMT) to form the ventricular, atrial and AV septae. At the meantime, the OT divides and forms the base of the ascending aorta, outlet of the LV, and pulmonary trunk, outlet of the RV.

Cells of the 2nd lineage ultimately contribute to the cardiac OT, RV and atria myocardium, while cells of the first lineage give rise to atria and LV (Kelly et al., 2001; Mjaatvedt et al., 2001; Waldo et al., 2001). The BA mesoderm also gives rise to a subset of craniofacial skeletal muscles that are specified in the mesodermal core of the BA. The cNC cells originate from the neural tube extending from the axial level of the mid otic placode to the third somite. The cells then migrate from the neural tube into the 3rd, 4th and 6th BA (Kirby et al., 1983). Some NC cells remain in the pharynx to support aortic arch artery development, while a subpopulation continues on to migrate into the OT of the heart and to the inflow tract near the cardiac conduction system (Kirby and Hutson, 2010). The cNC cells in the OT form the cardiac ganglia and the condensed mesenchyme at the junction of the presumptive sub-aortic and sub-pulmonary myocardium (Waldo et al., 1998). A third layer of cells, the epicardium derives from the pro-epicardial organs adjacent to the venous pole and forms a thin epithelium on the outer surface of the heart. The epicardium stimulates ventricular myocardial growth to become a thickened compact myocardial layer (Lavine and Ornitz, 2008; Sucov et al., 2009).

A combination of signaling molecules and SSTFs regulate each step of cardiac development. As the embryonic coelom forms, positive signals (BMP and FGFs) from the endoderm and negative signals (WNT) from the midline initiate the formation of the cardiac crescent and define the precise location of where SSTFs such as Nkx2.5, Tbx5, Gata4, and Mef2c, and the cardiac specific

chromatin remodeling subunit Smarcd3 will be expressed (Evans et al., 2010; Lopez-Sanchez and Garcia-Martinez, 2011). Activation of the SSTFs Gata4, Tbx5, and Smarcd3 within the cardiac crescent, initiates the mesoderm-derived cells to differentiate into cardiomyocytes (Takeuchi and Bruneau, 2009). Nkx2.5 is expressed in the 1st lineage and thus specifies the LV (Lyons et al., 1995; Tanaka et al., 1999; Yamagishi et al., 2001). Nkx2.5 suppress the expression of Fgf10 that regulates cell proliferation during cardiac looping (Prall et al., 2007) and interacts with Gata4 and Tbx5 (Garg et al., 2003). Tbx5 plays an important role in cell differentiation within the 1st lineage (Bruneau et al., 2001).

Fgf8, Fgf10, Isl1 (Cai et al., 2003) and Tbx1 (Theveniau-Ruissy et al., 2008) are expressed in the 2nd lineage and regulate the formation of OT and RV. Tbx1 regulates cell proliferation by activating Fgf10 (Watanabe et al., 2012). Isl1 is widely expressed in the BA mesoderm derived cells and regulates Mef2c (Dodou et al., 2004; Li et al., 2010). Foxh1 is essential for RV formation (von Both et al., 2004). Foxc1 and Foxc2 act upstream Tbx1 (Kume et al., 2001) and Tbx1 acts upstream of Foxa2 (Yamagishi et al., 2003). Hoxa1, Hoxb1 and Hoxa3 are expressed within the Isl1 and Tbx5 territory and contribute to the poles of the heart tube (Bertrand et al., 2011; Makki and Capecchi, 2010). Six1 its transcriptional cofactor Eya1 are important during OT remodeling and OT cushion formation activating Fgf8 (Guo et al., 2011). Pitx2 expresses in all cardiac lineages and plays critical role in OT and RV formation and remodeling (Gage et al., 1999b; Kioussi et al., 2002; Kitamura et al., 1999; Lin et al., 1999; Lu et al., 1999). Pitx2 acts upstream of Tbx1 (Harel, 2012), Isl1 and Mef2c (Ma et al. 2013), represses Fgf10 and together with Isl1 guide the 2nd lineage progenitor cells to transform into atrial cells (Galli et al., 2008). Pitx2 and Tbx1 are necessary for proper migration and proliferation of the 2nd lineage progenitor cells (Nowotschin et al., 2006).

SKELETAL MYOGENESIS

In the mammalian embryo, the majority of skeletal muscles are derived from transient developmental structures called somites. Somites develop in a cranial to caudal order as a result of the segmentation of the pre-somitic (paraxial) mesoderm that lies on each side of the neural tube and notochord (Borycki et al., 1999; Christ et al., 1983). After segmentation, somites give rise to epithelial dermomyotome on the dorsal side and mesenchymal sclerotome on the ventral side. The sclerotome later forms the cartilage and the bone of spine and ribs, while the dermomyotome gives rise to dermatome, which forms the dermis and myotome, which forms the skeletal muscles. Myogenic precursor cells undergo an epithelial-mesenchymal transition (EMT) response to signals from environmental cues, delaminate from the dermomyotome, and accumulate underneath to from myotome (Yusuf and Brand-Saberi, 2006). The myotome is further divided into the epaxial myotome which gives rise to deep back muscles, and the hypaxial myotome which gives rise to the limb and ventral trunk muscles. For the most part, craniofacial musculature is derived from the BA, while the most rostral somites also contribute some musculature to the head and neck. The ventrolateral lip (VLL) of the dermomyotome is part of the hypaxial dermomyotome and contributes to limb muscle formation. The forelimb muscle precursor cells delaminate from VLL and migrate towards forelimb bud. This process begins at about E10.5 in the forelimb and continues through about E12 in the forelimb. The same developmental process happened one day earlier in hindlimb. When the migratory muscle precursors reach the forelimb bud, they start to proliferate and position themselves along the developing bone anlagen. Soon after that, they start to form muscle anlagen of the limb, and resemble the shape and position of the adult muscle.

Forelimb muscle formation is characterized by the embryonic myogenesis

(from E 10.5- E14.5), fetal myogenesis (E 14.5-E18.5) and neonatal (P0) (Biressi et al., 2007a; Hutcheson et al., 2009; Stockdale, 1992). The embryonic myoblasts are derived from $Pax3^+/Pax7^-$ embryonic muscle precursors, which are characterized by embryonic and slow muscle heavy chains (MyHC). Fetal myoblasts are derived from $Pax3^+/Pax7^+$ muscle precursors and are characterized by a high proliferation rate and fast MyHC. These two types of myoblasts present distinctive differences in their shape, cell surface receptors, innervation, extracellular matrix proteins and morphology of the generated myotubes (Biressi et al., 2007b; Gunning and Hardeman, 1991; Nameroff and Rhodes, 1989; Ross et al., 1987). Embryonic myoblasts fuse to each other to generate a multinucleated embryonic myotubes which will recruit and fuse fetal myoblasts to form the fetal myotubes within the basal lamina of primary myotubes (Duxson et al., 1989).

Pax3 is expressed throughout the dermomyotome and is later confined to the lateral dermomyotome and the migrating precursor cells (Bober et al., 1994; Goulding et al., 1994; Williams and Ordahl, 1994). The migratory $Pax3^+$ cell population delaminates from the VLL and requires proper expression of c-MET and associated ligand HGF/SF. Absence of either result in muscle-less limbs (Birchmeier and Brohmann, 2000; Dietrich et al., 1999). In order to properly locate and move into the limb buds these migratory cells also require the expression of Lbx1 (Gross et al., 2000). The myogenic regulatory factors (MRF) Myf5, Myod, Myogenin (Myog) and Mrf4 are master regulators of skeletal myogenesis. Myf5 is the earliest MRF to be expressed in the dermomyotome at E8.0 and in the epaxial (Montarras et al., 1991) and hypaxial (Tajbakhsh et al., 1998) myotome. Myog is expressed after Myf5 at E8.5 and MRF4 at E9.0. Myod is the last one to be expressed in the somite at E10.5 (Wright et al., 1989) (Montarras et al., 1991). Myf5 and Myod are critical for myoblast determination and share redundant function. In contrast, Myog plays an essential role during

muscle differentiation (Hasty et al., 1993; Nabeshima et al., 1993). Mrf4 functions as a determination of myogenic lineage during primary myogenesis (Kassar-Duchossoy et al., 2004). Expression of Myf5 is directly regulated by Pax3 (Bajard et al., 2006). Pax7 expression occurs slightly later at E9, is first expressed in the somites and then in the limbs by E11.5, within post migratory cells (Jostes et al., 1990). Pax7 plays a critical role in satellite cell development and maintainance (Oustanina et al., 2004). Cells express both Pax7 and Pax3 are considered as fetal muscle precursors, which contribute to fetal myotube formation (Relaix et al., 2005). Pax7 is essential for fetal, postnatal and adult myogenesis (Murphy and Kardon, 2011). Similar to how some MRFs can be substituted for each other in some developmental networks; it appears that Pax3 and Pax7 can also substitute for each other when placed in the proper developmental context. The transcription factor nuclear factor one X (Nfix) is robustly expressed in fetal myoblasts (Biressi et al., 2007c) and functions as a transcriptional switch from embryonic to fetal myogenesis (Messina et al., 2010). Pitx2 is expressed in all states of embryonic and adult muscle cells (Shih et al., 2007c) and acts upstream of Pax3/Pax7 (Lozano-Velasco et al., 2011b) and Myod (L'Honore et al., 2010). Pitx3 is widely expressed in all skeletal muscle of the body and limb after Pitx2 is expressed. The compensational upregulation of Ptix2 as Pitx3 is absent suggests that Pitx2 and Pitx3 may partially redundant (L'Honore et al., 2007). Six family transcription factors (Six1, Six4) and Eya transcriptional cofactors (Eya1, Eya2) are also critical for hypaxial muscle specification and migration towards the limbs. Six1 and Six4 are expressed in overlapping domains in many embryonic tissues including the dermomyotome, myotome and limb buds, and are involved in the developmental network of fast versus slow muscle types (Niro et al., 2010). Six and Eya may function as upstream regulator of Pax3 during dermomyotome specification (Grifone et al., 2007; Grifone et al., 2005).

Understanding the gene networks that control embryonic and fetal organ development can lead to ways to treat and prevent birth defects and developmental disorders.

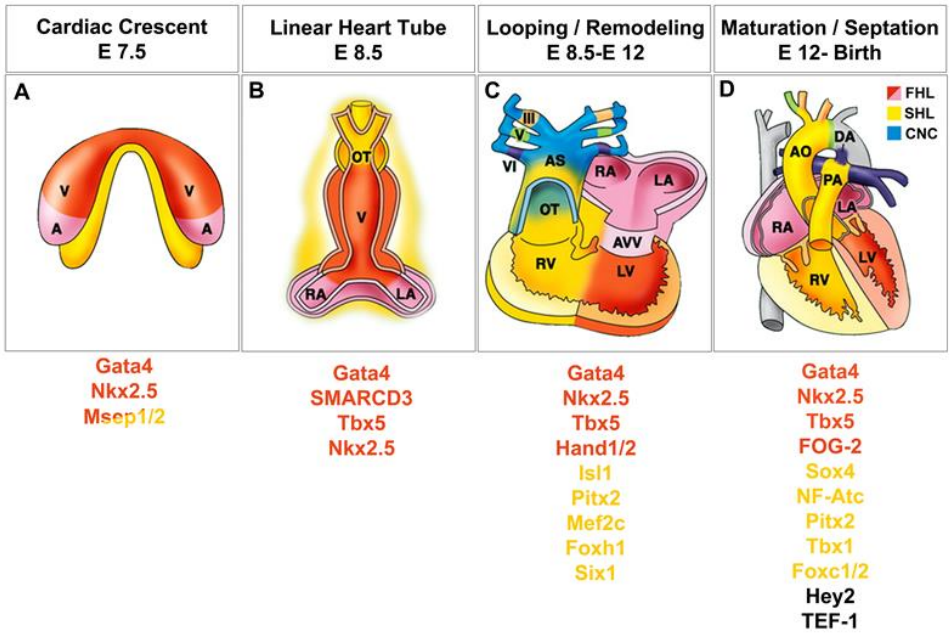

Figure 1.1

Figure 1.1 Cardiac Development. (A) Immediately after gastrulation at E7.5, the formation of the heart is initiated by the fusion of two cell linages, the 1st heart lineage (FHL) that forms a crescent shape in the anterior part of the embryo and the 2nd (SHL) in the medial and anterior to the FHL. **(B)** A day later at E8.5, cells of the SHL lie dorsal to the heart tube and migrate inside to form the right ventricle (RV), outflow tract (OT) and part of the atria (A). **(C)** Following the looping of the heart tube, the cardiac neural crest (CNC) cells also migrate into the OT to contribute to septation of the OT and to pattern the aortic arch arteries (III, IV and VI). This cellular remodeling results to the formation of the OT and atrioventricular valve (AVV) cushions form. **(D)** During the last week of gestation (E12- birth), continuously septation of the ventricles, atria and AVV results in the formation of the four-chambered heart. SSTFs essential for each developmental stage is color coordinated with the cell lineage that mark. The black colored SSTFs are not cell lineage specific.

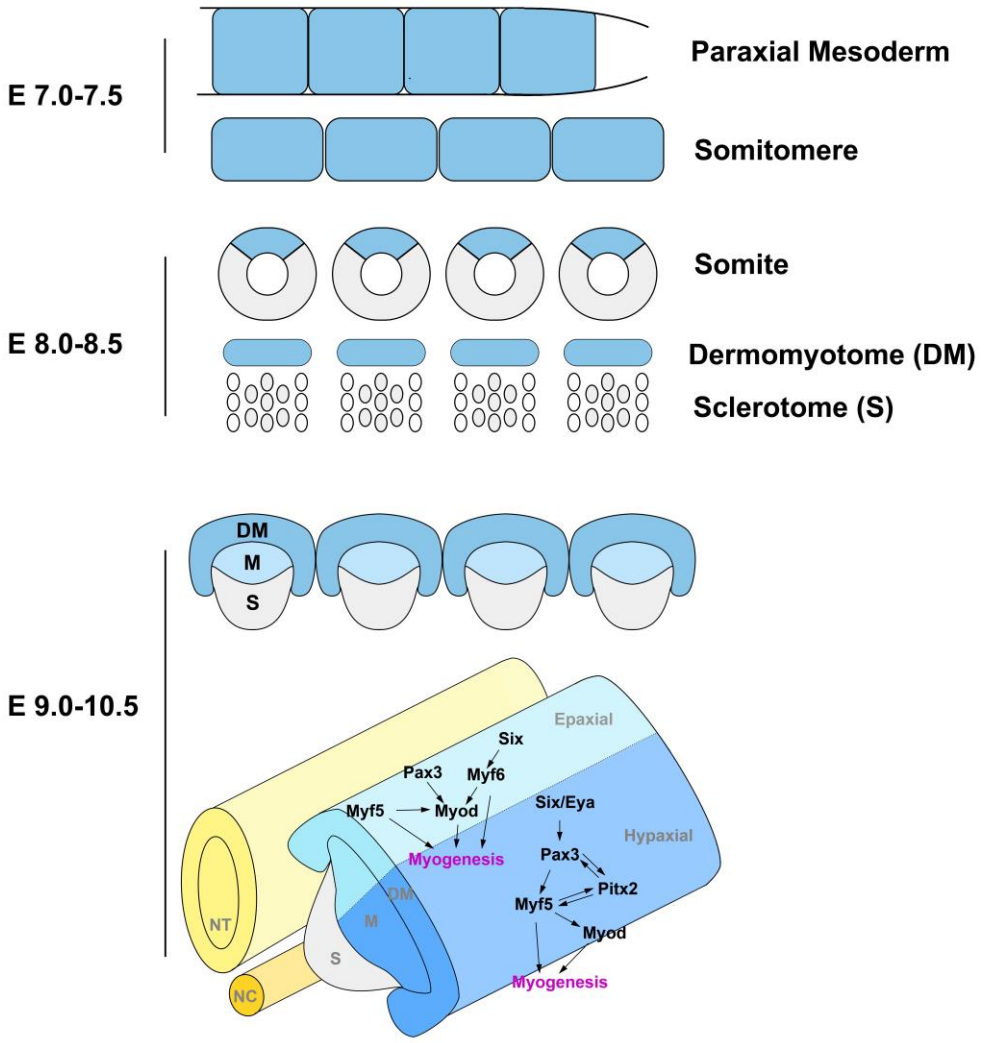
E 7.0-7.5
Paraxial Mesoderm
Somitomere
E 8.0-8.5
Somite
Dermomyotome (DM)
Sclerotome (S)
E 9.0-10.5
DM
M
S
Epaxial
Six
Pax3
Myf6
Myf5
Myod
Six/Eya
Hypaxial
Myogenesis
Pax3
Pitx2
Myf5
Myod
Myogenesis
DM
M
S
NT
NC

Figure 1.2

Figure 1.2 Skeletal Myogenesis. Paraxial mesoderm forms at E 7.0-E 7.5 along the axis of the body. Segmented somitomere is differentiated from paraxial mesoderm at E 8.0. Each somitomere differentiates into a somite which lies in a rostral to caudal manner on each side of the neural tube. The sclerotome (S) cells are delaminated from the dermomyotome (DM) which further give rise to myotome (M). As somites mature, they receive signals from the adjacent neural tube (NT) and notochord (NC). These signals result in the division of the somite into the S, DM and M. Cells in the epaxial region will give rise to the muscles of the deep back, while cells in the hypaxial region will give rise to muscles of the abdomen and limbs. Shh from the floor plate of the neural tube and from the notochord, and Wnt1 from the dorsal neural tube activate Myf5, which in turn activates Myod. Wnt7 and Pax3 from the dorsal neural tube also activate Myod to initiate myogenesis of the epaxial somites. Activation of Pax3, by Pitx2 and Six/Eya, activates Myf5 and Myod for initiation of hypaxial myogenesis.

REFERENCES

Bajard, L., Relaix, F., Lagha, M., Rocancourt, D., Daubas, P., and Buckingham, M.E. (2006). A novel genetic hierarchy functions during hypaxial myogenesis: Pax3 directly activates Myf5 in muscle progenitor cells in the limb. Genes & development *20*, 2450-2464.

Bertrand, N., Roux, M., Ryckebusch, L., Niederreither, K., Dolle, P., Moon, A., Capecchi, M., and Zaffran, S. (2011). Hox genes define distinct progenitor sub-domains within the second heart field. Developmental biology *353*, 266-274.

Birchmeier, C., and Brohmann, H. (2000). Genes that control the development of migrating muscle precursor cells. Curr Opin Cell Biol *12*, 725-730.

Biressi, S., Molinaro, M., and Cossu, G. (2007a). Cellular heterogeneity during vertebrate skeletal muscle development. Developmental biology *308*, 281-293.

Biressi, S., Tagliafico, E., Lamorte, G., Monteverde, S., Tenedini, E., Roncaglia, E., Ferrari, S., Cusella-De Angelis, M.G., Tajbakhsh, S., and Cossu, G. (2007b). Intrinsic phenotypic diversity of embryonic and fetal myoblasts is revealed by genome-wide gene expression analysis on purified cells. Developmental biology *304*, 633-651.

Biressi, S., Tagliafico, E., Lamorte, G., Monteverde, S., Tenedini, E., Roncaglia, E., Ferrari, S., Ferrari, S., Cusella-De Angelis, M.G., Tajbakhsh, S.*, et al.* (2007c). Intrinsic phenotypic diversity of embryonic and fetal myoblasts is revealed by genome-wide gene expression analysis on purified cells. Developmental biology *304*, 633-651.

Bober, E., Franz, T., Arnold, H.H., Gruss, P., and Tremblay, P. (1994). Pax-3 is required for the development of limb muscles: a possible role for the migration of dermomyotomal muscle progenitor cells. Development *120*, 603-612.

Borycki, A.G., Brunk, B., Tajbakhsh, S., Buckingham, M., Chiang, C., and Emerson, C.P., Jr. (1999). Sonic hedgehog controls epaxial muscle determination through Myf5 activation. Development *126*, 4053-4063.

Bruneau, B.G., Nemer, G., Schmitt, J.P., Charron, F., Robitaille, L., Caron, S., Conner, D.A., Gessler, M., Nemer, M., Seidman, C.E.*, et al.* (2001). A murine model of Holt-Oram syndrome defines roles of the T-box transcription factor Tbx5 in cardiogenesis and disease. Cell *106*, 709-721.

Cai, C.L., Liang, X., Shi, Y., Chu, P.H., Pfaff, S.L., Chen, J., and Evans, S. (2003). Isl1 identifies a cardiac progenitor population that proliferates prior to

differentiation and contributes a majority of cells to the heart. Developmental cell *5*, 877-889.

Christ, B., Jacob, M., and Jacob, H.J. (1983). On the origin and development of the ventrolateral abdominal muscles in the avian embryo. An experimental and ultrastructural study. Anatomy and embryology *166*, 87-101.

Dietrich, S., Abou-Rebyeh, F., Brohmann, H., Bladt, F., Sonnenberg-Riethmacher, E., Yamaai, T., Lumsden, A., Brand-Saberi, B., and Birchmeier, C. (1999). The role of SF/HGF and c-Met in the development of skeletal muscle. Development *126*, 1621-1629.

Dodou, E., Verzi, M.P., Anderson, J.P., Xu, S.M., and Black, B.L. (2004). Mef2c is a direct transcriptional target of ISL1 and GATA factors in the anterior heart field during mouse embryonic development. Development *131*, 3931-3942.

Duxson, M.J., Usson, Y., and Harris, A.J. (1989). The origin of secondary myotubes in mammalian skeletal muscles: ultrastructural studies. Development *107*, 743-750.

Evans, S.M., Yelon, D., Conlon, F.L., and Kirby, M.L. (2010). Myocardial lineage development. Circulation research *107*, 1428-1444.

Gage, P.J., Suh, H., and Camper, S.A. (1999a). The bicoid-related Pitx gene family in development. Mammalian genome : official journal of the International Mammalian Genome Society *10*, 197-200.

Gage, P.J., Suh, H., and Camper, S.A. (1999b). Dosage requirement of Pitx2 for development of multiple organs. Development *126*, 4643-4651.

Galli, D., Dominguez, J.N., Zaffran, S., Munk, A., Brown, N.A., and Buckingham, M.E. (2008). Atrial myocardium derives from the posterior region of the second heart field, which acquires left-right identity as Pitx2c is expressed. Development *135*, 1157-1167.

Garg, V., Kathiriya, I.S., Barnes, R., Schluterman, M.K., King, I.N., Butler, C.A., Rothrock, C.R., Eapen, R.S., Hirayama-Yamada, K., Joo, K.*, et al.* (2003). GATA4 mutations cause human congenital heart defects and reveal an interaction with TBX5. Nature *424*, 443-447.

Goulding, M., Lumsden, A., and Paquette, A.J. (1994). Regulation of Pax-3 expression in the dermomyotome and its role in muscle development. Development *120*, 957-971.

Grifone, R., Demignon, J., Giordani, J., Niro, C., Souil, E., Bertin, F., Laclef, C.,

Xu, P.X., and Maire, P. (2007). Eya1 and Eya2 proteins are required for hypaxial somitic myogenesis in the mouse embryo. Developmental biology *302*, 602-616.

Grifone, R., Demignon, J., Houbron, C., Souil, E., Niro, C., Seller, M.J., Hamard, G., and Maire, P. (2005). Six1 and Six4 homeoproteins are required for Pax3 and Mrf expression during myogenesis in the mouse embryo. Development *132*, 2235-2249.

Gross, M.K., Moran-Rivard, L., Velasquez, T., Nakatsu, M.N., Jagla, K., and Goulding, M. (2000). Lbx1 is required for muscle precursor migration along a lateral pathway into the limb. Development *127*, 413-424.

Gunning, P., and Hardeman, E. (1991). Multiple mechanisms regulate muscle fiber diversity. FASEB journal : official publication of the Federation of American Societies for Experimental Biology *5*, 3064-3070.

Guo, C., Sun, Y., Zhou, B., Adam, R.M., Li, X., Pu, W.T., Morrow, B.E., Moon, A., and Li, X. (2011). A Tbx1-Six1/Eya1-Fgf8 genetic pathway controls mammalian cardiovascular and craniofacial morphogenesis. The Journal of clinical investigation *121*, 1585-1595.

Harel, I., Maezawa, Y.,Avraham, R., Rinon, A., Ma, H., Cross, J. W., Leviatan, N., Hegesh, J. T., Roy, A., Jacob-Hirsch, J., Rechavi, G., Carvajhal, J., Tole, S., Kioussi, C., Quaggin, S.and Tzahor, E. (2012). Pharyngeal mesoderm regulatory network controls cardiac and head muscle morphogenesis. PNAS.

Harvey, R.P. (2002). Patterning the vertebrate heart. Nat Rev Genet *3*, 544-556.

Hasty, P., Bradley, A., Morris, J.H., Edmondson, D.G., Venuti, J.M., Olson, E.N., and Klein, W.H. (1993). Muscle deficiency and neonatal death in mice with a targeted mutation in the myogenin gene. Nature *364*, 501-506.

Hutcheson, D.A., Zhao, J., Merrell, A., Haldar, M., and Kardon, G. (2009). Embryonic and fetal limb myogenic cells are derived from developmentally distinct progenitors and have different requirements for beta-catenin. Genes & development *23*, 997-1013.

Jostes, B., Walther, C., and Gruss, P. (1990). The murine paired box gene, Pax7, is expressed specifically during the development of the nervous and muscular system. Mech Dev *33*, 27-37.

Kassar-Duchossoy, L., Gayraud-Morel, B., Gomes, D., Rocancourt, D.,

Buckingham, M., Shinin, V., and Tajbakhsh, S. (2004). Mrf4 determines skeletal muscle identity in Myf5:Myod double-mutant mice. Nature *431*, 466-471.

Kelly, R.G. (2005). Molecular inroads into the anterior heart field. Trends Cardiovasc Med *15*, 51-56.

Kelly, R.G., Brown, N.A., and Buckingham, M.E. (2001). The arterial pole of the mouse heart forms from Fgf10-expressing cells in pharyngeal mesoderm. Dev Cell *1*, 435-440.

Kioussi, C., Briata, P., Baek, S.H., Rose, D.W., Hamblet, N.S., Herman, T., Ohgi, K.A., Lin, C., Gleiberman, A., Wang, J.*, et al.* (2002). Identification of a Wnt/Dvl/beta-Catenin --> Pitx2 pathway mediating cell-type-specific proliferation during development. Cell *111*, 673-685.

Kirby, M.L., Gale, T.F., and Stewart, D.E. (1983). Neural crest cells contribute to normal aorticopulmonary septation. Science *220*, 1059-1061.

Kirby, M.L., and Hutson, M.R. (2010). Factors controlling cardiac neural crest cell migration. Cell adhesion & migration *4*, 609-621.

Kitamura, K., Miura, H., Miyagawa-Tomita, S., Yanazawa, M., Katoh-Fukui, Y., Suzuki, R., Ohuchi, H., Suehiro, A., Motegi, Y., Nakahara, Y.*, et al.* (1999). Mouse Pitx2 deficiency leads to anomalies of the ventral body wall, heart, extra- and periocular mesoderm and right pulmonary isomerism. Development *126*, 5749-5758.

Krumlauf, R. (1994). Hox genes in vertebrate development. Cell *78*, 191-201.

Kume, T., Jiang, H., Topczewska, J.M., and Hogan, B.L. (2001). The murine winged helix transcription factors, Foxc1 and Foxc2, are both required for cardiovascular development and somitogenesis. Genes & development *15*, 2470-2482.

L'Honore, A., Coulon, V., Marcil, A., Lebel, M., Lafrance-Vanasse, J., Gage, P., Camper, S., and Drouin, J. (2007). Sequential expression and redundancy of Pitx2 and Pitx3 genes during muscle development. Developmental biology *307*, 421-433.

L'Honore, A., Ouimette, J.F., Lavertu-Jolin, M., and Drouin, J. (2010). Pitx2 defines alternate pathways acting through MyoD during limb and somitic myogenesis. Development *137*, 3847-3856.

Lavine, K.J., and Ornitz, D.M. (2008). Fibroblast growth factors and Hedgehogs: at the heart of the epicardial signaling center. Trends in genetics : TIG *24*,

33-40.

Li, P., Pashmforoush, M., and Sucov, H.M. (2010). Retinoic acid regulates differentiation of the secondary heart field and TGFbeta-mediated outflow tract septation. Developmental cell *18*, 480-485.

Lin, C.R., Kioussi, C., O'Connell, S., Briata, P., Szeto, D., Liu, F., Izpisua-Belmonte, J.C., and Rosenfeld, M.G. (1999). Pitx2 regulates lung asymmetry, cardiac positioning and pituitary and tooth morphogenesis. Nature *401*, 279-282.

Liu, Y., Cserjesi, P., Nifuji, A., Olson, E.N., and Noda, M. (1996). Sclerotome-related helix-loop-helix type transcription factor (scleraxis) mRNA is expressed in osteoblasts and its level is enhanced by type-beta transforming growth factor. The Journal of endocrinology *151*, 491-499.

Lopez-Sanchez, C., and Garcia-Martinez, V. (2011). Molecular determinants of cardiac specification. Cardiovascular research *91*, 185-195.

Lozano-Velasco, E., Contreras, A., Crist, C., Hernandez-Torres, F., Franco, D., and Aranega, A.E. (2011). Pitx2c modulates Pax3+/Pax7+ cell populations and regulates Pax3 expression by repressing miR27 expression during myogenesis. Developmental biology *357*, 165-178.

Lu, M.F., Pressman, C., Dyer, R., Johnson, R.L., and Martin, J.F. (1999). Function of Rieger syndrome gene in left-right asymmetry and craniofacial development. Nature *401*, 276-278.

Lyons, I., Parsons, L.M., Hartley, L., Li, R., Andrews, J.E., Robb, L., and Harvey, R.P. (1995). Myogenic and morphogenetic defects in the heart tubes of murine embryos lacking the homeo box gene Nkx2-5. Genes & development *9*, 1654-1666.

Makki, N., and Capecchi, M.R. (2010). Hoxa1 lineage tracing indicates a direct role for Hoxa1 in the development of the inner ear, the heart, and the third rhombomere. Developmental biology *341*, 499-509.

McGinnis, W., Levine, M.S., Hafen, E., Kuroiwa, A., and Gehring, W.J. (1984). A conserved DNA sequence in homoeotic genes of the Drosophila Antennapedia and bithorax complexes. Nature *308*, 428-433.

Messina, G., Biressi, S., Monteverde, S., Magli, A., Cassano, M., Perani, L., Roncaglia, E., Tagliafico, E., Starnes, L., Campbell, C.E.*, et al.* (2010). Nfix regulates fetal-specific transcription in developing skeletal muscle. Cell *140*,

554-566.

Mjaatvedt, C.H., Nakaoka, T., Moreno-Rodriguez, R., Norris, R.A., Kern, M.J., Eisenberg, C.A., Turner, D., and Markwald, R.R. (2001). The outflow tract of the heart is recruited from a novel heart-forming field. Developmental biology *238*, 97-109.

Montarras, D., Chelly, J., Bober, E., Arnold, H., Ott, M.O., Gros, F., and Pinset, C. (1991). Developmental patterns in the expression of Myf5, MyoD, myogenin, and MRF4 during myogenesis. The New biologist *3*, 592-600.

Murphy, M., and Kardon, G. (2011). Origin of vertebrate limb muscle: the role of progenitor and myoblast populations. Curr Top Dev Biol *96*, 1-32.

Nabeshima, Y., Hanaoka, K., Hayasaka, M., Esumi, E., Li, S., Nonaka, I., and Nabeshima, Y. (1993). Myogenin gene disruption results in perinatal lethality because of severe muscle defect. Nature *364*, 532-535.

Nameroff, M., and Rhodes, L.D. (1989). Differential response among cells in the chick embryo myogenic lineage to photosensitization by Merocyanine 540. Journal of cellular physiology *141*, 475-482.

Niro, C., Demignon, J., Vincent, S., Liu, Y., Giordani, J., Sgarioto, N., Favier, M., Guillet-Deniau, I., Blais, A., and Maire, P. (2010). Six1 and Six4 gene expression is necessary to activate the fast-type muscle gene program in the mouse primary myotome. Developmental biology *338*, 168-182.

Nowotschin, S., Liao, J., Gage, P.J., Epstein, J.A., Campione, M., and Morrow, B.E. (2006). Tbx1 affects asymmetric cardiac morphogenesis by regulating Pitx2 in the secondary heart field. Development *133*, 1565-1573.

Oustanina, S., Hause, G., and Braun, T. (2004). Pax7 directs postnatal renewal and propagation of myogenic satellite cells but not their specification. The EMBO journal *23*, 3430-3439.

Prall, O.W., Menon, M.K., Solloway, M.J., Watanabe, Y., Zaffran, S., Bajolle, F., Biben, C., McBride, J.J., Robertson, B.R., Chaulet, H.*, et al.* (2007). An Nkx2-5/Bmp2/Smad1 negative feedback loop controls heart progenitor specification and proliferation. Cell *128*, 947-959.

Relaix, F., Rocancourt, D., Mansouri, A., and Buckingham, M. (2004). Divergent functions of murine Pax3 and Pax7 in limb muscle development. Genes & development *18*, 1088-1105.

Relaix, F., Rocancourt, D., Mansouri, A., and Buckingham, M. (2005). A

Pax3/Pax7-dependent population of skeletal muscle progenitor cells. Nature *435*, 948-953.

Ross, J.J., Duxson, M.J., and Harris, A.J. (1987). Formation of primary and secondary myotubes in rat lumbrical muscles. Development *100*, 383-394.

Shih, H.P., Gross, M.K., and Kioussi, C. (2007). Expression pattern of the homeodomain transcription factor Pitx2 during muscle development. Gene expression patterns : GEP *7*, 441-451.

Stockdale, F.E. (1992). Myogenic cell lineages. Developmental biology *154*, 284-298.

Sucov, H.M., Gu, Y., Thomas, S., Li, P., and Pashmforoush, M. (2009). Epicardial control of myocardial proliferation and morphogenesis. Pediatric cardiology *30*, 617-625.

Suga, H., Tschopp, P., Graziussi, D.F., Stierwald, M., Schmid, V., and Gehring, W.J. (2010). Flexibly deployed Pax genes in eye development at the early evolution of animals demonstrated by studies on a hydrozoan jellyfish. Proceedings of the National Academy of Sciences of the United States of America *107*, 14263-14268.

Tajbakhsh, S., Borello, U., Vivarelli, E., Kelly, R., Papkoff, J., Duprez, D., Buckingham, M., and Cossu, G. (1998). Differential activation of Myf5 and MyoD by different Wnts in explants of mouse paraxial mesoderm and the later activation of myogenesis in the absence of Myf5. Development *125*, 4155-4162.

Takeuchi, J.K., and Bruneau, B.G. (2009). Directed transdifferentiation of mouse mesoderm to heart tissue by defined factors. Nature *459*, 708-711.

Tanaka, M., Wechsler, S.B., Lee, I.W., Yamasaki, N., Lawitts, J.A., and Izumo, S. (1999). Complex modular cis-acting elements regulate expression of the cardiac specifying homeobox gene Csx/Nkx2.5. Development *126*, 1439-1450.

Theveniau-Ruissy, M., Dandonneau, M., Mesbah, K., Ghez, O., Mattei, M.G., Miquerol, L., and Kelly, R.G. (2008). The del22q11.2 candidate gene Tbx1 controls regional outflow tract identity and coronary artery patterning. Circulation research *103*, 142-148.

von Both, I., Silvestri, C., Erdemir, T., Lickert, H., Walls, J.R., Henkelman, R.M., Rossant, J., Harvey, R.P., Attisano, L., and Wrana, J.L. (2004). Foxh1 is essential for development of the anterior heart field. Developmental cell *7*,

331-345.

Waldo, K., Miyagawa-Tomita, S., Kumiski, D., and Kirby, M.L. (1998). Cardiac neural crest cells provide new insight into septation of the cardiac outflow tract: aortic sac to ventricular septal closure. Developmental biology *196*, 129-144.

Waldo, K.L., Kumiski, D.H., Wallis, K.T., Stadt, H.A., Hutson, M.R., Platt, D.H., and Kirby, M.L. (2001). Conotruncal myocardium arises from a secondary heart field. Development *128*, 3179-3188.

Watanabe, Y., Zaffran, S., Kuroiwa, A., Higuchi, H., Ogura, T., Harvey, R.P., Kelly, R.G., and Buckingham, M. (2012). Fibroblast growth factor 10 gene regulation in the second heart field by Tbx1, Nkx2-5, and Islet1 reveals a genetic switch for down-regulation in the myocardium. Proceedings of the National Academy of Sciences of the United States of America *109*, 18273-18280.

Williams, B.A., and Ordahl, C.P. (1994). Pax-3 expression in segmental mesoderm marks early stages in myogenic cell specification. Development *120*, 785-796.

Wright, W.E., Sassoon, D.A., and Lin, V.K. (1989). Myogenin, a factor regulating myogenesis, has a domain homologous to MyoD. Cell *56*, 607-617.

Yamagishi, H., Maeda, J., Hu, T., McAnally, J., Conway, S.J., Kume, T., Meyers, E.N., Yamagishi, C., and Srivastava, D. (2003). Tbx1 is regulated by tissue-specific forkhead proteins through a common Sonic hedgehog-responsive enhancer. Genes & development *17*, 269-281.

Yamagishi, H., Yamagishi, C., Nakagawa, O., Harvey, R.P., Olson, E.N., and Srivastava, D. (2001). The combinatorial activities of Nkx2.5 and dHAND are essential for cardiac ventricle formation. Developmental biology *239*, 190-203.

Yusuf, F., and Brand-Saberi, B. (2006). The eventful somite: patterning, fate determination and cell division in the somite. Anatomy and embryology *211 Suppl 1*, 21-30.

Gene Networks During Cardiogenesis And Skeletal Myogenesis

Chapter 2

Pitx2-Mediated Cardiac Outflow Tract Remodeling

Hsiao-Yen Ma, Jun Xu, Diana Eng, Michael K. Gross, Chrissa Kioussi

Development Dynamics

Published March 12, 2013

Dec Dyn 242(5):456-68

doi: 10.1002/dvdy.23934

SUMMARY

Heart morphogenesis involves sequential anatomical changes from a linear tube of a single channel peristaltic pump to a four-chamber structure with two channels controlled by one-way valves. The developing heart undergoes continuous remodeling, including septation.

Pitx2-null mice are characterized by cardiac septational defects of the atria, ventricles, and outflow tract. Pitx2-null mice also exhibited a short outflow tract, including unseptated conus and deformed endocardial cushions. Cushions were characterized with a jelly-like structure, rather than the distinct membrane-looking leaflets, indicating that endothelial mesenchymal transition was impaired in Pitx2$^{-/-}$ embryos. Mesoderm cells from the branchial arches and neural crest cells from the otic region contribute to the development of the endocardial cushions, and both were reduced in number. Members of the Fgf and Bmp families exhibited altered expression levels in the mutants.

We suggest that Pitx2 is involved in the cardiac outflow tract septation by promoting and/or maintaining the number and the remodeling process of the mesoderm progenitor cells. Pitx2 influences the expression of transcription factors and signaling molecules involved in the differentiation of the cushion mesenchyme during heart development.

INTRODUCTION

Congenital heart defects are the leading non-infectious cause of death in newborns. Approximately half of all cases are associated with septational malformations in the outflow tract (OT) and/or ventricles (Hoffman and Kaplan, 2002). The mammalian heart develops from cells of four embryonic origins: (1) the cardiac crescent, first lineage or first heart field; (2) the branchial arch (BA)-derived mesoderm, second lineage or secondary heart field; (3) the cardiac neural crest (cNC) cells and (4) the epicardium. The first lineage appears shortly after gastrulation as a population of mesodermal cells that differentiate into endocardial and myocardial types and form a tubular structure (Harvey, 2002). The second lineage arises from a population of splanchnic mesodermal cells that contribute to the formation of OT and right ventricle (RV) (Buckingham et al., 2005; Kelly et al., 2001). The OT is a tubular structure consisting of striated cardiac musculature lined with endocardium. The OT follows a dramatic remodeling to form the aorto-pulmonary (AP) septum that separates the initially single OT vessel to form the ascending aorta (Ao) and the pulmonary trunk (Webb et al., 2003). Between E9.5 and E10.5, endocardial cushions start to form across the common OT, the conotruncus, and the atrioventricular canal. The conotruncal endocardial cushions further divide into proximal and distal conotruncal cushions. The distal conotruncal cushions will form the AP septum at E12.5 - E13.5. The linear heart tube consists of the external layer of myocardium and the internal layer of endocardium, which are separated by the myocardium-produced extracellular matrix, the cardiac jelly. As endocardial cushions develop, endocardial cells proliferate and undergo an epithelial-to-mesenchymal transformation (EMT) and infiltrate the cardiac jelly. As the two cushions come closer, the endocardial cell barrier degenerates and the mesenchymal cells form a bridge to stabilize the fusion of the two cushions (Ray and Niswander, 2012). When tissue alignment, fusion or rotation is

disrupted, transposition of the great arteries (TGA) or double-outlet right ventricle (DORV) occurs. Complete failure of OT septation results in persistent truncus arteriosus (PTA).

At the early stages, cNC cells penetrate the second lineage, which is adjacent to the pharyngeal ectoderm, for the formation of the OT. The unspecified mesoderm receives extracellular cues that orchestrate its sequential differentiation into cardiogenic mesoderm, myocardium and smooth muscle. These cues are primarily signaling molecules, such as the bone morphogenetic proteins (BMPs) and the fibroblast growth factors (FGFs). BMP signaling is involved in the induction of the cardiac differentiation. Bmp2 and Bmp4 induce Nkx2.5 and Gata4, which regulate differentiation of cardiac mesoderm into first and second heart lineages (Monzen et al., 1999). *BMP* signaling promotes specification and differentiation of the second lineage to a cardiac fate by inhibiting FGF signaling (Tirosh-Finkel et al., 2006). *Bmp4* is expressed in the splachnic mesoderm, BA mesoderm, and OT myocardium, and is required for OT septation and endocardial cushion remodeling (Liu et al., 2004). FGF signaling is involved in cardiac induction, septation, cell proliferation and OT alignment (Ilagan et al., 2006; Kelly et al., 2001; Park et al., 2008).

Sequence-specific transcription factors (SSTFs) are also involved in guiding proper cardiac cellular proliferation, differentiation and migration. The LIM-homeodomain protein Islet-1 (Isl1) is expressed in the pharyngeal mesoderm and is required for the development of the SHF lineage and its derivatives (Cai et al., 2003). Isl1 marks proliferating, undifferentiated pluripotent cardiovascular progenitors of the second lineage (Buckingham et al., 2005; Cai et al., 2003). *Isl1*-null mice die at E10 with hearts lacking OT septation. The bHLH protein Mef2c marks a subpopulation of the second lineage (Dodou et al., 2004) and, when mutated, leads to similar defects as *Isl1*, including defective heart looping and malformed OT (Buckingham et al., 2005;

Lin et al., 1997). *Tbx1* is expressed in the non-cNC-derived mesoderm of the caudal pharyngeal region, which is part of the second lineage and contributes to the formation of OT and RV (Hu et al., 2004; Xu et al., 2004). *Fgf8* and *Fgf10* act downstream of Tbx1 in the second lineage (Kelly and Papaioannou, 2007; Vitelli et al., 2002).

Pitx2, a paired-like homeobox SSTF, is transiently expressed on the left side of the cardiac crescent and linear heart tube during early development (E8), and later (E9-E14.5) is expressed in the OT and RV. Genomic screens for inherited atrial fibrillation patients have found deficiencies in the Pitx2 locus (Schnabel, 2011). Pitx2-null embryos are characterized by a non-septated atrium, valvular and OT deficiencies, including PTA, DORV and TGA (Gage et al., 1999b; Kioussi et al., 2002; Kitamura et al., 1999; Lin et al., 1999; Lu et al., 1999). Pitx2 controls the specification of cardiac cells within the second lineage by repressing Fgf10 and Isl1 (Galli et al., 2008). Pitx2 and Tbx1 are necessary for proper migration and proliferation of secondary lineage cardiac progenitors (Nowotschin et al., 2006). The observed phenotypes of the knockout mouse models indicated that Pitx2 is critical in regulating the OT formation. Here we report that Pitx2 acts in a network kernel during cardiogenesis and controls the state of the cells of the second lineage as they migrate from the BA to OT and enter the remodeling state to form the valves.

EXPERIMENTAL PROCEDURES

Mice

ICR *Pitx2*$^{+/LacZ}$ (*Pitx2*$^{+/Z}$) mice (Lin et al., 1999) were bred and females were checked for the presence of a vaginal plug (E0). Embryos were isolated at

different developmental stages and the yolk sacs were used for genotyping. *Mef2c*^{Cre} mice (Verzi et al., 2005) and *Wnt1*^{Cre} mice (Jackson Lab) (Echelard et al., 1994) were crossed with *Rosa26*^{EGFP}(*Rosa*^{EGFP}) (Jackson Lab) (Mao et al., 2001) mice to obtain *Mef2c*^{Cre}|*Rosa*^{EGFP} and *Wnt1*^{Cre}|*Rosa*^{EGFP} double heterozygotes, respectively. *Pitx2*$^{+/Z}$ mice were crossed with *Mef2c*^{Cre}|*Rosa*^{EGFP} or *Wnt1*^{Cre}|*Rosa*^{EGFP} to generate green *Pitx2* wild type and mutant mice. PCR analysis from tail genomic DNA identified the 380 bp EGFP and 400 bp Cre bands.

Immunohistochemistry, TUNEL and BrdU

Immunohistochemistry on cryosections was performed as described by (Shih, 2007). Sections were photographed on an AxioImager Z1, Zeiss microscope. TUNEL assay was also performed as recommended by the manufacturer (Dead End kit; Promega). Pregnant female *Pitx2*$^{+/Z}$ mice were injected with 5 mg/ml BrdU 2 hr before dissection. Embryos from injected mice were processed, as previously described (Shih et al., 2007b). Immunohistochemistry of whole-mount embryos was performed according to standard protocol (Joyner and Wall, 2008). Whole embryos were photographed with a discovery V8, Zeiss microscope. Primary antibodies are listed as follows: MF20 (Mouse, 1:50, DHSB), ß-galactosidase (Rabbit, 1:1000, Cappel), BrdU (Rat, 1:100, Accurate Chemical Scientific Corporation), EGFP [Rat, 1:1500, (Shih et al., 2007c)], Isl1 (Mouse, 1:30, DHSB), PECAM (Rat, 1:10, BD Biosciences), Neurofilament 200 (Rabbit, 1:100, Sigma).

Quantitative Real-time PCR(qPCR)

cDNA from BA (n=5) and heart (n=5) were prepared by RNeasy Micro Kit

(Qiagen). cDNA (25ng) was analyzed by qPCR using SYBR Green I methodology as previously described (Hilton et al., 2010). All samples were analyzed in triplicate and normalized by glyceraldehyde-3-phosphate dehydrogenase. All qPCR primer sets are listed in Table 2.1.

Pitx2-Binding Site Analysis

An in house Perl script, binding_site_compare.pl was used for identifying the absolute location and evolutionary conservation of potential Pitx2-binding sites TAATCY (Amendt et al., 1998; Campbell et al., 2012a; Eng et al., 2010; Eng and Dubovoy, 2012). The alignments for each gene, along with the 20kb region upstream of the gene, were download from the UCSC Genome Browser on Mouse July 2007 (NCBI37/mm9) Assembly, available at http://genome.ucsc.edu/. The alignments were then formatted for our script, which identified the absolute location of potential Pitx2 binding sites and the species conserved for each binding site. Excel was used to map binding site locations and species to each gene.

Chromatin Immuno-Precipitation (ChIP)

Heart and BA biopsies from 6-8 embryos of E10.5 *Pitx2* wild type and *Pitx2*$^{Z/Z}$ mice were harvested per ChIP. Samples were collected and processed as previously described (Hilton et al., 2010). Primers were designed for binding sites identified as conserved sites. Control primers were designed for regions on the genome with no putative binding site within a minimum of a 1kb window on the mouse genome. All primer sets are listed in Table 2.1.

RNA *in situ* Hybridization

Whole-mount RNA *in situ* hybridization was performed according to standard procedures (Oliver et al., 1995). RNA *in situ* hybridization on sections was performed on 16 ìm cryosections, as previously described (Kyrylkova et al., 2012). Digoxigenin-labeled antisense RNA in situ probes were generated by an in vitro transcription kit (Dig RNA labeling kit, Roche Molecular Biochemicals). AP-conjugated anti-DIG antibody (1:500) was used to detect the hybridization signals (Roche Molecular Biochemicals).

RESULTS

Hypocellular OT Endothelial Cushions in Pitx2 Mutants

Pitx2-null mice (*Pitx2*$^{LacZ/LacZ}$, *Pitx2*$^{Z/Z}$) die at E14.5 due to arrest of organ development (Gage et al., 1999b; Kitamura et al., 1999; Lin et al., 1999; Lu et al., 1999). The heart is one of the organs that is severely affected, displaying atrial and ventricular septal defects, hypoplastic RV, RA isomerism, DORV, TGA, PTA and abnormal aortic arch remodeling (Campione et al., 2001; Gage et al., 1999b; Kitamura et al., 1999; Lin et al., 1999; Liu et al., 2002; Lu et al., 1999). The phenotype of the developing OT was analyzed at E10.5 and E12.5 in mutant and wild type mice (Fig. 2.1). At E10.5, the heart was already smaller, with delayed looping (Fig. 2.1A, B). The length of the OT was measured in at least three groups of mice, and a 20% decrease was identified (Fig. 2.1C), as has been also previously described (Ai et al., 2006). As the heart matures, it undergoes remodeling, and at E12.5 the OT divides and forms two structures, the aorta (Ao) and pulmonary artery (PA) (Fig. 2.1E). The septation of the OT occurs by (1) the initial division of the aortic sac by the cNC cells, (2) the septation of the distal part of the OT (truncus), and (3) the zipper-like closure of

the proximal part (conus) through the fusion of the cushions (Kirby, 2007). By E12.5, septation of the truncus, including the semilunar OT valves, has been completed. The conus closes from distal to proximal towards the ventricles. The ridges beneath the endocardium start to bulge, and when they meet in the middle of the lumen, the endocardium breaks down and a septum is formed (Waldo et al., 1998; Waldo et al., 1999). This conal septum separates the pulmonary and aortic roots. The Pitx2 mutants that exhibited DORV (Fig. 2.1F) continued to exhibit a shorter OT by 20% (Fig. 2.1G). Histological analysis on transverse sections at the conus level (Fig. 2.1E1, F1) indicated a thin and loose epithelium, a non-septated conus with randomly arranged mesenchymal cells within the semilunar valves, in the mutants (Fig. 2.1F1). Cell-counts of serial transverse sections through the OT of three individual mice for each stage indicated a slow but consistent cell reduction during OT valve formation, starting with no significant reduction at E10.5 (Fig. 2.1D) followed by a 17.5% reduction at E12.5 (Fig. 2.1H). Double labeling immunohistochemistry for MF20 and Pitx2(ß-Gal) on transverse sections at the level of the pulmonary and aortic roots at E12.5 (Fig. 2.1I, J) indicated lack of $MF20^+$ cells between the roots in mutants (Fig. 2.1J). Pitx2 was expressed in the muscularized semilunar pulmonary and aortic valves (Fig. 2.1I, yellow cells). No $MF20^+$ cells were detected in these cells in mutants (Fig. 2.1J). These data collectively suggest that Pitx2 is involved in the formation of the OT septum and in the muscularization process of the pulmonary and aortic valves.

Cell Death and Proliferation Defects of OT Mesenchymal Cells in Pitx2 Mutants

During cardiac remodeling, the OT cushions undergo EMT and become the membranous valves upon activation of cell apoptosis. To determine if Pitx2 is involved in this mechanism, Pitx2-mutant and heterozygote littermates were

examined for TUNEL and BrdU incorporation (Fig. 2.2). No cell death differences were detected at E10.5 (Fig. 2.2A, B). By E12.5, the OT undergoes remodeling and mesenchymal cells follow programmed cell death (Fig. 2.2C, arrows). No such cells were detected in the mutants (Fig. 2.2D). Cell-counts of OT serial sections at E12.5 showed significant decrease of TUNEL$^+$ cells in the mutants (Fig. 2.2E). To assay for cell proliferation, BrdU$^+$ and BrdU$^+$/Pitx2$^+$(ß-Gal$^+$) mesenchymal cells were detected by double labeling immunohistochemistry at E10.5 (Fig. 2.2F, G) and E12.5 (Fig. 2.2I, J). Cells were counted in five serial sections from three independent embryos at each stage and genotype. The number of BrdU$^+$ cells was 20% higher in mutants at both stages, while the number of BrdU$^+$/Pitx2$^+$ cells was increased by 57% at E10.5 and 65% at E12.5 (Fig. 2.2H, K). Collectively these data suggest that Pitx2 maintains the number of mesenchymal cells by inhibiting them from entering the cell cycle and promoting their exit, for further differentiation and/or apoptotic fate.

Second Cell Lineage and cNC Cell Defects in Pitx2 Mutants

Expression of Pitx2 in the OT cushions is detected as early as E10, and absence of Pitx2 results in a non-septated aorta and pulmonary trunk (Gage et al., 1999b; Kioussi et al., 2002; Kitamura et al., 1999; Lin et al., 1999). To investigate the cellular events, the Mef2c-lineage tracer mouse was crossed to *Rosa*^{EGFP} to detect the second cell lineage (Verzi et al., 2005). Double labeling immunohistochemistry was used to determine the distribution of EGFP(Mef2c) and Isl1 in BAs (Fig. 2.3A, B) and OT (Fig. 2.3D, E) at E10.5. Mef2c is restricted to the second lineage, while Isl1 primarily marks the cardiac progenitor cells (Cai et al., 2003) and, to a lesser extent, the cNC cells (Engleka et al., 2012). EGFP$^+$/Isl1$^+$ cells were detected as they enter the heart tube (Fig. 2.3A) and were severely reduced in the mutants (Fig. 2.3B). The EGFP$^+$ cells

were also already very much reduced in the BAs (Fig. 2.3B). The EGFP$^+$/Isl1$^+$ cells located in several layers of the OT epithelium (Fig. 2.3D) were reduced in mutants (Fig. 2.3E). The EGFP$^+$ cells that contribute to the formation of the epithelium and leaflets (Fig. 2.3D) were also reduced in the mutants (Fig. 2.3E). These cellular defects were more prominent at E12.5 (Fig. 2.3G, H). Very few EGFP$^+$ and almost no Isl1$^+$ cells were detected in the OT epithelium and leaflets. Quantitative assays indicated almost 50% reduction of EGFP(Mef2c) in BA (Fig. 2.3C) and the entire heart (Fig. 2.3F, I) compared to wild type embryos. Isl1 RNA levels were also reduced in the tested biopsies but in less extent (Fig. 2.3C, F, I). RNA levels for both EGFP and Mef2c were measured and no difference was detected in both BA and OT, suggesting that EGFP levels correspond to the endogenous Mef2c.

The cNC cells also contribute to the OT endocardial cushions. Postotic NC cells contribute to OT endocardial cushions (Kirby, 2007); preotic NC cells distribute to the contruncus and coronary artery formation (Arima et al., 2012). To test the cNC distribution in the OT of the Pitx2 mutants, the *Wnt1^{Cre}*|*Rosa^{EGFP}* reporter mouse was crossed to the *Pitx2^{LacZ}* line. Although the contribution of the Wnt1$^+$ cells to the OT under the Pitx2 influence was previously reported, (Ai et al., 2006), we performed the analysis at earlier developmental stages. At E9.5 the OT is already shorter in the Pitx2 mutants, (Fig. 2.4B) and the Wnt1$^+$ cells just populated the OT; while in the control wild type mice, they start to fuse and widely populate the area (Fig. 2.4A). At E10.5, a thick stream of Wnt1$^+$ cells was located in the OT (Fig. 2.4C); while in the mutants, this population seems restricted to the truncated truncus (Fig. 2.4D). At E12.5 this delay of the Wnt1$^+$ cells to populate the truncus and conus seems to be recovered in the mutants (Fig. 2.4E, F). However, the expression levels of another cNC marker, Ap2α, were reduced in the OT in mutants (Fig. 2.4G, H) at E12.5. These data suggest that Pitx2 influences the distribution of the BA

mesoderm derived and cNC cells during OT and endocardial cushion development.

Pitx2 Occupancy at SSTF Loci in BAs and Heart

Our data have shown that Pitx2 regulates the expression of both Mef2c and Isl1 in the BAs and OT, indicating this regulation might be on a transcriptional level. Chromatin-occupancy analyses provided another means to assess the interaction between Pitx2 and the SSTF that were altered in E10.5 *Pitx2* mutants. Embryos from approximately 2-3 synchronous litters were rapidly genotyped. Tissue biopsies, including BA (mandibular part of 1st, 2nd and 3rd BA) and heart (OT, atria and ventricles), were dissected from 6-8 embryos of each genotype and pooled for two independent experiments. From each experiment, a pair of wild type and mutant chromatin extract was generated with sufficient material for one immunoprecipitation, using an anti-Pitx2 antibody. Each immunoprecipitate provided enough material for 15 triplicate qPCR analyses. Amplicons within the *Mef2c, Isl1*, *Gat4* and *Nkx2.5* loci were identified, as described previously for T-box (Hilton et al., 2010) and Hox (Eng et al., 2012a) genes. Core motifs for bicoid class homeodomains (TAATCY) that were embedded in evolutionarily conserved non-coding regions and were, themselves, evolutionarily conserved, were identified (Fig. 2.5). Each red diamond represents a different species in which the core motif was conserved and expected to be essential for biological function. Core motifs with the most diamonds were selected as candidate *cis* regulatory modules, and primer pairs were designed to encompass a 70-150 bp context around these sites. The initially selected primer pairs were tested by endpoint PCR on purified genomic DNA. Amplified pairs were selected for SSTF chromatin occupancy analyses by ChIP-qPCR (Table S1). The mutant extract lacks Pitx2 protein and is, therefore, expected to have 0% occupancy. The signal measured in the mutant

precipitate, for any given amplicon, is a direct measurement of the background. Pitx2 occupied *Mef2c* (Fig. 2.5A, B) and *Isl1* (Fig. 2.5C, D) in the BA biopsies at positions -521 and +1983, respectively. No Pitx2 occupancy was detected on *Gata4* (Fig. 2.5F) at the positions -1065, +29818 and +36199, despite being evolutionarily conserved (Fig. 2.5E). Pitx2 occupancy was also not detected on *Nkx2.5* (Fig. 2.5H) at the positions -10523 and -1952 (Fig. 2.5G). Pitx2 occupancy on *Tbx1* BA biopsies has previously been reported in E10.5 mice (Shih et al., 2007b). The Pitx2 occupancy on the SSTF *Mef2c* and *Isl1* correlates well with their altered expression profiles in the developing BA. It has been shown that Pitx2 regulates *Gata4* expression (Lozano-Velasco et al., 2011a), and *Nkx2.5* has synergistic activity with Pitx2 (Ganga et al., 2003). However, this might not be due to Pitx2 occupancy at this developmental stage.

Pitx2 and FGF/BMP Signaling

FGF signaling in the second cardiac lineage is essential for OT cushion formation and remodeling. *Fgf8* expression in the ectoderm of the 1st and 2nd BA regulates proliferation and differentiation of post-migratory cNC cells. FGF signaling in the OT myocardium controls extracellular matrix formation; while BMP signaling is essential for endothelial cell transformation and invasion of cNC cells (Park et al., 2008). RNA in situ hybridization at E10.5 was used to determine the expression profile of *Fgf8, Fgf3, Bmp4* and *Notch* (Fig. 2.6). *Fgf8* is detected in the ectoderm of the 2nd, 3rd and 4th BA in wild type and heterozygote embryos (Fig. 2.6A, B) and was barely detectable in the 4th BA in mutants (Fig. 2.6C), as previously described (Liu et al., 2003). Similarly, the area of *Fgf3* expression in the 3rd - 6th BA (Fig. 2.6E, F) was reduced in mutants (Fig. 2.6G). The *Notch* signaling has been implicated in regulating EMT during valve development. *Notch2* is expressed in the cNC-derived vascular smooth muscle cells and is critical in mammalian OT development (Niessen and

Karsan, 2008). *Notch2* was expressed in the 3rd and 4th aortic arch (Fig. 2.6I, J), with significantly reduced expression levels in the mutants (Fig. 2.6K). *Bmp4* is expressed in the ventral splanchnic mesoderm, BA mesoderm, and OT myocardium. Bmp4 promotes proliferation of cushion mesenchyme and concurrently represses cell proliferation in the OT myocardium (Liu et al., 2004). The *Bmp4*-distinct area of mesenchymal expression in the OT (Fig. 2.6M, N) was not detected in mutants (Fig. 2.6O). The thinner OT epithelium was prominent in all mutants (Fig. 2.5M, N, O, red and black dotted line). Quantitative PCR analysis further confirmed the lower expression levels of *Fgf8* (Fig. 2.6D), *Fgf3* (Fig. 2.6H), *Notch2* (Fig. 2.6L) and *Bmp4* (Fig. 2.6P) in the mutant BA and heart (only for *Bmp4*) biopsies at E10.5. No significant difference between wild type and heterozygote was detected. Collectively, these results suggest that the combination of the altered *FGF*, *BMP* and *Notch* signaling results in the hypoproliferative mesenchymal cells in the OT cushions and their delayed EMT.

Cardiac Vascular and Innervation Defects in Pitx2 Mutants

Unilateral ablation of *Pitx2* results in asymmetric remodeling of the BA system, which leads to randomized laterality of the aortic arch (Yashiro et al., 2007). We investigated the aortic arch system defects, found in the Pitx2 mutants at the cellular level, by whole mount antibody staining with platelet-endothelial cell adhesion molecule (PECAM) at E10.5 (Fig. 2.7A, B, D, E). Endothelial cells were detected in the well-developed 3rd and 4th BAs and, to a lesser extent, in the 6th BA (Fig. 2.7A). An increased number of endothelial cells were extending into the OT and RV in wild type mice (Fig. 2.7A, D). In contrast, endothelial cells were severely reduced in mutant BAs (Fig. 2.7B) and OT (Fig. 2.7E). A similar phenotype was also observed at E11.5 (data not shown). Quantitative PCR further confirmed the reduced PECAM level of expression in mutant BA

(Fig. 2.7C) and heart biopsies (Fig. 2.7F). The BA innervation process was also affected in Pitx2-null mutant mice as detected by whole mount neurofilament (NF) antibody staining (Fig. 2.7G, H, J, K). The maxillary (V2) (Fig. 2.7G, H, red dotted line) and mandibular (V3) (Fig. 2.7G, H, star) branch of the trigeminal nerve (V) that innervates mastication muscles was not prominent in the mutants. Pitx2 mutants do not form mastication muscles (Shih et al., 2007b); and, thus, V2 and V3 were unable to migrate to their final destinations, as the supportive tissue was missing. The facial nerve (VII) that innervates the facial muscles and receives the sense from the anterior tongue was distorted. It failed to reach the edge of the 2nd BA (Fig. 2.7G, H). The sensory acoustic nerve (VIII) that migrates parallel to VII had a similar phenotype (Fig. 2.7G, H). The glossopharyngeal nerve (IX) provides special innervation to the stylopharyngeus. The vagus nerve (X) provides brachiomotor innervation to the majority of laryngeal and pharyngeal muscles and has three nuclei associated with the cardiovascular control the dorsal motor nucleus, the nucleus ambiguous, and the solitary nucleus. The afferent fibers of the autonomic nervous system transmit signals to the medulla by cranial nerves X and IX. Both IX and X nerves, located in the jugular area, were thinner, shorter, and not properly aligned in mutants, possibly as a result of the severe distortion or absence of several facial muscles (Fig. 2.7G, H). The X nerve innervates the OT to sense the aortic blood pressure and to slow the heart rate (Fig. 2.7G, arrow). NF expression was detected in the wild type (Fig. 2.7J) heart but in much lower levels than in mutants (Fig. 2.7K). This signal reduction may explain the observed arrhythmias and conduction deficiencies in Pitx2-mutant mice and human patients (Schnabel, 2011). Quantitative analyses for NF (Fig. 2.7I, L) were also performed in BAs (Fig. 2.7I) and heart (Fig. 2.7L) biopsies, indicating significant reduction of NF in mutants.

DISCUSSION

Homeobox genes are key players for cell specification and organ formation as members of network kernels at early developmental stages. Pitx2 specifies tooth, pituitary, (Gage et al., 1999b; Kitamura et al., 1999; Lin et al., 1999; Lu et al., 1999; Shih et al., 2007c), facial (ocular and mastication) (Gage et al., 2005; Shih et al., 2007b) and abdominal (Hilton et al., 2010) muscle development, while regulating the developmental process of organs including heart , intestine and lung (Gage et al., 1999b; Kitamura et al., 1999; Lin et al., 1999; Lu et al., 1999; Shih et al., 2007c). The human Axenfeld-Rieger syndrome associated with mutations in *PITX2* locus 4q25 is characterized by umbilical hernia, glaucoma, myopathies and cardiac arrhythmias (Perveen et al., 2000; Schnabel, 2011). The close correlation of mouse phenotypes to the human syndrome demonstrates the evolutionarily conserved functions of Pitx2. Pitx2 loss of function results in severe cardiovascular defects, including atrial isomerism, DORV, TGA, PTA and abnormal aortic arch remodeling (Campione et al., 2001; Gage et al., 1999b; Kitamura et al., 1999; Lin et al., 1999; Liu et al., 2002; Lu et al., 1999). Genetic studies have shown that Pitx2-mediated signaling during cardiogenesis is conducted within BA mesoderm cells (Ai et al., 2006), pharyngeal arch mesenchyme (Franco and Campione, 2003) and cNC cells (Hamblet et al., 2002; Kioussi et al., 2002). Our data show that *Pitx2* is a member of a network kernel, including *Mef2c*, *Isl1*, *Tbx1*, *Gata4* and *Nkx2.5*, that synergistically regulates endocardial cushion development and separation of the great arteries. We have demonstrated that Pitx2 occupies *cis* regulatory elements of *Mef2c*, *Isl1* and *Tbx1* (Harel I, 2012) in BA mesoderm.

Conotruncal defects, including TGA, DORV, tetralogy of Fallot, and PTA, result in abnormal OT development, including hypocellular cushions, altered conotruncal rotation, and misalignment of septal components. Endocardial cushion formation starts with a swelling of the OT region at E9.5 and their

formation is induced by signals from the myocardium that inhibit expression of chamber-specific genes and the active expression of extracellular matrix genes. BMPs are the major myocardial signals that initiate endocardial cushion formation and remodeling by promoting EMT (Lyons et al., 1990; Ma et al., 2005). Bmp4 is required for endocardial cushion expansion and OT septation (McCulley et al., 2008). Loss of Bmp4 in the second cardiac lineage results in a limited number of cells in the developing OT cushions and a defective remodeling process, a very similar phenotype to the one observed in the *Pitx2*-mutant mice. BMP signaling in the endocardium and cNC cells is vital to OT septation and formation of the aorta and pulmonary arteries.

TGFßs are among the early signaling molecules implicated in endocardial cushion development. TGFß ligands and receptors are expressed in the OT during cushion formation and EMT (Brown et al., 1996). TGFß signaling acts through SMADs to induce expression of the SSTF Slug that, in turn, promotes endocardial cushion formation of the antrioventricular canal (AVC) via EMT mechanisms (Romano and Runyan, 2000). Wnt/ß-catenin regulates cardiac valve formation (Hurlstone et al., 2003) and, together with TGFß, regulates cushion EMT. Notch signaling induces the expression of the pro-migratory SSTF Snail in AVC and OT endocardial cushion endothelial cells undergoing EMT. Snail inhibits VE-cadherin activity, and mesenchymal cells break contact with their neighboring cells. Notch signaling is also required for TGFß2 and several TGFß receptors in AVC and OT to further support endocardial EMT.

Fgf10, a target of the Wnt-ß-catenin pathway in the cardiac mesoderm, is expressed in the second cardiac lineage (Kelly et al., 2001). However, Fgf10-null mice do not exhibit apparent cardiac defects. Fgf8 is also expressed in the second cardiac lineage and, when mutated, results to DORV and PTA (Abu-Issa et al., 2002; Frank et al., 2002). Fgf8 is essential for mesoderm-derived cell proliferation and survival during OT elongation.

Reduced expression of Fgf8 in mesoderm- and ectoderm-derived cells, resulting in apoptotic cNC cell death in the developing pharyngeal arches (Ilagan et al., 2006).

Cardiac NC cells migrate into the OT endocardial cushions and contribute to the formation of aortic and pulmonary valves. Ablation of cNC cells results in OF defects, including shortening in length, delayed rotation and caudal displacement, dextroposed aorta (DORV), PTA, and interruption of the aortic arch. The shorter OT is also characterized by decreased second cardiac lineage cell migration (Waldo et al., 2005). This reciprocal interaction between the two cell lineages is essential for the OT septation.

Pitx2 acts upstream of the Wnt11/TGFß2 signaling pathway that regulates extracellular matrix composition, cytoskeletal rearrangements and polarized cell movement required for tissue morphogenesis (Zhou et al., 2007). *BMP* and *Notch* expression was Pitx2-dependet in the OT of the linear heart tube in areas where cushions will be formed (Fig. 2.6I-K, M-O). This further supports the involvement of Pitx2 in a multi-signaling network during cushion formation and EMT induction and maintenance. *Pitx2*-mutant mice also exhibit remodeling malformations of intraventricular septum and ventricular myocardium (Tessari et al., 2008). The formation of AVC and the ventricular septation is another type of cell fusion that requires EMT.

Thus, we conclude that Pitx2 regulates the maintenance and epithelial-mesenchymal transitions of the BA mesoderm cells as they enter the linear heart tube to form the OT endocardial cushions. Pitx2 promotes the healthy interaction of the mesoderm-derived and cNC cells for proper OT septation by acting as a node of a sophisticated network kernel.

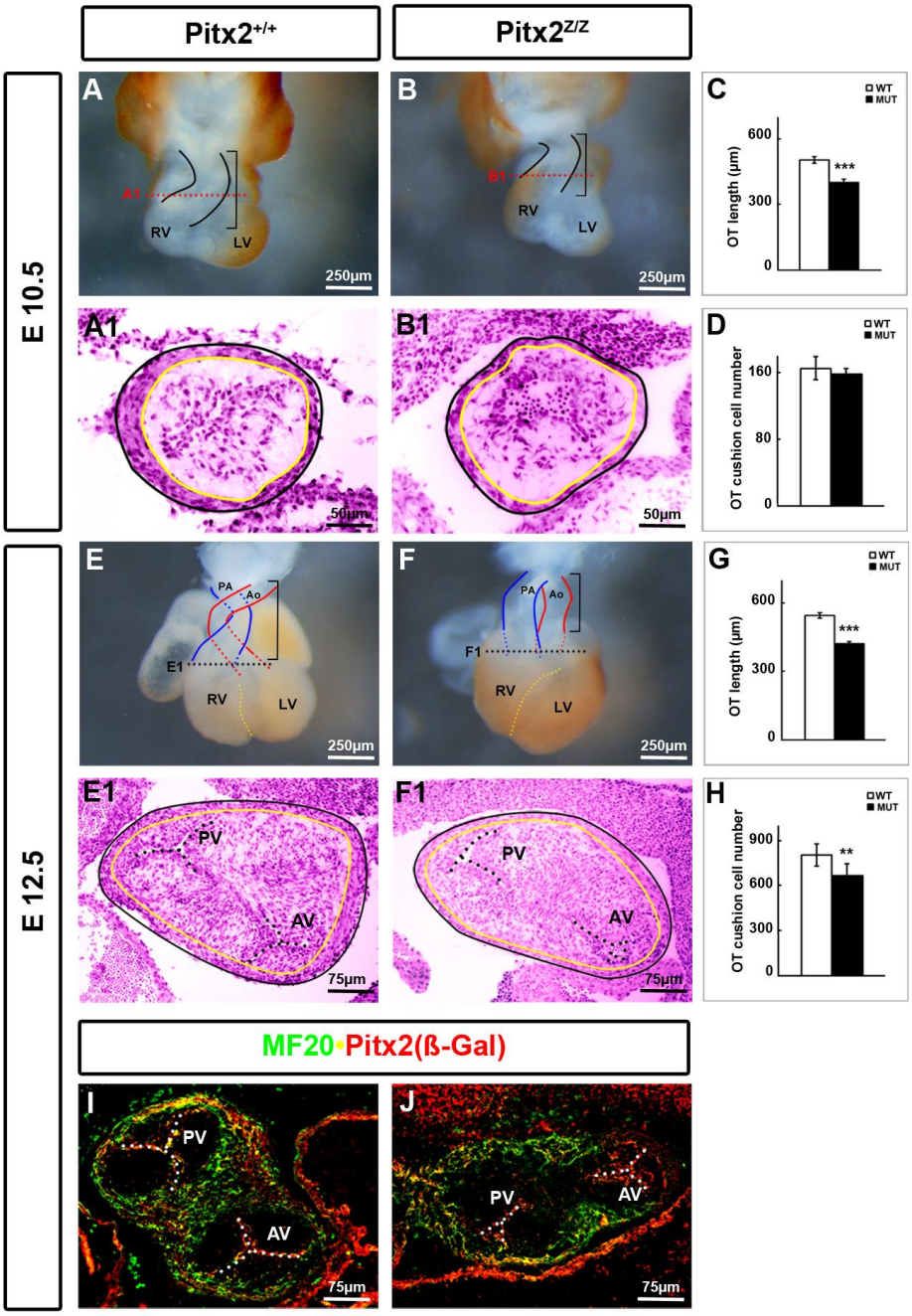
Pitx2+/+
Pitx2Z/Z
E 10.5
E 12.5
A
B
C
A1
B1
D
E
F
G
E1
F1
H
I
J
RV
LV
PA
Ao
PV
AV
A1
B1
E1
F1
250µm
50µm
75µm
WT
MUT
OT length (µm)
OT cushion cell number
600
300
0
160
80
900
***
**
MF20•Pitx2(ß-Gal)

Figure 2.1

Figure 2.1 Shorter and hypocellular cardiac OT in *Pitx2* mutants . Ventral view of the entire heart at E10.5 **(A, B)** and E12.5 **(E, F)** showed a shortened OT with a prominent DORV in *Pitx2*-mutant mice **(F)**. **(C, G)** The length of the OT was measured as indicated by brackets. Statistics were based on results from 3 different embryos at each stage. HE staining on 14 µm transverse cryosections at E10.5 **(A1, B1**) and E 12.5 **(E1, F1)** mice indicated thinner OT epithelium in the conus. The black and yellow lines correspond to the outer and inner epithelium, respectively. **(D, H)** Cell counts of a set of 5-8 serial sections along the OT showed reduction of cells in the cushions of mutants. ***: $p<0.01$, **: $p<0.05$. **(I, J)** Double labeling immunohistochemistry on E12.5 mouse transverse sections for MF20 and Pitx2 (ß-Gal). No $MF20^{+}$ cells were detected in the conal septum and semilunar valves in the mutants. Ao, aorta; AV, aortic valve; LV, left ventricle; PA, pulmonary artery; PV, pulmonary valve; RV, right ventricle.

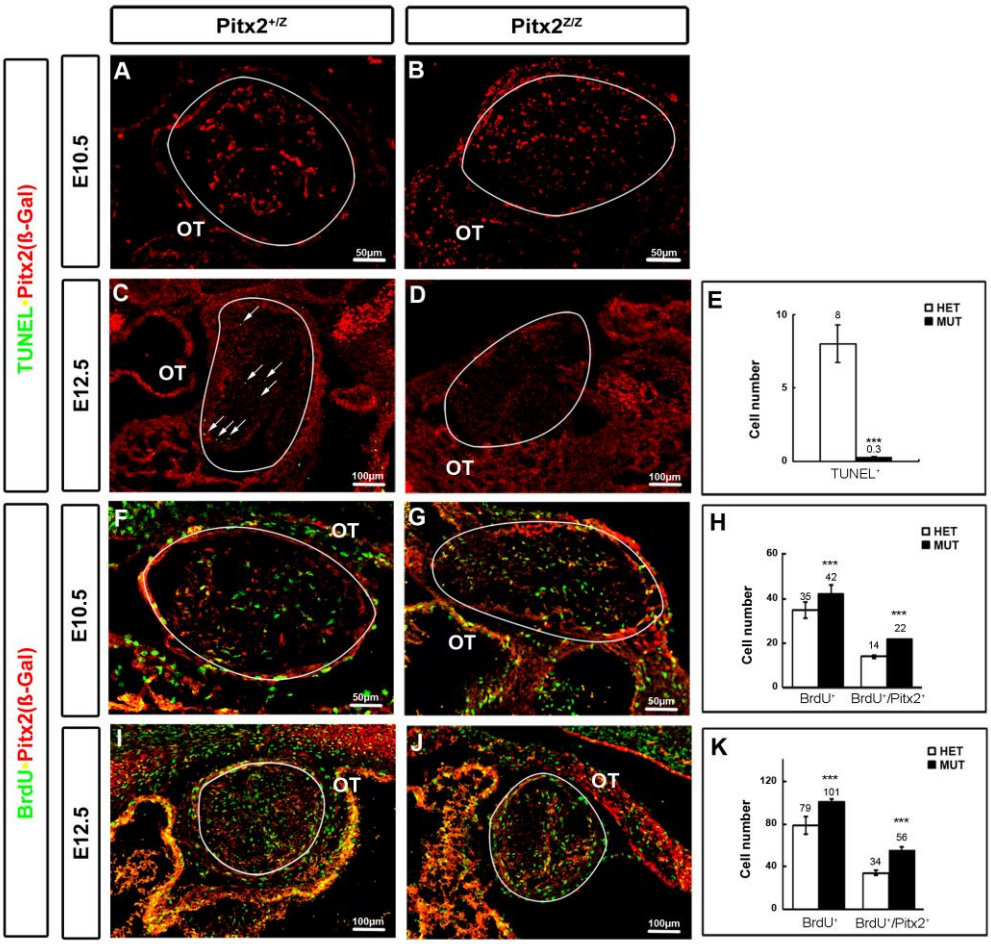
Pitx2+/Z
Pitx2Z/Z
TUNEL/Pitx2(ß-Gal)
BrdU/Pitx2(ß-Gal)
E10.5
E12.5
A
B
C
D
E
F
G
H
I
J
K
OT
50µm
100µm
HET
MUT
Cell number
TUNEL+
BrdU+
BrdU+/Pitx2+
***
8
0.3
35
42
14
22
79
101
34
56

Figure 2.2

Figure 2.2 OT Cushion mesenchymal cell proliferation and apoptosis defects in *Pitx2* mutants. (A-D) TUNEL assay was performed on 14 µm frontal sections to identify the cell apoptosis index during OT remodeling. **(A, B)**TUNEL signal was not detected at E10.5 in either OT mesenchyme of the heterozygote or in mutant littermates. The TUNEL signal was detected in heterozygote OT cushion mesenchyme (**C**, white arrows) but not in mutant littermate **(D)** at E12.5. **(E)** The number of apoptotic cells in the OT cushion was counted based on eight continuous sections for three individual embryos at E12.5. **(F, G, I, J)** Double labeling of ß-gal and Bromodeoxyuridine (BrdU) on 14 µm frontal sections showed Pitx2 effects on cell proliferation. The number of proliferative cells was increased in *Pitx2* mutants at E10.5 and E12.5, respectively **(H, K)**. The $BrdU^+$ and $BrdU^+/Pitx2^+$ cells were counted based on five continuous sections for three individual embryos in each stage. The OT cushion was traced by a white line. Statistics were based on results from 3 different embryos at each stage. ***: $p<0.01$.

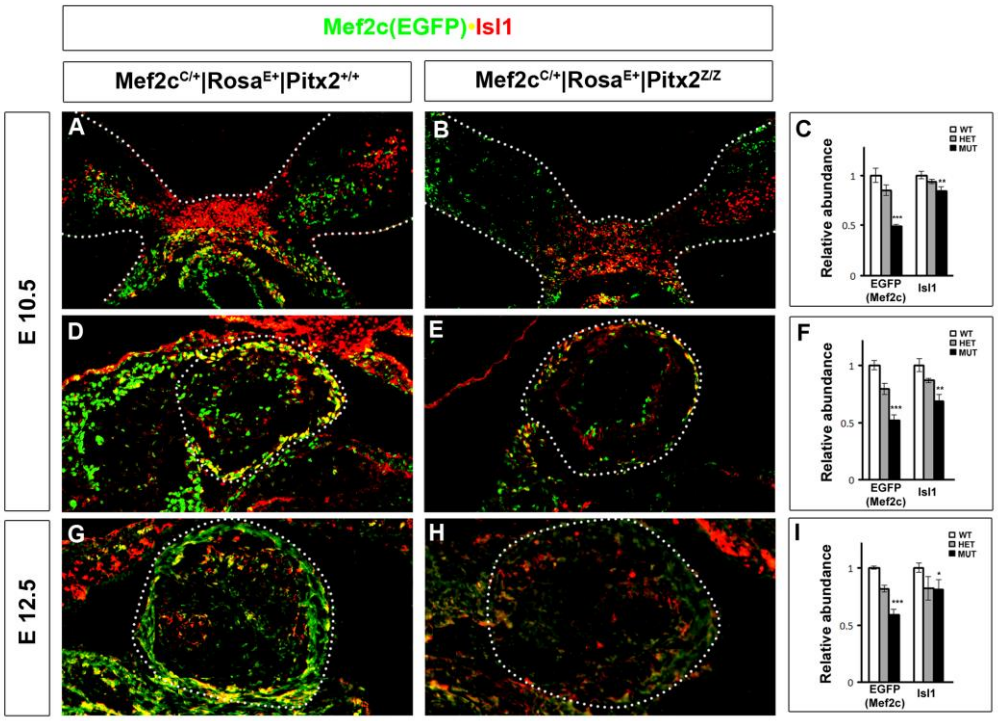

Figure 2.3

Figure 2.3 Defects of the second cardiac cell lineage in *Pitx2* mutants. Double labeling immunohistochemistry of transverse cryosections sections of *Mef2c*$^{Cre/+}$ | *Rosa*$^{EGFP/+}$ | *Pitx2*$^{+/+}$ **(A, D, G)** and *Mef2c*$^{Cre/+}$ | *Rosa*$^{EGFP/+}$ | *Pitx2*$^{Z/Z}$ **(B, E, H)** for EGFP (Mef2c) and Isl1 indicated reduction of cell populations in the mutant BA **(B)** at E10.5 and OT at E10.5 **(E)** and E12.5 **(H)**. **(G, F, I)** Quantitative analysis by qPCR for *EGFP* and *Isl1* indicated reduced levels in E10.5 BA (C) and OT (F, I). ***: p<0.01; **: p<0.05; *: p<0.1.

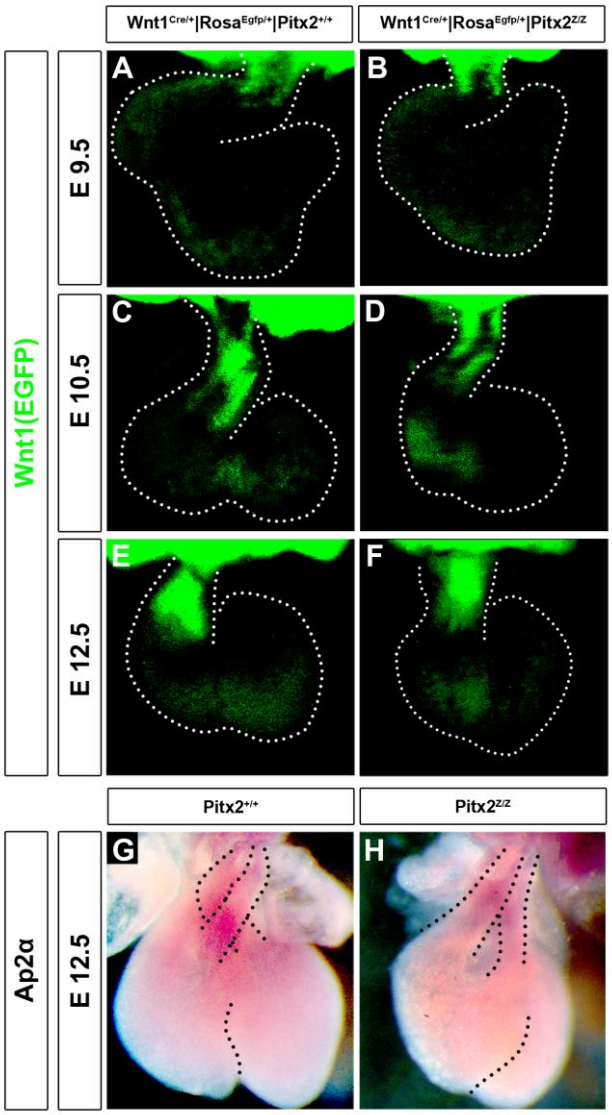

Figure 2.4

Figure 2.4 Impaired cNC cells in Pitx2 mutants. Wnt1$^{Cre/+}$|Rosa^{EGFP}|Pitx2$^{+/+}$ **(A, C, E)** and Wnt1$^{Cre/+}$|Rosa^{EGFP}|Pitx2$^{Z/Z}$ **(B, D, F)** hearts were dissected at E 9.5 **(A, B),** E 10.5 **(C, D)** and E 12.5 **(E, F)**. The green fluorescent cNC cells that migrated towards the OT were reduced in mutants, with more prominent phenotype at E9.5 and E10.5. **(G, H)** Whole mount RNA in situ hybridization at E12.5 hearts for Ap2α expression in OT indicated reduced levels in the great arteries in mutants.

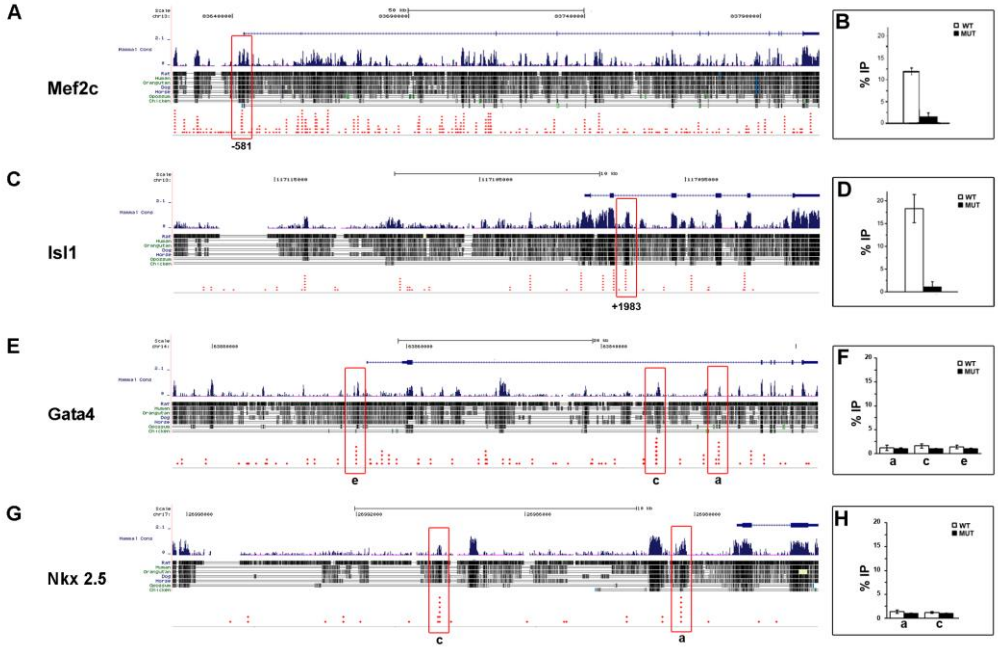

Figure 2.5

Figure 2.5 Pitx2 occupancy on SSTF gene loci in BA and heart chromatin. Sonically sheared chromatin, isolated from E10.5 mice, was used to detect Pitx2 protein occupancy on *Mef2c* **(A)** and *Isl1* **(B)** in BA biopsies and *Gata4* **(E)** and *Nkx2.5* **(G)** in heart biopsies. PCR amplicons of 70-150bp (red boxes) were designed around highly evolutionarily conserved bicoid core motif TAATCY. Each red diamond indicated a single vertebrate species, containing the biocoid core motif. Bar graphs show the average relative amount of signal precipitated from wild type (white bar) and mutant (black bar). Pitx2 was found to occupy the *Mef2c* and *Isl1* gene on the conserved -521 **(B)** and +1983 **(D)** sites in E10.5 embryonic BA biopsies, respectively. No significant difference was measured for Pitx2 occupancy in conserved regions of Gata4 **(F)** and Nkx2.5 **(H)** in E10.5 heart biopsies.

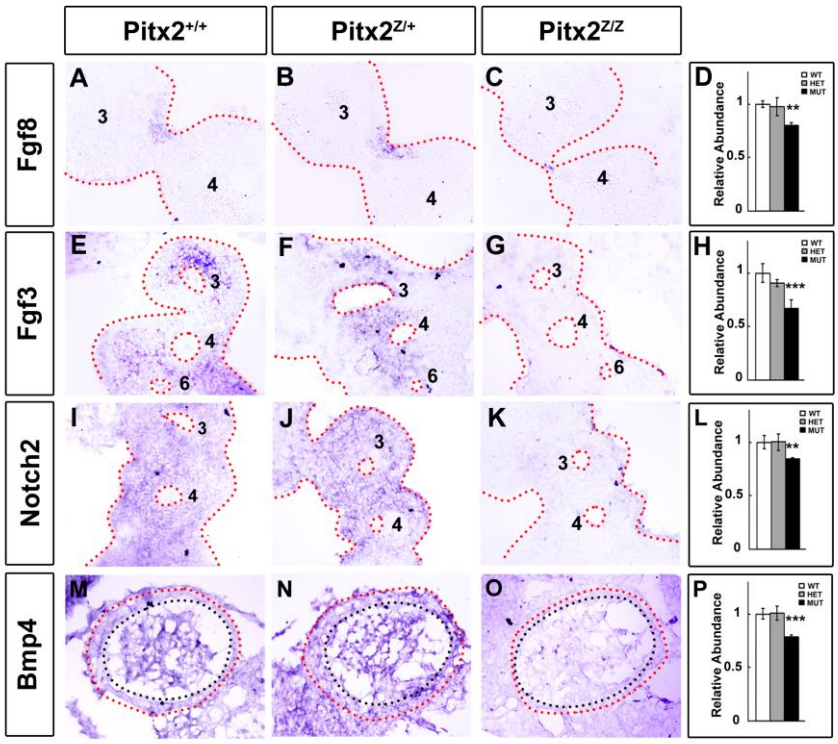

Figure 2.6

Figure 2.6 Alteration of FGF, BMP and Notch signaling in *Pitx2* mutants. RNA in situ hybridization on cryostat sections revealed altered *Fgf8* **(A-C)**, *Fgf3* **(E-G)**, *Notch2* **(I-K)** and *Bmp4* **(M-O)** expression in E10.5 *Pitx2* control (wild type and heterozygote) and mutant mice. **(C)** The *Fgf8* expression in 3rd and 4th BA ectoderm was decreased in mutants compared to control embryos. **(G)** *Fgf3* expression levels were reduced in the 2nd - 6th BA mutants. *Notch2* expression levels, detected in the 3rd and 4th BA in wild type **(I)** and heterozygote **(J)**, were barely detectable in 3rd and 4th BA in mutants **(K)**. No *Bmp4* expression was detected in the OT mesenchymal cushions (area inside the black dotted line) in mutants **(O)** compare to the control **(M, N)**. Thinner OT wall (between red and black dotted line) was consistently observed in Pitx2 mutants **(O)**. Quantitative PCR assay indicated the significantly decreased mRNA expression levels of *Fgf8* **(D)**, *Fgf3* **(H)**, *Notch2* **(L)** and *Bmp4* **(P)** at E10.5 BA **(D, H, L)** and heart **(P)** biopsies, respectively.

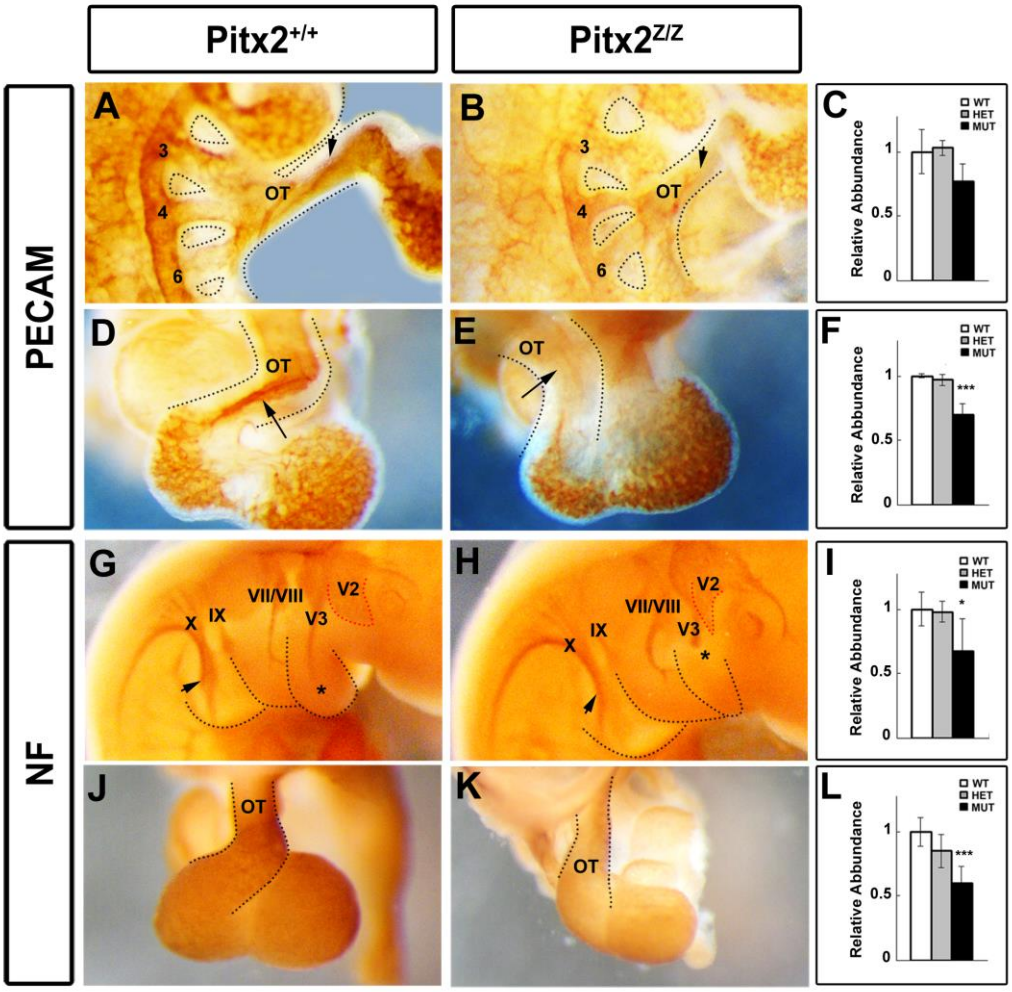
Pitx2+/+
Pitx2Z/Z
PECAM
NF
A
B
C
D
E
F
G
H
I
J
K
L
3
4
6
OT
V2
VII/VIII
V3
X
IX
*
WT
HET
MUT
Relative Abbundance
1
0.5
0
***

Figure 2.7

Figure 2.7 Vascular and nervous system defects in *Pitx2* mutants. Whole mount antibody staining with PECAM **(A, B, D, E)** and NF **(G, H, J, K)** was performed on E10.5 *Pitx2* wild type and mutant mice. **(A**, **B)** PECAM expression is reduced in BA (3, 4 and 6) and OT (arrowhead). **(D, E)** The dorsal view of the OT indicated the septational vasculature (arrow) was disrupted in Pitx2-null mice. **(C, F)** Quantitative qPCR for PECAM mRNA levels in *Pitx2* wild type, heterozygote and mutant in BAs **(C)** and heart **(F)** biopsies. The expression levels of PECAM in heart were significantly decreased in E10.5 mutants. Innervation of BAs and OT was detected by NF antibody in both control and mutant embryos **(G, H, J, K)**. V2 (red dotted line) and V3 (stars) and X (arrow head) were shorter and thinner in mutants (H). NF signals were reduced in mutant hearts **(K)**. Quantitative qPCR assay indicated significantly decreased levels in mutants in BA **(I)** and OT **(L)** biopsies, with no difference between wild type and heterozygote at this stage. V2: maxillary nerve; V3: Mandibular nerve; VII/VIII: Facial nerve; IX: Glossopharyngeal nerve; X: Vagus nerve.

Primer	Forward	Reverse
qPCR		
EGFP	ACGTAAACGGCCACAAGTTC	AAGTCGTGCTGCTTCATGTG
Isl1	ATGATGGTGGTTTACAGGCTAAC	TCGATGCTACTTCACTGCCAG
Fgf8	CCGAGGAGGGATCTAAGGAAC	CTTCCAAAAGTATCGGTCTCCAC
Fgf3	TGCGCTACCAAGTACCACC	CACTTCCACCGCAGTAATCTC
Notch2	ATGTGGACGAGTGTCTGTTGC	GGAAGCATAGGCACAGTCATC
Bmp4	TTCCTGGTAACCGAATGCTGA	CCTGAATCTCGGCGACTTTTT
PECAM	ACGCTGGTGCTCTATGCAAG	TCAGTTGCTGCCCATTCATCA
NF	ACAGCTCGGCTATGCTCAG	CGGGACAGTTTGTAGTCGCC
GAPDH	AGGTCGGTGTGAACGGATTTG	TGTAGACCATGTAGTTGAGGTCA
ChIP-qPCR		
Isl1	TTGGGGTGACTCTTCCTTTG	GATGGGCAATTTGATCTGCT
Mef2c	CCATGACCATCCAGTTTTGA	GCACACACTTGCTTCATTTCA
Nkx2.5a	GGGCGAGGGTCCTGGGAGTC	CGGCCCCCAATATAGCTCCCC
Nkx2.5c	ACTGACACACACTGCAGGGGC	GTGGGTGGTCCTCTCTCAGCAGT
Gata4a	TGTCCAACAATGGCTGTGGAGTGC	TCCCTAGTTCCTCTGTCCCTTGCC
Gata4c	AAGCCCCCATCCCCTGCACTT	ACTGGACAGAACCTTGCCTGCTCA
Gata4e	TTCTCTCCCCGGCACCGGTTT	GTCCTCGAACTGCGGGAGCC

Table 2.1

REFERENCES

Abu-Issa, R., Smyth, G., Smoak, I., Yamamura, K., and Meyers, E.N. (2002). Fgf8 is required for pharyngeal arch and cardiovascular development in the mouse. Development *129*, 4613-4625.

Ai, D., Liu, W., Ma, L., Dong, F., Lu, M.F., Wang, D., Verzi, M.P., Cai, C., Gage, P.J., Evans, S.*, et al.* (2006). Pitx2 regulates cardiac left-right asymmetry by patterning second cardiac lineage-derived myocardium. Dev Biol *296*, 437-449.

Amendt, B.A., Sutherland, L.B., Semina, E.V., and Russo, A.F. (1998). The molecular basis of Rieger syndrome. Analysis of Pitx2 homeodomain protein activities. The Journal of biological chemistry *273*, 20066-20072.

Arima, Y., Miyagawa-Tomita, S., Maeda, K., Asai, R., Seya, D., Minoux, M., Rijli, F.M., Nishiyama, K., Kim, K.S., Uchijima, Y.*, et al.* (2012). Preotic neural crest cells contribute to coronary artery smooth muscle involving endothelin signalling. Nature communications *3*, 1267.

Brown, C.B., Boyer, A.S., Runyan, R.B., and Barnett, J.V. (1996). Antibodies to the Type II TGFbeta receptor block cell activation and migration during atrioventricular cushion transformation in the heart. Dev Biol *174*, 248-257.

Buckingham, M., Meilhac, S., and Zaffran, S. (2005). Building the mammalian heart from two sources of myocardial cells. Nature reviews Genetics *6*, 826-835.

Cai, C.L., Liang, X., Shi, Y., Chu, P.H., Pfaff, S.L., Chen, J., and Evans, S. (2003). Isl1 identifies a cardiac progenitor population that proliferates prior to differentiation and contributes a majority of cells to the heart. Developmental cell *5*, 877-889.

Campbell, A.L., Eng, D., Gross, M.K., and Kioussi, C. (2012). Prediction of gene network models in limb muscle precursors. Gene *509*, 16-23.

Campione, M., Ros, M.A., Icardo, J.M., Piedra, E., Christoffels, V.M., Schweickert, A., Blum, M., Franco, D., and Moorman, A.F. (2001). Pitx2 expression defines a left cardiac lineage of cells: evidence for atrial and ventricular molecular isomerism in the iv/iv mice. Developmental biology *231*, 252-264.

Dodou, E., Verzi, M.P., Anderson, J.P., Xu, S.M., and Black, B.L. (2004). Mef2c is a direct transcriptional target of ISL1 and GATA factors in the anterior heart field during mouse embryonic development. Development *131*, 3931-3942.

Echelard, Y., Vassileva, G., and McMahon, A.P. (1994). Cis-acting regulatory sequences governing Wnt-1 expression in the developing mouse CNS. Development *120*, 2213-2224.

Eng, D., Campbell, A., Hilton, T., Leid, M., Gross, M.K., and Kioussi, C. (2010). Prediction of regulatory networks in mouse abdominal wall. Gene *469*, 1-8.

Eng, D., and Dubovoy, A. (2012). High Left Ventricular Vent Return After Left and Right Ventricular Assist Device Placement in a Patient With a Mechanical Aortic Valve. J Cardiothorac Vasc Anesth.

Eng, D., Ma, H.Y., Xu, J., Shih, H.P., Gross, M.K., and Kiouss, C. (2012). Loss of abdominal muscle in Pitx2 mutants associated with altered axial specification of lateral plate mesoderm. PLoS One *7*, e42228.

Engleka, K.A., Manderfield, L.J., Brust, R.D., Li, L., Cohen, A., Dymecki, S.M., and Epstein, J.A. (2012). Islet1 derivatives in the heart are of both neural crest and second heart field origin. Circulation research *110*, 922-926.

Franco, D., and Campione, M. (2003). The role of Pitx2 during cardiac development. Linking left-right signaling and congenital heart diseases. Trends Cardiovasc Med *13*, 157-163.

Frank, D.U., Fotheringham, L.K., Brewer, J.A., Muglia, L.J., Tristani-Firouzi, M., Capecchi, M.R., and Moon, A.M. (2002). An Fgf8 mouse mutant phenocopies human 22q11 deletion syndrome. Development *129*, 4591-4603.

Gage, P.J., Rhoades, W., Prucka, S.K., and Hjalt, T. (2005). Fate maps of neural crest and mesoderm in the mammalian eye. Invest Ophthalmol Vis Sci *46*, 4200-4208.

Gage, P.J., Suh, H., and Camper, S.A. (1999). Dosage requirement of Pitx2 for development of multiple organs. Development *126*, 4643-4651.

Galli, D., Dominguez, J.N., Zaffran, S., Munk, A., Brown, N.A., and Buckingham, M.E. (2008). Atrial myocardium derives from the posterior region of the second heart field, which acquires left-right identity as Pitx2c is expressed. Development *135*, 1157-1167.

Ganga, M., Espinoza, H.M., Cox, C.J., Morton, L., Hjalt, T.A., Lee, Y., and Amendt, B.A. (2003). PITX2 isoform-specific regulation of atrial natriuretic factor expression: synergism and repression with Nkx2.5. J Biol Chem *278*, 22437-22445.

Hamblet, N.S., Lijam, N., Ruiz-Lozano, P., Wang, J., Yang, Y., Luo, Z., Mei, L., Chien, K.R., Sussman, D.J., and Wynshaw-Boris, A. (2002). Dishevelled 2 is essential for cardiac outflow tract development, somite segmentation and neural tube closure. Development *129*, 5827-5838.

Harel I, M.Y., Avraham R, Rinon A, Ma HY, Cross J.W, Leviatan N, Hegesh J. T, Roy A, Jacob-Hirsch J, Rechavi G, Carvajal J, Tole S, Kioussi C, Quaggin S, and Tzahor E (2012). Pharyngeal mesoderm regulatory network controls cardiac and head muscle morphogenesis. Proceedings of the National Academy of Sciences. PNAS *in press*.

Harvey, R.P. (2002). Patterning the vertebrate heart. Nat Rev Genet *3*, 544-556.

Hilton, T., Gross, M.K., and Kioussi, C. (2010). Pitx2-dependent occupancy by histone deacetylases is associated with T-box gene regulation in mammalian abdominal tissue. J Biol Chem *285*, 11129-11142.

Hoffman, J.I., and Kaplan, S. (2002). The incidence of congenital heart disease. J Am Coll Cardiol *39*, 1890-1900.

Hu, T., Yamagishi, H., Maeda, J., McAnally, J., Yamagishi, C., and Srivastava, D. (2004). Tbx1 regulates fibroblast growth factors in the anterior heart field through a reinforcing autoregulatory loop involving forkhead transcription factors. Development *131*, 5491-5502.

Hurlstone, A.F., Haramis, A.P., Wienholds, E., Begthel, H., Korving, J., Van Eeden, F., Cuppen, E., Zivkovic, D., Plasterk, R.H., and Clevers, H. (2003). The Wnt/beta-catenin pathway regulates cardiac valve formation. Nature *425*, 633-637.

Ilagan, R., Abu-Issa, R., Brown, D., Yang, Y.P., Jiao, K., Schwartz, R.J., Klingensmith, J., and Meyers, E.N. (2006). Fgf8 is required for anterior heart field development. Development *133*, 2435-2445.

Joyner, A., and Wall, N. (2008). Immunohistochemistry of whole-mount mouse embryos. CSH Protoc *2008*, pdb prot4820.

Kelly, R.G., Brown, N.A., and Buckingham, M.E. (2001). The arterial pole of the mouse heart forms from Fgf10-expressing cells in pharyngeal mesoderm. Dev Cell *1*, 435-440.

Kelly, R.G., and Papaioannou, V.E. (2007). Visualization of outflow tract development in the absence of Tbx1 using an FgF10 enhancer trap transgene. Dev Dyn *236*, 821-828.

Kioussi, C., Briata, P., Baek, S.H., Rose, D.W., Hamblet, N.S., Herman, T., Ohgi, K.A., Lin, C., Gleiberman, A., Wang, J.*, et al.* (2002). Identification of a Wnt/Dvl/beta-Catenin --> Pitx2 pathway mediating cell-type-specific proliferation during development. Cell *111*, 673-685.

Kirby, M. (2007). Cardiac Development (Oxford University Press, New York).

Kitamura, K., Miura, H., Miyagawa-Tomita, S., Yanazawa, M., Katoh-Fukui, Y., Suzuki, R., Ohuchi, H., Suehiro, A., Motegi, Y., Nakahara, Y.*, et al.* (1999). Mouse Pitx2 deficiency leads to anomalies of the ventral body wall, heart, extra- and periocular mesoderm and right pulmonary isomerism. Development *126*, 5749-5758.

Kyrylkova, K., Kyryachenko, S., Kioussi, C., and Leid, M. (2012). Determination of gene expression patterns by in situ hybridization in sections. Methods Mol Biol *887*, 23-31.

Lin, C.R., Kioussi, C., O'Connell, S., Briata, P., Szeto, D., Liu, F., Izpisua-Belmonte, J.C., and Rosenfeld, M.G. (1999). Pitx2 regulates lung asymmetry, cardiac positioning and pituitary and tooth morphogenesis. Nature *401*, 279-282.

Lin, Q., Schwarz, J., Bucana, C., and Olson, E.N. (1997). Control of mouse cardiac morphogenesis and myogenesis by transcription factor MEF2C. Science *276*, 1404-1407.

Liu, C., Liu, W., Palie, J., Lu, M.F., Brown, N.A., and Martin, J.F. (2002). Pitx2c patterns anterior myocardium and aortic arch vessels and is required for local cell movement into atrioventricular cushions. Development *129*, 5081-5091.

Liu, W., Selever, J., Lu, M.F., and Martin, J.F. (2003). Genetic dissection of Pitx2 in craniofacial development uncovers new functions in branchial arch morphogenesis, late aspects of tooth morphogenesis and cell migration. Development *130*, 6375-6385.

Liu, W., Selever, J., Wang, D., Lu, M.F., Moses, K.A., Schwartz, R.J., and Martin, J.F. (2004). Bmp4 signaling is required for outflow-tract septation and branchial-arch artery remodeling. Proc Natl Acad Sci U S A *101*, 4489-4494.

Lozano-Velasco, E., Chinchilla, A., Martinez-Fernandez, S., Hernandez-Torres, F., Navarro, F., Lyons, G.E., Franco, D., and Aranega, A.E. (2011). Pitx2c modulates cardiac-specific transcription factors networks in differentiating cardiomyocytes from murine embryonic stem cells. Cells, tissues, organs *194*, 349-362.

Lu, M.F., Pressman, C., Dyer, R., Johnson, R.L., and Martin, J.F. (1999). Function of Rieger syndrome gene in left-right asymmetry and craniofacial development. Nature *401*, 276-278.

Lyons, K.M., Pelton, R.W., and Hogan, B.L. (1990). Organogenesis and pattern formation in the mouse: RNA distribution patterns suggest a role for bone morphogenetic protein-2A (BMP-2A). Development *109*, 833-844.

Ma, L., Lu, M.F., Schwartz, R.J., and Martin, J.F. (2005). Bmp2 is essential for cardiac cushion epithelial-mesenchymal transition and myocardial patterning. Development *132*, 5601-5611.

Mao, X., Fujiwara, Y., Chapdelaine, A., Yang, H., and Orkin, S.H. (2001). Activation of EGFP expression by Cre-mediated excision in a new ROSA26 reporter mouse strain. Blood *97*, 324-326.

McCulley, D.J., Kang, J.O., Martin, J.F., and Black, B.L. (2008). BMP4 is required in the anterior heart field and its derivatives for endocardial cushion remodeling, outflow tract septation, and semilunar valve development. Dev Dyn *237*, 3200-3209.

Monzen, K., Shiojima, I., Hiroi, Y., Kudoh, S., Oka, T., Takimoto, E., Hayashi, D., Hosoda, T., Habara-Ohkubo, A., Nakaoka, T.*, et al.* (1999). Bone morphogenetic proteins induce cardiomyocyte differentiation through the mitogen-activated protein kinase kinase kinase TAK1 and cardiac transcription factors Csx/Nkx-2.5 and GATA-4. Mol Cell Biol *19*, 7096-7105.

Niessen, K., and Karsan, A. (2008). Notch signaling in cardiac development. Circ Res *102*, 1169-1181.

Nowotschin, S., Liao, J., Gage, P.J., Epstein, J.A., Campione, M., and Morrow, B.E. (2006). Tbx1 affects asymmetric cardiac morphogenesis by regulating Pitx2 in the secondary heart field. Development *133*, 1565-1573.

Oliver, G., Wehr, R., Jenkins, N.A., Copeland, N.G., Cheyette, B.N., Hartenstein, V., Zipursky, S.L., and Gruss, P. (1995). Homeobox genes and connective tissue patterning. Development *121*, 693-705.

Park, E.J., Watanabe, Y., Smyth, G., Miyagawa-Tomita, S., Meyers, E., Klingensmith, J., Camenisch, T., Buckingham, M., and Moon, A.M. (2008). An FGF autocrine loop initiated in second heart field mesoderm regulates morphogenesis at the arterial pole of the heart. Development *135*, 3599-3610.

Perveen, R., Lloyd, I.C., Clayton-Smith, J., Churchill, A., van Heyningen, V., Hanson, I., Taylor, D., McKeown, C., Super, M., Kerr, B.*, et al.* (2000). Phenotypic variability and asymmetry of Rieger syndrome associated with PITX2 mutations. Invest Ophthalmol Vis Sci *41*, 2456-2460.

Ray, H.J., and Niswander, L. (2012). Mechanisms of tissue fusion during development. Development *139*, 1701-1711.

Romano, L.A., and Runyan, R.B. (2000). Slug is an essential target of TGFbeta2 signaling in the developing chicken heart. Dev Biol *223*, 91-102.

Schnabel, R.B. (2011). Comparison of approaches to fine-map first-generation genome-wide association study results at chromosome 9p21. Circ Cardiovasc Genet *4*, 577-578.

Shih, H.P., Gross, M.K., and Kioussi, C. (2007a). Cranial muscle defects of Pitx2 mutants result from specification defects in the first branchial arch. Proc Natl Acad Sci U S A *104*, 5907-5912.

Shih, H.P., Gross, M.K., and Kioussi, C. (2007b). Expression pattern of the homeodomain transcription factor Pitx2 during muscle development. Gene expression patterns : GEP *7*, 441-451.

Tessari, A., Pietrobon, M., Notte, A., Cifelli, G., Gage, P.J., Schneider, M.D., Lembo, G., and Campione, M. (2008). Myocardial Pitx2 differentially regulates the left atrial identity and ventricular asymmetric remodeling programs. Circ Res *102*, 813-822.

Tirosh-Finkel, L., Elhanany, H., Rinon, A., and Tzahor, E. (2006). Mesoderm progenitor cells of common origin contribute to the head musculature and the cardiac outflow tract. Development *133*, 1943-1953.

Verzi, M.P., McCulley, D.J., De Val, S., Dodou, E., and Black, B.L. (2005). The right ventricle, outflow tract, and ventricular septum comprise a restricted expression domain within the secondary/anterior heart field. Dev Biol *287*, 134-145.

Vitelli, F., Morishima, M., Taddei, I., Lindsay, E.A., and Baldini, A. (2002). Tbx1 mutation causes multiple cardiovascular defects and disrupts neural crest and cranial nerve migratory pathways. Hum Mol Genet *11*, 915-922.

Waldo, K., Miyagawa-Tomita, S., Kumiski, D., and Kirby, M.L. (1998). Cardiac neural crest cells provide new insight into septation of the cardiac outflow tract: aortic sac to ventricular septal closure. Developmental biology *196*, 129-144.

Waldo, K.L., Hutson, M.R., Stadt, H.A., Zdanowicz, M., Zdanowicz, J., and Kirby, M.L. (2005). Cardiac neural crest is necessary for normal addition of the myocardium to the arterial pole from the secondary heart field. Dev Biol *281*, 66-77.

Waldo, K.L., Lo, C.W., and Kirby, M.L. (1999). Connexin 43 expression reflects neural crest patterns during cardiovascular development. Dev Biol *208*, 307-323.

Webb, S., Qayyum, S.R., Anderson, R.H., Lamers, W.H., and Richardson, M.K. (2003). Septation and separation within the outflow tract of the developing heart. J Anat *202*, 327-342.

Xu, H., Morishima, M., Wylie, J.N., Schwartz, R.J., Bruneau, B.G., Lindsay, E.A., and Baldini, A. (2004). Tbx1 has a dual role in the morphogenesis of the cardiac outflow tract. Development *131*, 3217-3227.

Yashiro, K., Shiratori, H., and Hamada, H. (2007). Haemodynamics determined by a genetic programme govern asymmetric development of the aortic arch. Nature *450*, 285-288.

Zhou, W., Lin, L., Majumdar, A., Li, X., Zhang, X., Liu, W., Etheridge, L., Shi, Y., Martin, J., Van de Ven, W.*, et al.* (2007). Modulation of morphogenesis by noncanonical Wnt signaling requires ATF/CREB family-mediated transcriptional activation of TGFbeta2. Nat Genet *39*, 1225-1234.

Gene Networks During Cardiogenesis And Skeletal Myogenesis

Chapter 3

Pitx2 acts a Transcriptional Switch from Embryonic to Fetal Skeletal Muscle Cell Fate

Hsiao-Yen Ma, Jun Xu, Diana Eng, Adam Campbell, Michael K. Gross, Chrissa Kioussi

To be submitted

SUMMARY

During myogenesis cells enter developmental states that are defined by specific gene regulatory networks. Cell states characterized by distinct shape, cell surface receptors, extracellular matrix proteins and functions. Embryonic myoblasts derive from embryonic muscle progenitors that fuse together to establish the muscle anlagen. As development progress, fetal myoblasts are formed from the fetal progenitors and the embryonic myoblasts and consequently form the fetal or secondary large fiber. Specific gene regulatory networks identify each cell type, as a constellation of a two and/or three sequence specific transcription factors. Embryonic ($Pax3^{+}Lbx1^{+}$) to fetal ($Pax3^{-}Pax7^{+}$) progenitor transition occurs at E11.5. Pitx2 is expressed in embryonic progenitors as they have moved into the forelimb muscle anlagen and have specified the transition state from embryonic to fetal progenitors. Pitx2 expression was remained within the fetal progenitors and both embryonic and fetal myoblasts. Myf5 specifies the myoblast fate. In absence of Pitx2 the number of embryonic/fetal progenitors ($Pax3^{+}Pax7^{+}$) and embryonic myoblasts ($Pax3^{+}Myf5^{+}$) was increased. Myoblasts failed to exit the cell cycle, exhibited G1 arrest and their entry to myogenic fate ($Myog^{+}$) was delayed. These data suggest that Pitx2 acts as the transcriptional switch from the embryonic to fetal fate during muscle development.

INTRODUCTION

Vertebrate skeletal muscles derive from somites, the paraxial mesoderm-derived epithelial structures located lateral to neural tube. Cells of the ventromedial part of the somite lose their epithelial structure to become mesenchymal sclerotome cells while the remainders form the dermomyotome. Dermomyotome further subdivides by partially overlapping expression patterns of homeodomain sequence specific transcription factors (SSTFs). The dorsomedial dermomyotome gives rise to the epaxial muscles that include the deep muscles of the back. The ventrolateral dermomyotome gives rise to the hypaxial muscles that include the appendicular and abdominal body wall muscles (Burke and Nowicki, 2003). Muscle progenitors become specified and committed to myoblasts, which later differentiate into myocytes that fuse to each other and form the multinucleated myofibers.

SSTFs are required for molecular specification, movement and myogenic progression during muscle development and represent the nodes of the gene regulatory networks. Combinatorial codes of SSTFs mark specific regions of the somite and dermomyotome before the onset of myogenic progression (Cheng et al., 2004). The cell types of myoblasts are specified by a different combination of SSTFs; yet, the timing, location, and nature of this specification process are not yet known. The paired domain homeobox genes Pax3 and Pax7 are expressed in somitic cells, and the $Pax3^+$ and $Pax7^+$ cells form the muscle progenitor pool of the limb (Kassar-Duchossoy et al., 2005; Relaix et al., 2005). Pax3 is required for somite segmentation and formation of the dermomyotomal lips (Goulding et al., 1994; Relaix et al., 2004; Schubert et al., 2001). When Pax3 is mutated or absent, dermomyotomal cells fail to delaminate and hypaxial muscles fail to form (Bober et al., 1994). Pax7 is required for proper fetal myogenesis and maintenance of “juvenile" adult satellite cells, a self-renewing population of myogenic precursors (Relaix et al.,

2005). A complex set of genetic interactions has been well documented between Pax3 and the different bHLH myogenic regulatory factors (MRFs, Myf5, Mrf4, Myod, Myog) in anatomically distinct muscle groups (Braun et al., 1992; Maroto et al., 1997; Rudnicki et al., 1992; Rudnicki et al., 1993; Tajbakhsh et al., 1997).

The muscle pattern formation of the limb is established during embryonic myogenesis. The first Pax3^{+} muscle progenitors migrating into the forelimb at E10.0-E12.5 are considered embryonic muscle progenitors (EMP) (Relaix et al., 2004). At E11.5, Pax3 expression starts to be reduced while Pax7 starts to be expressed in these cells as they transit to Pax3^{-}Pax7^{+} fetal muscle progenitors (FMP) (Hutcheson et al., 2009). The Pax3^{+}/Pax7^{+} cells characterize a transient stage from EMP to FMP. Pax7 is expressed though out the adult muscle progenitors (AMP), which give rise to satellite cells (Seale and Rudnicki, 2000). At E10.5, the Pax3^{+} EMP start to express Myf5 and called embryonic myoblasts (EMB). Myf5 continues to be expressed in fetal (FMB) and adult myoblasts (AMP) (Biressi et al., 2007c; Kassar-Duchossoy et al., 2005). Embryonic or primary fibers appear around E11 as the result of fusion of the embryonic myoblasts (EMB). Fetal or secondary fibers arise from the fusion of fetal myoblasts (FMB) either with primary fibers or with other FMB during fetal (E14.5-P0) and neonatal (P0-P21) myogenesis. Adult myogenesis is initiated in postnatal stages and continues throughout the life span to support muscle growth, maturation, and regeneration (Biressi et al., 2007a; Stockdale, 1992). The transition from EMB to FMB is initiated by the transcription nuclear factor IX (Nfix). Pax7 directly binds to Nfix and activates its expression (Messina et al., 2010). Specification of FMB also requires Mrf4 expression (Gayraud-Morel et al., 2007; Hinterberger et al., 1991), while Myod is expressed in differentiated myocytes and myofibers (Cornelison and Wold, 1997; Hinterberger et al., 1991; Ontell et al., 1993).

EMF are short, incorporate less myoblasts to FMB and adopt different myosin heavy chain (MyHC) isoforms. EMF express embryonic (MyHCemb) and I/β MyHC, FMB express MyHCemb and perinatal (MyHCperi) and the heterogeneous AMF express both I and II MyHC (Wigmore and Evans, 2002; Zhang et al., 1998). Vertebrate muscles consist of fatigue-resistant slow twitch fibers (SF) that express MyHC I/β and of oxidative metabolism and glycolytic fast twitch fibers (FF) that express MyHCemb, MyHCperi, MyHCIIa, MyHCIIb and MyHCIId (Bottinelli, 2001; Weiss et al., 2001).

Pitx2, a homeobox SSTF marks all muscle anlagen form embryogenesis to adult hood (Shih et al., 2007c). Pitx2 specifies the masseter (Shih et al., 2007a) and abdominal wall musculature (Eng et al., 2012), while regulates the higher muscle assembly in limbs (Campbell et al., 2012b). Pitx2 acts downstream of the Pax3 and Lbx1, after the muscle progenitors have been delaminated and start to migrate into the forelimb muscle anlagen. Pitx2^{+} cells are first detected in the dermomyotome at E10.25 (Shih et al., 2007c). In these studies we have shown that Pitx2, a key player of organ specification and maturation (Gage et al., 1999b; Kioussi et al., 2002; Kitamura et al., 1999; Lin et al., 1999; Lu et al., 1999), regulates the Pax3^{+}Pax7^{+} population as they transit from EM to FM during limb myogenesis.

EXPERIMENTAL PROCEDURES

Mice

ICR *Pitx2*$^{+/LacZ}$ (*Pitx2*$^{+/Z}$) mice (Lin et al., 1999) were bred and females were checked for the presence of a vaginal plug (E0.5). The yolk sacs of the isolated embryos were used for X-gal staining to distinguish the wild type and

heterozygote mice, while mutant null embryos were identified by their anatomical phenotype. To obtain $Pax3^{Cre}$|$Pitx2^{FL/Z}$ ($Pitx^{Pax3}$) and MCK^{Cre}|$Pitx^{FL/Z}$ ($Pitx2^{MCK}$) mice, $Pitx2^{FL/+}$ mice were crossed with $Pitx2^{Z/+}$, to generate $Pitx2^{FL/Z}$, $Pax3^{Cre}$|$Pitx2^{FL/+}$ and MCK^{Cre}|$Pitx2^{FL/+}$ respectively. The $Pax3^{Cre}$|$Pitx2^{FL/+}$ and MCK^{Cre}|$Pitx2^{FL/+}$ mice bred with the $Pitx2^{FL/Z}$ to generate $Pitx2^{Pax3}$ and $Pitx^{MCK}$ mice respectively. PCR analysis from tail genomic DNA identified the 360 bp FL and 380 bp Cre bands. PCR analysis from MCK^{Cre}|$Pitx^{FL/Z}$ skeletal muscle and non-muscle DNA identified Pitx2 deletion with a 360bp FL band and non-deletion with a 1.4kb Pitx2 band.

Immunohistochemistry

Immunohistochemistry on cryosections was performed as described by (Shih, 2007). Sections were photographed on an AxioImager Z1, Zeiss microscope. Antibodies used: Pax3 (Rat 1:100, (Gross et al., 2002)), Pax7 (mouse 1:30, Hybridoma Bank), Myf5 (Rabbit 1:100, Santa Cruz Biotechnology Inc.), Myog (Rabbi, 1:100, Pharmingen), (Mouse, 1:100, Santa Cruz Biotechnology Inc.).

Cell counting and data analysis

Immunostained cells with different antibodies were counted. Cryosections of 16µm from E10.5, E11.5 and E12.5 mouse right forelimb, WT (n=3) and MUT (n=3) mice were used for each stage. The reported cell number was mean counted through all slides of forelimb tissue and divided by slides numbers, with standard deviation (mean ± sd). Five to eight slides were counted for each stage. The significant difference between WT and MUT was determined via t-test statistical analysis. Two tailed *p*-value < 0.1, < 0.05 and < 0.01 was indicated by *, ** and *** respectively to show statistic significant difference.

Quantitative Real-time PCR (qPCR)

cDNA from limb buds was prepared by RNeasy Micro Kit (Qiagen). cDNA (25ng) was analyzed by qPCR using SYBR Green I methodology as previously described (Hilton et al., 2010). All samples were analyzed in triplicate and normalized by glyceraldehyde-3-phosphate dehydrogenase. Primer sets are listed in Table 3.1.

RNA *in situ* Hybridization

Whole-mount RNA *in situ* hybridization was performed as previously described by (Ma et al., 2013).

Stable Transfected C2C12 Cells

C2C12 cells were transfected using Neon transfection system (Invitrogen) according to manufacturer's protocol. Briefly, C2C12 cells were grown to 90% confluence in growth media and then trypsinized. Cells were centrifuged and washed several times with PBS (Ca^{2+}/Mg^{2+} free). Cells were resuspended to a density of $1x10^7$ cells/ml with resuspension buffer and electroporated with 3µg plasmid DNA using the following parameters: pulse voltage = 1650V, pulse width = 10ms, pulse number = 3. Cells were then seeded into 6-well tissue culture plates in growth media without antibiotics or G418 overnight in humidified incubator at 37°C, 5% CO_2. The subsequent day the media was changed growth media with antibiotics and G418. When transfected cells reached 90% confluence single clones were generated using dilution method using a 96-well tissue culture plate. Cells were serial diluted 1:2 from 4000 cells/well to 1 cell/well. Cells were maintained in growth media in humidified incubator 37°C, 5% CO_2 changing media every 48 hrs. Cell growth in wells that

were initially seeded with less than 4 cells was assumed to arise from single cells.

Cell Growth and Differentiation Conditions

C2C12 cells were maintained in growth media + 250µg/ml G418 (DMEM/F12 Gibco), 2.5mM Glutamine (Hyclone), 10% FBS, 50U/ml Pen/Strep (Cellgro), 0.25µg/ml Fungizone (Invitrogen), and 250µg/ml G418 (Invitrogen) in incubator 37°C, 90% humidity, 5% CO_2 and media was changed every 2-3 days. For differentiation, cells were grown to 90% confluence and media was changed to differentiation media + 250µg/ml G418 (DMEM/F12 Gibco), 2.5mM Glutamine (Hyclone), 2% horse serum, 50U/ml Pen/Strep (Cellgro), 0.25µg/ml Fungizone (Invitrogen), and 250µg/ml G418 (Invitrogen) and changed daily.

Cell Cycle Analysis

C2C12 cells were grown to 90% confluence, trypsinized, and centrifuged at 300 x g for 5 min. The supernatant was discarded and the cells were resuspended in PBS. Cells were centrifuged, supernatant was discarded and the pellet resuspended in 0.5 ml PBS, 0.1% Triton-X 100 in addition to 10 µl of RNAse A (10 µg/ml Invitrogen) and 10 µl Propidium Iodide (PI; 1 mg/ml Sigma-Aldrich). Cells were incubated for 30 min at room temp prior to cell cycle using FC500 flow cytometer Beckman Coulter, analyzing $\geq$ 30,000 cells.

Cell Proliferation Analysis

Cell proliferation was measured using Click-it EdU Flow Cytometry Assay Kit [Invitrogen] using Alexa Fluor 647 azide (Invitrogen), according to manufacturer protocol. Cells were grown to 90% confluence in growth media, EdU was

added to media (final concentration 10 µM) for 2 hrs. Cells were trypsinized and washed with 1% BSA in PBS solution. Cells were centrifuged and resuspended in Click-it fixative reagent, mixed and incubated at room temp for 15 min in the dark. Cells were washed with 1% BSA in PBS solution, centrifuged, resuspended in Click-it saponin-based permeabilization/wash reagent, and incubated at room temp for 15 min in the dark. During incubation Click-it reaction cocktail was prepared and 0.5 ml of cocktail was added to cells after incubation was completed. Cells were incubated for 30 min at room temp in the dark. Cells were then washed with saponin-based permeabilization/wash reagent and resuspended in the same reagent to final volume of 0.5 ml. Cells were then analyzed using FC500 flow cytometer Beckman Coulter, analyzing $\geq$ 30,000 cells.

Grasp Strength Analysis and H&E Staining

Four weeks old Pitx2^{Pax3} mice (n=3) and its control littermates (n=4) have been used for grasp strength test. Mice were placed on the top of the cage cover. The cover was turned over while mice grabbed the metal wire. Time started to be recorded right after the cage cover turned over, and ended when mouse discharged from the wire. Each mouse was tested 5 times. Right after the grasp strength analysis, skeletal muscle from fore- and hind-limbs was isolated. The tissue was rapidly put into liquid nitrogen cold isopentane. Snap frozen tissue was embedded into OCT and cryosectioned to obtain 14µm transverse sections. H&E staining was followed using standard protocol. Stained sections were photographed on an AxioImager Z1, Zeiss microscope.

RESULTS

Deformed Forelimb Muscle Anlagen in Pitx2 Mutants

Forelimb muscle progenitors are delaminated from ventrolateral lip of dermomyotome at E 10.5 and migrate towards forelimb bud for myogenesis. X-gal staining indicated the expression of Pitx2 in forelimb in Pitx2$^{Z/+}$ (HET) and Pitx2$^{Z/Z}$ (MUT) mice. X-gal staining was first detected within the forelimb bud at E10.5 (Fig 3.1A, B). By E11.5, the Pitx2 expression pattern was well established and looked similar in both HET and MUT (Fig 3.1F, G). At E 12.5, distinct muscle populations with clear boundaries start to form (Fig 3.1K). However, in MUT the shape of the muscles appeared truncated and disorganized with not clear boundaries (Fig 3.1L). The expression of Pitx2 in wild type (WT) was increased from E10.5 to E12.5 (Fig 3.1E, J, O). Myog is expressed in all differentiated myofibers and whole mount in situ hybridizations was used to detect all forming myofibers (Fig 3.1C, D, H, I, M, N). Myog expression was not detected at E11.5 in WT forelimbs (Fig 3.1H) and in lesser extend in MUT (Fig 3.1I), with a stronger presence at E12.5 (Fig 3.1M, N). Myog expression levels were increased during muscle development (Fig 3.1E, J, O). Myog expression was decreased in MUT at E11.5 (Fig 3.1J), but by E12.5 no difference was detected between MUT and WT (Fig 3.1O). These data further support previous observations (Campbell et al., 2012b) that myogenesis is progressing in absence of Pitx2 but the higher order muscle assembly is disordered or delayed.

Extended Embryonic Progenitors in Pitx2 Mutants

Skeletal muscle consists of different myofibers that derive from myoblasts which are specified from different progenitors (Ontell et al., 1993). Pitx2 is expressed in all myogenic states from myoblasts to myofibers (Shih et al.,

2007c). Delamination of Pax3$^+$ EMP from the dermomyotome to the forelimb progressed normally in absence of Pitx2 (Fig 3.2A, B) in a dorsal ventral distribution pattern. Very few myoblast were Pax3$^+$Pax7$^+$, which represent the transition state from embryonic to fetal myoblasts (E/FMB) (Fig 3.2A, B). The number of EMP (Pax3$^+$), E/FMP (Pax3$^+$Pax7$^+$) or FMP (Pax7$^+$) remained the same between WT and MUT (Fig 3.2C). By E11.5, muscle progenitors exhibit a dorsal-ventral pattern independent of the Pitx2 presence (Fig 3.2D, E) with the Pax3$^+$Pax7$^+$ FMP located in the inner part of the anlagen (Fig 3.2D-E1). Although there was no change in the distribution of any of the three populations, the number of E/FMP was increased by 16%, while the number of FMP was decreased by 29% in the MUT (Fig 3.2F). By E12.5, EMP were still present in both WT and MUT, half of the population entered the transition E/FMP state (Fig 3.2G, H) with the FMP occupying the most outer forelimb muscle anlagen space (Fig 3.2G-H1). No change in the number of FMP was detected, but the E/FMP population was increased by 18% in MUT (Fig 3.2I). Pax3 is transiently expressed in EMP and its mRNA levels were decreased as progenitors progress to myoblasts (Fig 3.2J). Pax7 expression is increased as EMP progress to FMP. In MUT, Pax7 expression did not follow this trend (Fig 3.2J). Collectively these data suggest that in absence of Pitx2 the transition from EMP to FMP was problematic. The intermediate E/FMP state was extended in time and cell numbers with more cells remained in EMP state and less in FMP state. Thus, Pitx2 might promote the transition from EMP to FMP during early forelimb myogenesis.

Reduced Embryonic Myoblasts in Pitx2 Mutants

Myf5 is expressed in both EMP and FMP as they migrate to forelimb at E10.5 and determines the myoblast embryonic and fetal fate (Biressi et al., 2007c;

Kassar-Duchossoy et al., 2005) (Fig 3.3A, B). The numbers of Myf5$^+$ and Pax3$^+$Myf5$^+$ cells were reduced by 32% and 33% respectively in MUT mice (Fig 3.3B, C). This pattern of reduced Myf5$^+$ and Pax3$^+$Myf5$^+$ cells continued at E11.5 (Fig 3.3D-E1) and E12.5 (Fig 3.3G-H1) but with smaller changes (Fig 3.3F, I). Quantitative analysis of forelimbs indicated that Myf5 levels were reduced as myogenesis proceeds and cells commit to further differentiation (Fig 3.3J), (Ontell et al., 1993; Sassoon et al., 1989). However, Myf5 levels in MUT were increased during myogenesis (Fig 3.3J) indicating that the EMB enter the differentiation state faster in absence of Pitx2. Collectively, these data suggest that Pitx2 promotes Myf5 expression in the EMP as they progress to the myoblast state.

Pitx2-Mediated Myoblast Cell Cycle Exit

As proliferating myoblasts migrate to their final destinations, they exit the cell cycle, adapt a new gene regulatory kernel, and enter a new developmental state. Pitx2-EGFP and EGFP stable transfected C2C12 myoblasts were used to study the function of Pitx2 during cell cycle. Myoblasts growing in presence of serum were stained with propidium iodine and flow sorted. The distribution of cells in control (EGFP) samples was 71 ± 0.3% (G1), 14 ± 4% (G2), 16 ± 4% (S), while for the Pitx2-overexpressing cells the distribution was 76 ± 1% (G1), 19 ± 4% (G2), 7 ± 2% (S), (Fig 3.4A). In presence of Pitx2, 7% G1 and 36% G2 arrest was observed, followed by a 56% sorter S-phase (Fig 3.4A). To determine if the proliferation index differed between the treatment groups, EdU proliferation assay was performed after switching C2C12 cells to differentiation media. Double labeling immunohistochemistry in control and CMV-Pitx2 myoblasts indicated 14% decreased EdU$^+$ cells in the Pitx2-cells compared to control cells (Fig 3.4B). Increased expression level of cell cycle marker, cyclin

D1 (Ccnd1) and cyclin D2 (Ccnd2), in E12.5 MUT forelimb was observed by qPCR analysis (Fig 3.4C). These data suggest that Pitx2 promotes G1 arrest in myoblasts and inhibits their re-entry to the cell cycle. The observed decrease in EdU incorporation in Pitx2 cells and increased expression of Ccnds in Pitx2 null mice is consistent with the withdrawal from the cell cycle and cell cycle arrest.

Reduced Fetal Myoblasts in Pitx2 Mutants

To determine the Pitx2 function in FMB, the expression profile of Pax7 was studied. Pax7 was detected for the first time in the dermomyotome at E10.5 in both WT and MUT (Fig 3.5A, B), of which some were also Myf5^{+}. At E11.5, Pax7^{+} FMB have been migrated into the forelimb (Fig 3.5D-E1), primarily in the anterior proximal area. The Pax7^{+} FMB increase in number as the forelimb grows (Fig 3.5A-G2). Although Myf5 is expressed in the forelimb at E10.5 (Fig 3.5A), the FMP specification occurs at E11.5 (Fig 3.5D). FMB (Pax7^{+}Myf5^{+}) started to be detected in the proximal part of the forelimb (Fig 3.5D1, E1). In MUT, the number of FMB declines by 32% at E11.5 (Fig 3.5F) and 29% at E12.5 (Fig 3.5I), with a higher decrease within the Myf5^{+}Pax7^{+} population (Fig 3.5F, I). Furthermore, Nfix as FMB marker was significantly reduced in its mRNA expression at E12.5 (Fig 3.5J). These data suggest that Pitx2 promotes the progression to myogenic commitment for both EMP and FMP cells.

Reduced Myofibers in Pitx2 Mutants

Embryonic and fetal myoblasts fuse and form the embryonic (EMF) and fetal (FMF) Myog^{+} myofibers. At E10.5, only a few cells in the proximal part of the forelimb were Myog^{+} (data not shown) and their number was increasing as muscle grows and matures (Fig 3.6A-F). The Myog mRNA levels were also

increased as detected by quantitative analysis assays (Fig 3.1E, J, O). The number of Myog^{+} myofibers was decreased in the MUT with a more severe reduction of 19% at E11.5 (Fig 3.6A, B, C). The Pax3^{+}Myog^{+} EMF were almost half in number by E12.5 in MUT forelimbs (Fig 3.6F). Pax7^{+} cell number was increased as the forelimb growth (Fig 3.6G-L). Pax7^{+}Myog^{+} FMF was 25% less in the MUT compare to WT at E11.5 (Fig 3.6I). It caught up in the MUT by E12.5 (Fig 3.6L). In absence of Pitx2 the formation of EMF and FMF is delayed. However, Pitx2 is critical for EMF formation rather than FMF formation. EMF establishes the basic muscle pattern, and Pitx2 regulates them, then Pitx2 might control the higher order muscle assembly to form secondary myofibers and the slow/fast muscles.

Generation of conditional Pitx2 knockout mice

Since ablation of Pitx2 in mice causes lethality at E10.5-E14.5 due to arrest of multiple organ development (Gage et al., 1999; Kioussi et al., 2002; Kitamura et al., 1999; Lin et al., 1999; Lu et al., 1999), the muscle type study after E14.5 can't be analyzed. To explore the function of Pitx2 in late stage during muscle formation, we generated a conditional mouse null allele of Pitx2 (Pitx2^{FL}) (Fig 3.7). To specifically ablate *Pitx2* in the muscle tissue, we have generated a Pitx2-floxed (Pitx2^{FL}) mouse by homologous recombination (Fig 3.7A). Pitx2^{FL} targeted ES cell clones were selected by treatment with G418 and microinjected into blastocysts to generate chimeric mice. Cre-mediated deletion of the Pitx2^{FL} allele (Pitx2$^{\Delta}$) was confirmed by Southern blotting of BamHI and KpnI digestion (Fig 3.7B). Pitx2$^{FL/+}$ mice were bred with Pitx2$^{Z/+}$ mice to generate the Pitx2$^{FL/Z}$ mouse. Pitx2$^{FL/Z}$ mice were viable and fertile. Pitx2$^{FL/Z}$ mice were bred these with the Pax3$^{Cre/+}$ (Engleka et al., 2005) and MCK$^{Cre/+}$ (Bruning et al., 1998) mice to generate skeletal muscle specific Pitx2 knockout mice Pax3^{Cre}|Pitx2$^{FL/Z}$ (Pitx2^{Pax3}) and MCK^{Cre}|Pitx2$^{FL/Z}$ (Pitx2^{MCK}). The

skeletal muscle specific Pitx2 deletion was detected by PCR analysis using genomic DNA. Pitx2 homeodmain deletion was only detected in different skeletal muscle tissues of 1-month old Pitx2^{MCK} mouse (Fig 3.7C).

Histological Defects in Muscle Specific Pitx2-Null Mice

The EMP give rise to EMF which determine the basic muscle pattern, while FMP give rise to FMF which contributes to muscle growth and maturation. EMF and FMF are distinct in morphology as indicated by the MyHC isoforms. The role of Pitx2 during myofibers formation, assembly and maturation are still remains elusive. To explore the function of Pitx2 in these different myofiber formation, Pitx2^{Pax3} and Pitx2^{MCK} mice were bred for EMF and FMF study respectively. Both of their offspring grow to adulthood and fertilizable.

The grasp strength analysis for four weeks old Pitx2^{Pax3} mice and its control littermates showed weakened limb strength in Pitx2^{Pax3} mice (Fig 3.8A-C). The hindlimb muscles were isolated right after the grasp strength analysis and analyze the morphology further by using HE staining. The centrally localized nuclei were observed in Pitx2^{Pax3} mice (Fig 3.8D, E). This uneven nuclei distribution implies the EMB fusion and EMF assembly defects may occur in absence of Pitx2.

DISCUSSION

Muscle is a heterogeneous tissue consisting of different muscle fibers derived from distinct progenitor and myoblast cells. Embryonic, fetal and adult muscle derived from related but distinct progenitor populations (Fig 3.9). Each myogenic cell type is determined by a specific SSTF network. Our studies have shown that Pitx2 is expressed in all skeletal muscle cell phase, progenitors,

myoblasts and myofibers (Shih et al., 2007c), is essential for the proper formation of mastication (Shih et al., 2007a), abdominal wall (Eng et al., 2012b) and forelimb muscles (Campbell et al., 2012b) and regulates exit from the cell cycle affects the proper muscle growth (Campbell et al., 2012b). In this study we have shown that Pitx2 functions as embryonic-to-fetal progenitor switch during forelimb myogenesis.

Pitx2 Promotes the Embryonic-to-Fetal Progenitor State

Myogenic progenitors located in dermomyotome require Pax3 for their delamination. Pax3 activates c-mets that is essential for the delamination and migration of muscle precursors (Epstein et al., 1996; Relaix et al., 2003). Lbx1 is expressed in a very small window and marks the muscle migratory cells (Gross et al., 2000). The expression domain and timing of Pitx2 suggested that the muscle progenitor migration would not be disrupted. Pitx2 mutant forelimbs do not exhibit obvious gross anatomical defects in $Pax3^+$ cells. Moreover, Pax7, Myf5 and Myog expression were not influenced by the loss of Pitx2, suggesting that Pitx2 is not essential for the myogenic pattern formation. $Pax3^+Pax7^+$ E/FMP give rise to and required for fetal myogenesis. Pitx2 is expressed for the first time in this population. During embryonic myogenesis, the proliferating $Pax3^+$ cells gradually minimize the Pax3 expression and iniaite the Pax7 expression. This progression is slower down in the MUT and results to the increased number of E/FMP ($Pax3^+Pax7^+$) (Fig 2, Fig 3.9). In addition, Pitx2 promotes the exit of the myoblast from the cell cycle (Campbell et al., 2012b). Thus, Pitx2 may promote EMP to FMP transition via repressing Pax3 and activating Pax7 expression, which results to the establishment of a new kernel and a new cell state.

Pitx2 and Pitx3 in Embryonic and Fetal Myogenesis

Pitx genes encode highly homologous proteins, identical within their homeodomains and varying mainly in the N-terminal region. Pitx gene family has three members including Pitx1, Pitx2 and Pitx3. Pitx3 is also expressed in limb muscle and implicated in developmental myogenesis (L'Honore et al., 2007). Pitx3 null mice do not show any obvious skeletal muscle defect, which indicates it is not essential to myogenesis when acting alone (L'Honore et al., 2007). However, Pitx2 expression is increasing as progenitors and myoblasts transition from the embryonic to fetal state at E11.5, and might compensate the Pitx3 function. Pitx3 expression did not change in the Pitx2 MUT at E11.5, but it was significantly increased in the MUT a day later when the majority of the cells are in the fetal state (Fig S3.1). The onset of Pitx3 is observed at E11.0, shortly after the onset of Pix2 at E10.5 (L'Honore et al., 2007). The delay of the Pitx3 expression suggests that there is no redundancy during the sensate window of E10.5 to E11. Pitx3 might be partially redundant and compensate the Pitx2 function each at later fetal states. The significant decrease of Pax7, Myf5 and Myog mRNA levels was happened in MUT (Fig 3.2J, 3.3J and 3.1E) is combined with a decreased number of FMP ($Pax7^+$), MB ($Myf5^+$) and MF ($Myog^+$) (Fig 3.2F, 3.3F, 3.5F and 3.6C, I) at E11.5. After activation of Pitx3 at E12.5, the expression of Pax7 and Myog and the number of MF ($Myog^+$) was corrected in the MUT (Fig 3.2J and 3.6F, L). Thus Pitx2 and Pitx3 are working together timely for the establishment of the fetal state.

Pitx2 in Fetal Myoblast Formation

Nfix is robustly and specifically expressed in FMB (Biressi et al., 2007c) and functions as a transcriptional switch from EMB to FMB by activating Pax7

(Messina et al., 2010). In absence of Pitx2, Pax7 was decreased in FMB at E11.5 (Fig 3.2D-F, J). However, the elevated levels of Pitx3 might rescue the decline of Pax7 by E12.5 (Fig 3.2J). Nfix is expressed at E12.5 when FMB have been formed (Fig 3.5J) and its expression was not Pitx3-dependent, which further supports the essential role of Pitx2 for the EMB to FMB transition.

We have identified new kernels that specify delicate and time sensitive developmental states during forelimb muscle development. Pitx2 mutants indeed form forelimb muscles but the ration of embryonic and fetal cells is disrupted that leads to future structural defects during the higher order muscle assembly and the formation of fibers.

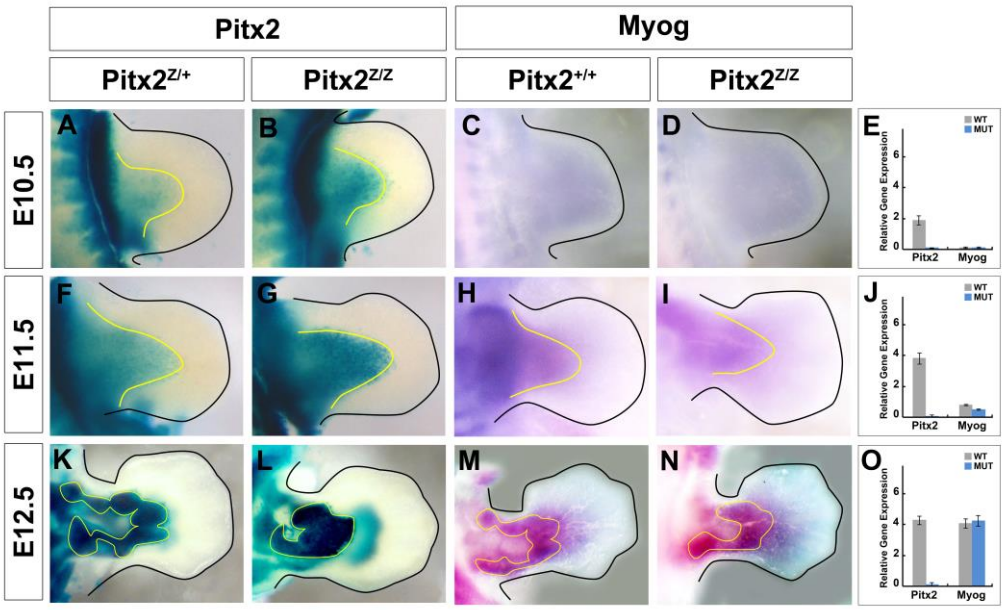

Figure 3.1

Figure 3.1 Forelimb muscle defects in Pitx2 mutants. Whole mount X-gal staining used to trace and compare the forelimb muscles in HET **(A, F, K)** and MUT **(B, G, L)** mouse embryos. **(A, B)** X-gal was first detected in the forelimb at E10.5. **(F, G)** At E11.5, the basic shape of muscle mass had established. **(K)** Muscles start to develop in HET at E12.5. **(L)** In MUT, muscles were truncated without clear boundaries among different muscle groups. Myog expression in the forelimb muscle was detected by whole mount *in situ* hybridization in WT **(C, H, M)** and MUT **(D, I, N)** mouse embryos. **(C, D)** No Myog signal was observed at E10.5. At E11.5, Myog started to be detectable in WT forelimb buds **(H)**, with reduced expression in MUT **(I)**. **(M, N)** At E12.5, the Myog expression pattern was similar to the X-gal stained well-developed HET muscle **(K)** and truncated, disordered MUT muscles **(L)**. **(E, J, O)** Pitx2 and Myog expression measured by qPCR analysis was increased as forelimb growth. **(J)** Myog expression was decreased in MUT at E11.5.

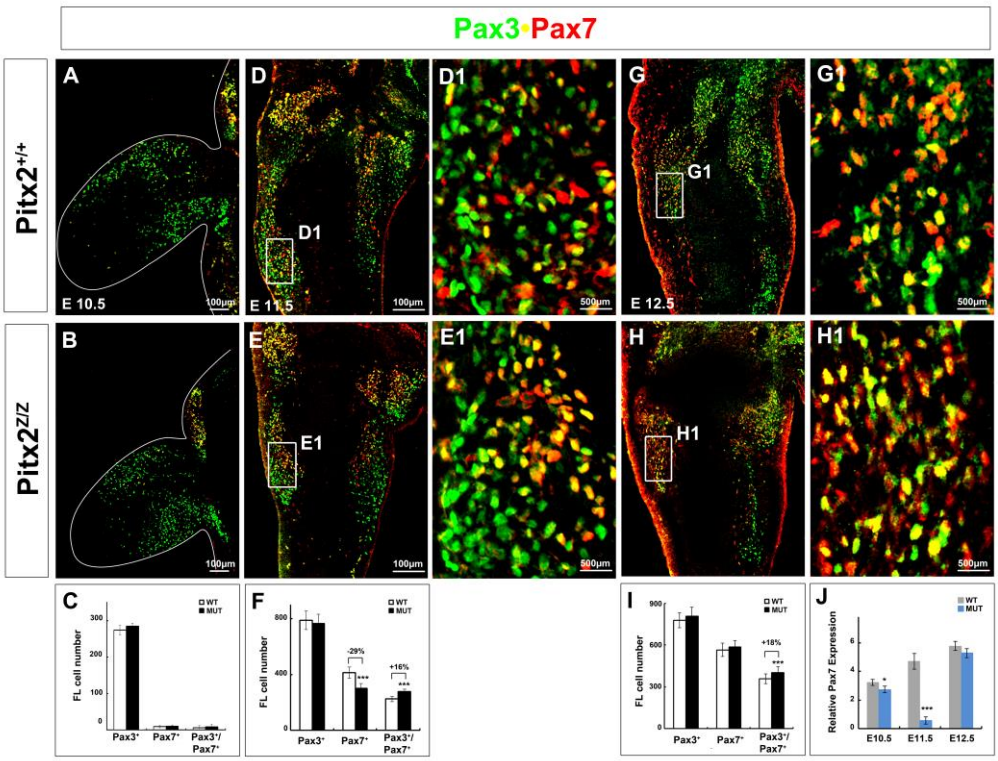

Figure 3.2

Figure 3.2 Extended embryonic muscle progenitors in Pitx2 mutants. Immunohistochemistry on transverse sections of WT and MUT at E10.5 **(A, B)**, E11.5 **(D, E)** and E12.5 **(G, H)**. **(A)** Migrating Pax3$^+$ muscle progenitors, delaminate from dermomyotome and migrate to the forelimb bud. **(A, C)** Pax7 is expressed in dermomyotome and in very few Pax3$^+$ EMP in forelimb. Loss of Pitx2 did not affect the pattern and migration of progenitors. **(D, E)** Pax3$^+$Pax7$^+$ cells were present at E 11.5 in both WT and MUT. **(F)** At this stage, the number of Pax7$^+$ was decreased by 29%, while the number of Pax3$^+$Pax7$^+$ cells was increased by 16% in the MUT. **(D1, E1)** Higher magnification. **(I)** At E12.5, the number of Pax7 was no difference between WT and MUT. **(G, H, I)** In the MUT, 18% more Pax3$^+$Pax7$^+$ was detected as compared to WT. **(G1, H1)** Higher magnification. **(J)** Pax7 mRNA levels measured by qPCR analysis. Pax7 expression was dramatically decreased at E11.5. At E12.5, the expression level was increased in MUT with no difference in WT and MUT.

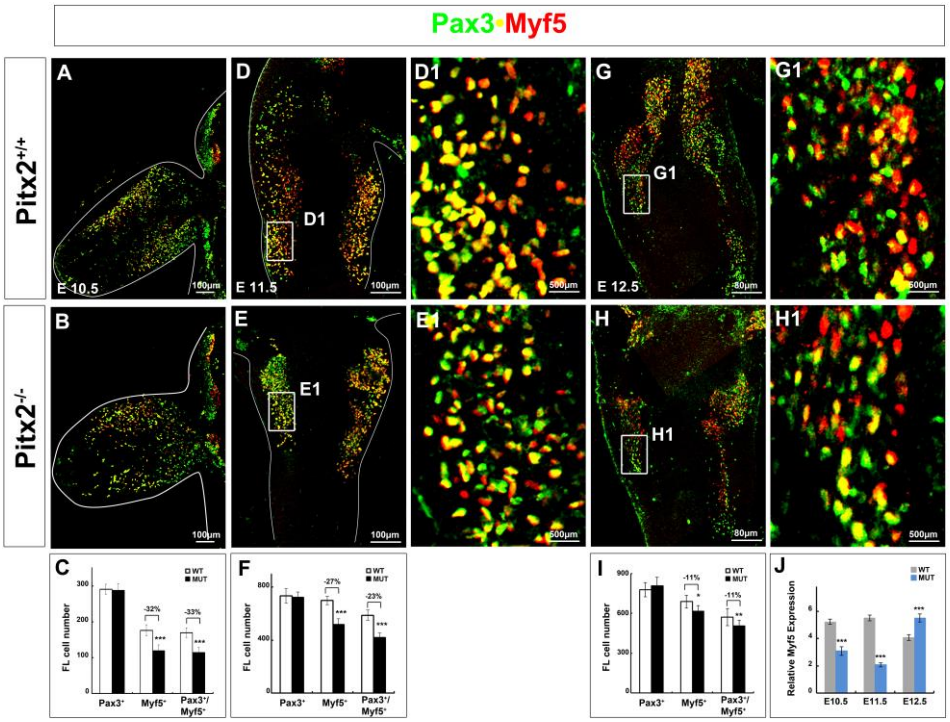

Figure 3.3

Figure 3.3 Reduced embryonic myoblasts in Pitx2 mutants. Immunohistochemistry on transverse sections WT and MUT mice to detect the alteration of Myf5 expression in developing forelimb from E10.5 to E12.5. **(A)** Myf5^{+} committed myoblasts were detected in the myotome and forelimb bud at E10.5. **(A, B)** Pax3^{+} EMP were committed to myogenic fate by expressing Myf5. Loss of Pitx2 did not alter the dosal-ventral pattern of myogenic precursors. **(C)** The number of Myf5^{+} and Pax3^{+}Myf5^{+} were reduced by 32% and 33% in the MUT respectively. At E 11.5, although more embryonic muscle progenitors were committed to myogenic fate **(D, E)**, the number of Myf5^{+} and Pax3^{+}Myf5^{+} remained reduced by 27% and 23% in MUT **(F)**. **(D1, E1)** Higher magnification. **(G, H, G1, H1)** At E 12.5, EMP are specified to myoblasts. **(I)** The number of Myf5^{+} and Pax3^{+}Myf5^{+} cells in forelimb was still reduced by 11% in MUT. **(J)** Myf5 mRNA levels measured by qPCR analysis. In MUT, Myf5 expression levels were decreased from E10.5 to E11.5, and then increased at E12.5.

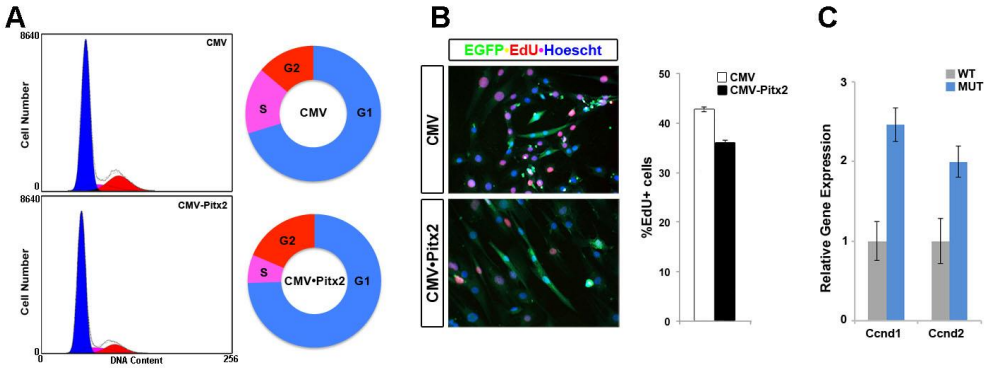

Figure 3.4

Figure 3.4 Pitx2 promotes myoblast exit from the cell cycle. (A) The distribution of cells analyzed found that (mean ± sem) in control was 71 ± 0.3% (G1), 14 ± 4% (G2), 16 ± 4% (S); while, Pitx2-overexpressing cells had a distribution of 76 ± 1% (G1), 19 ± 4% (G2), 7 ± 2% (S). The 9% decrease of the cells in S phase and the 7% increase of cells in G1 phase was statistically significant. **(B)** EdU proliferation assay. Compared to CMV control group, 14% less EdU signal was detected in the CMV-Pitx2 group. **(C)** mRNA levels of Ccnd1 and Ccnd2 measured by qPCR at E12.5 WT and Pitx2 MUT forelimb tissue. Increased levels of Ccnd1 and Ccnd2 transcripts were detected in MUT.

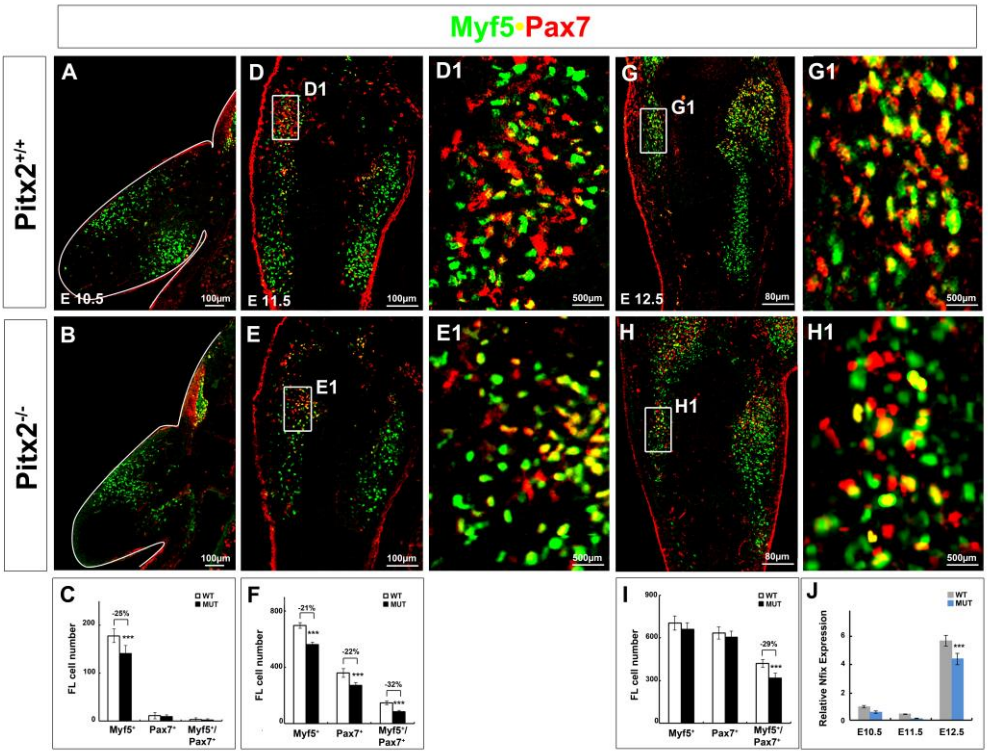

Figure 3.5

Figure 3.5 Reduced fetal myoblasts in Pitx2 mutants. Immunohistochemistry on transverse sections of WT and MUT at E10.5 **(A, B)**, E11.5 **(D, E)** and E12.5 **(G, H)**. **(A, B)** Myf5^{+} myoblasts were detected in the forelimb bud at E10.5. Pax7 is not expressed in the forelimb at this stage. **(C)** The number of Myf5^{+} cells and was reduced by 25% in MUT. **(D, E)** At E 11.5, Pax7 expression was detected in distal part of the forelimb. **(F)** The numbers of Myf5^{+}, Pax7^{+} and Pax7^{+}Myf5^{+} were 21%, 22% and 32% less in the MUT respectively. **(I)** At E 12.5, the number of Myf5^{+} and Pax7^{+}Myf5^{+} FMB **(G, H, G1, H1)** was still reduced in MUT by 29%.

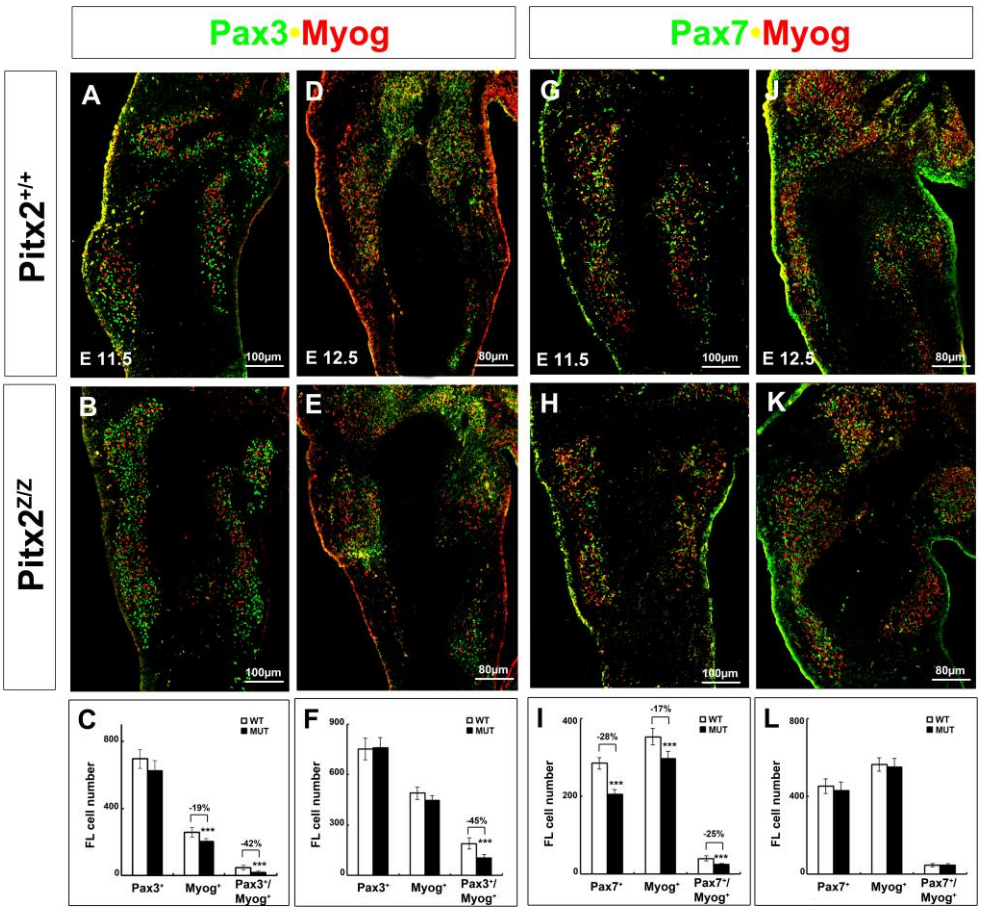

Figure 3.6

Figure 3.6 Reduced embryonic myofibers in Pitx2 mutant. Immunohistochemistry on transverse sections of WT and MUT at E11.5 **(A, B, G, H)** and E12.5 **(D, E, J, K). (A, B, G, H)** At E 11.5, Myog was expressed in both WT and MUT forelimb**. (A, G)** EMP ($Pax3^+Myog^-$), FMP ($Pax7^+Myog^-$), myofibers ($Myog^+$) and committed embryonic ($Pax3^+Myog^+$) and fetal ($Pax7^+Myog^+$) muscle precursor were all present in WT. **(C, I)** In MUT the number of $Myog^+$, $Pax3^+Myog^+$, $Pax7^+$ and $Pax7^+Myog^+$ was reduced by 19%, 42%, 28% and 25% respectively. **(D, J)** At E 12.5, more $Pax3^+$ and $Pax7^+$ cells differentiated into $Myog^+$ cells. **(F, L)** The committed EMP were reduced in number by 46% in MUT, while the committed FMP were rescued by that time MUT.

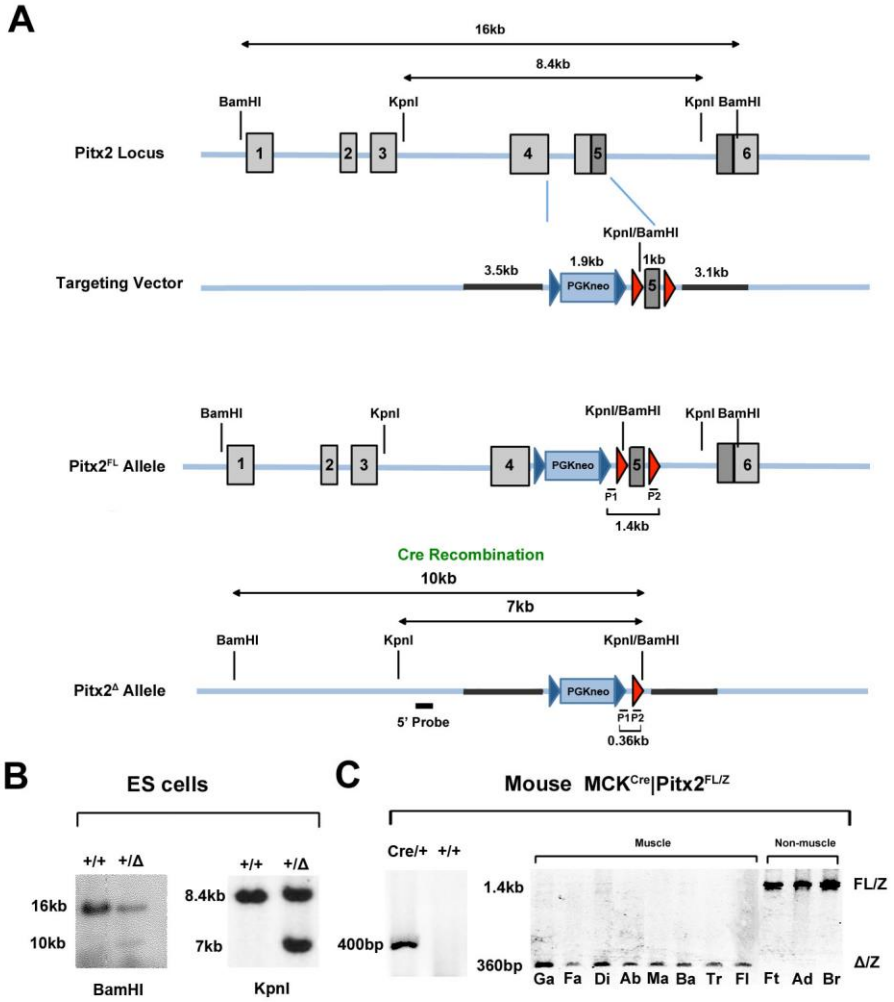
A
16kb
8.4kb
BamHI
KpnI
KpnI BamHI
Pitx2 Locus
1
2
3
4
5
6
KpnI/BamHI
1.9kb
1kb
Targeting Vector
3.5kb
PGKneo
3.1kb
Pitx2FL Allele
P1
P2
1.4kb
Cre Recombination
10kb
7kb
Pitx2Δ Allele
5' Probe
0.36kb
B
ES cells
+/+ +/Δ
16kb
10kb
BamHI
8.4kb
7kb
KpnI
C
Mouse MCKCre|Pitx2FL/Z
Cre/+ +/+
400bp
Muscle
Non-muscle
1.4kb
360bp
FL/Z
Δ/Z
Ga Fa Di Ab Ma Ba Tr Fl Ft Ad Br

Figure 3.7

Figure 3.7 Generation of conditional Pitx2 knockout mice. (A) Schematic representation of the Pitx2 locus, targeting vector, $Pitx2^{FL}$ allele and $Pitx2^{\Delta}$ allele. Part of the homeodomain (exon 5) has been floxed with loxp sites (red arrowhead), and a neo-frt (blue box with blue arrowhead) cassette has been inserted between exon 4 and 5. After homologous recombination, $Pitx2^{FL}$ allele was generated. Cre recombination after that resulted to the generation of the $Pitx2^{\Delta}$ allele. **(B)** Diagnosis of homologous recombination and cre recombination in ES cells by genomic DNA Southern blot assay using a 5' probe using BamHI and KpnI restriction sites. **(C)** muscle tissue specific Pitx2 knockout mice were obtained via crossing MCK^{Cre} with $Pitx2^{FL/Z}$ mice. PCR analysis from tail genomic DNA identified the 380 bp Cre bands. PCR analysis from MCK^{Cre}|$Pitx^{FL/Z}$ skeletal muscle and non-muscle DNA identified Pitx2 deletion with a 360bp FL band and non-deletion with a 1.4kb Pitx2 band.

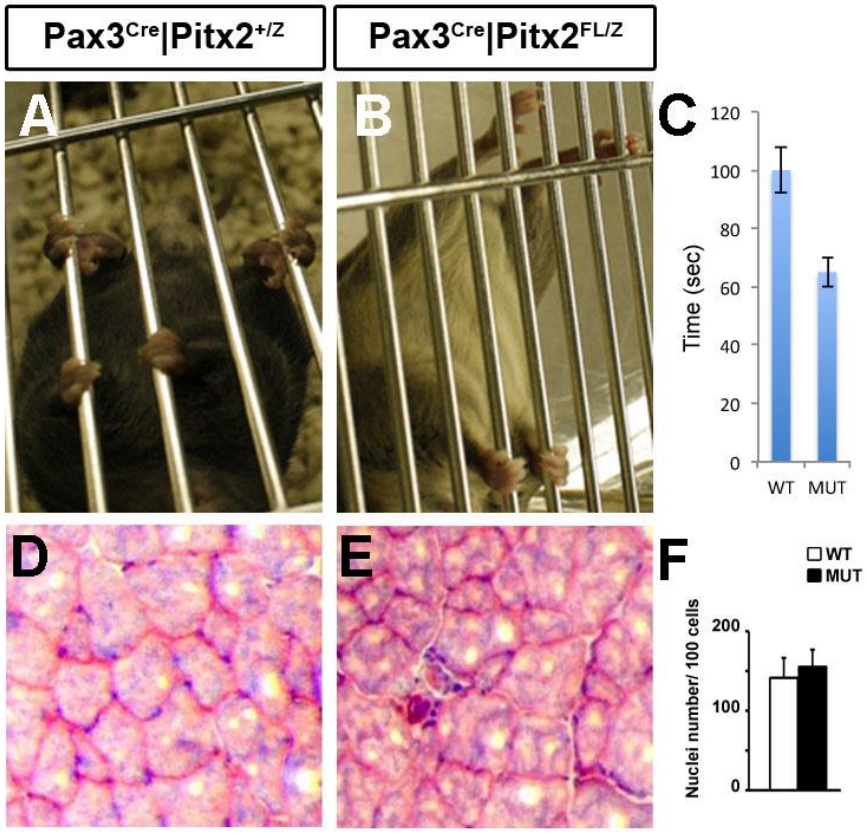

Figure 3.8

Figure 3.8 Grasp and histological defects in conditional mutant Pitx2 mice. (A, B) Reduced forelimb grasp strength in tissue-specific Pitx2^{Pax3} mice. **(C)** Pitx2^{Pax3} mice were able to hold onto wire for 35% less time than the control littermates. **(D, E)** Centrally localized nuclei were observed in Pitx2^{Pax3} mice via HE staining on hindlimb cross sections. **(F)** Increased number of nuclei/cell in mutants.

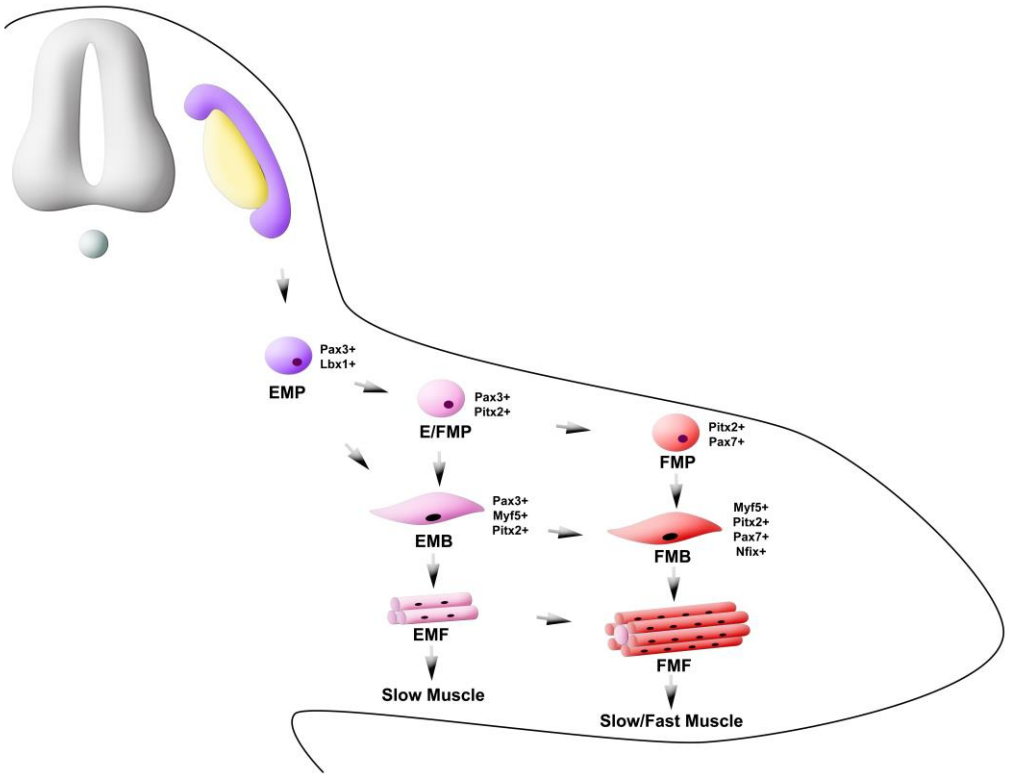

Figure 3.9

Figure 3.9 Developmental states of forelimb myogenesis. After delaminating from the demomyogome at E8.5 the Pax3^{+} EMP migrate towards limb bud and start to express Lbx1 at E9.5. Expression of Pitx2 specifies the E/FMP at E10.5 and expression of Pax7 at E11.5 specifies the fetal state. Myf5 expression marks all myoblasts, embryonic and fetal. FMB differentiate themselves from the EMB by expressing Nfix. EMB fuse each other to form EMF and FMB fuse to EMF or to other FMB to form large FMF. EMF give rise to slow muscle and FMF give rise to both slow and fast muscle in the future.

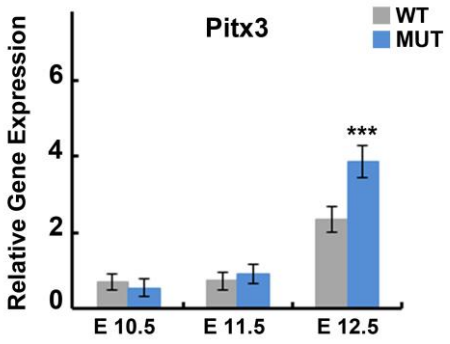

Figure S3.1

Figure S3.1 Pitx3 expression in Pitx2 mutants. Pitx3 expression was increased from E10.5 to E12.5 in WT forelimbs. In MUT, Pitx3 expression did not change at E10.5 and E11.5, but it was significantly increased at E12.5.

Primer	Forward	Reverse
Myf5	AAGGCTCCTGTATCCCCTCAC	TGACCTTCTTCAGGCGTCTAC
Myog	GGTGTGTAAGAGGAAGTCTGTG	TAGGCGCTCAATGTACTGGAT
Pax7	TGGGGTCTTCATCAACGGCT	ATCGGCACAGAATCTTGGAGA
Pitx2	TGGACCAACCTTACGGAAGC	GACAGAGACGTTGACGTGAGG
Pitx3	TGCGCTGTCGTTATCGGAC	GGTAGCGATTCCTCTGGAAGG
Nfix	AGCCCCAGCTACTACAACATA	AGTCCAGCTTTCCTGACTTCT
Ccnd1	TTCGTGGCCTCTAAGATGAAGG	GAGCAGCTCCATTTGCAGC
Ccnd2	ACCTTCCGCAGTGCTCCTA	CCCAGCCAAGAAACGGTCC
GAPDH	ACACCCATCACAAACATGGG	CATCAACGGGAAGCCCAT

Table 3.1

REFERENCES

Biressi, S., Molinaro, M., and Cossu, G. (2007a). Cellular heterogeneity during vertebrate skeletal muscle development. Developmental biology *308*, 281-293.

Biressi, S., Tagliafico, E., Lamorte, G., Monteverde, S., Tenedini, E., Roncaglia, E., Ferrari, S., Ferrari, S., Cusella-De Angelis, M.G., Tajbakhsh, S.*, et al.* (2007b). Intrinsic phenotypic diversity of embryonic and fetal myoblasts is revealed by genome-wide gene expression analysis on purified cells. Developmental biology *304*, 633-651.

Bober, E., Franz, T., Arnold, H.H., Gruss, P., and Tremblay, P. (1994). Pax-3 is required for the development of limb muscles: a possible role for the migration of dermomyotomal muscle progenitor cells. Development *120*, 603-612.

Bottinelli, R. (2001). Functional heterogeneity of mammalian single muscle fibres: do myosin isoforms tell the whole story? Pflugers Archiv : European journal of physiology *443*, 6-17.

Braun, T., Rudnicki, M.A., Arnold, H.H., and Jaenisch, R. (1992). Targeted inactivation of the muscle regulatory gene Myf-5 results in abnormal rib development and perinatal death. Cell *71*, 369-382.

Burke, A.C., and Nowicki, J.L. (2003). A new view of patterning domains in the vertebrate mesoderm. Dev Cell *4*, 159-165.

Campbell, A.L., Shih, H.P., Xu, J., Gross, M.K., and Kioussi, C. (2012). Regulation of motility of myogenic cells in filling limb muscle anlagen by Pitx2. PloS one *7*, e35822.

Cheng, L., Alvares, L.E., Ahmed, M.U., El-Hanfy, A.S., and Dietrich, S. (2004). The epaxial-hypaxial subdivision of the avian somite. Dev Biol *274*, 348-369.

Cornelison, D.D., and Wold, B.J. (1997). Single-cell analysis of regulatory gene expression in quiescent and activated mouse skeletal muscle satellite cells. Developmental biology *191*, 270-283.

Eng, D., Ma, H.Y., Xu, J., Shih, H.P., Gross, M.K., and Kioussi, C. (2012). Loss of abdominal muscle in Pitx2 mutants associated with altered axial specification of lateral plate mesoderm. PloS one *7*, e42228.

Epstein, J.A., Shapiro, D.N., Cheng, J., Lam, P.Y., and Maas, R.L. (1996). Pax3 modulates expression of the c-Met receptor during limb muscle development. Proceedings of the National Academy of Sciences of the United States of America *93*, 4213-4218.

Gage, P.J., Suh, H., and Camper, S.A. (1999). Dosage requirement of Pitx2 for development of multiple organs. Development *126*, 4643-4651.

Gayraud-Morel, B., Chretien, F., Flamant, P., Gomes, D., Zammit, P.S., and Tajbakhsh, S. (2007). A role for the myogenic determination gene Myf5 in adult regenerative myogenesis. Developmental biology *312*, 13-28.

Goulding, M., Lumsden, A., and Paquette, A.J. (1994). Regulation of Pax-3 expression in the dermomyotome and its role in muscle development. Development *120*, 957-971.

Gross, M.K., Dottori, M., and Goulding, M. (2002). Lbx1 specifies somatosensory association interneurons in the dorsal spinal cord. Neuron *34*, 535-549.

Gross, M.K., Moran-Rivard, L., Velasquez, T., Nakatsu, M.N., Jagla, K., and Goulding, M. (2000). Lbx1 is required for muscle precursor migration along a lateral pathway into the limb. Development *127*, 413-424.

Hinterberger, T.J., Sassoon, D.A., Rhodes, S.J., and Konieczny, S.F. (1991). Expression of the muscle regulatory factor MRF4 during somite and skeletal myofiber development. Developmental biology *147*, 144-156.

Hutcheson, D.A., Zhao, J., Merrell, A., Haldar, M., and Kardon, G. (2009). Embryonic and fetal limb myogenic cells are derived from developmentally distinct progenitors and have different requirements for beta-catenin. Genes & development *23*, 997-1013.

Kassar-Duchossoy, L., Giacone, E., Gayraud-Morel, B., Jory, A., Gomes, D., and Tajbakhsh, S. (2005). Pax3/Pax7 mark a novel population of primitive myogenic cells during development. Genes Dev *19*, 1426-1431.

Kioussi, C., Briata, P., Baek, S.H., Rose, D.W., Hamblet, N.S., Herman, T., Ohgi, K.A., Lin, C., Gleiberman, A., Wang, J.*, et al.* (2002). Identification of a Wnt/Dvl/beta-Catenin --> Pitx2 pathway mediating cell-type-specific proliferation during development. Cell *111*, 673-685.

Kitamura, K., Miura, H., Miyagawa-Tomita, S., Yanazawa, M., Katoh-Fukui, Y., Suzuki, R., Ohuchi, H., Suehiro, A., Motegi, Y., Nakahara, Y.*, et al.* (1999). Mouse Pitx2 deficiency leads to anomalies of the ventral body wall, heart, extra- and periocular mesoderm and right pulmonary isomerism. Development *126*, 5749-5758.

L'Honore, A., Coulon, V., Marcil, A., Lebel, M., Lafrance-Vanasse, J., Gage, P., Camper, S., and Drouin, J. (2007). Sequential expression and redundancy of Pitx2 and Pitx3 genes during muscle development. Developmental biology *307*, 421-433.

Lin, C.R., Kioussi, C., O'Connell, S., Briata, P., Szeto, D., Liu, F., Izpisua-Belmonte, J.C., and Rosenfeld, M.G. (1999). Pitx2 regulates lung asymmetry, cardiac positioning and pituitary and tooth morphogenesis. Nature *401*, 279-282.

Lu, M.F., Pressman, C., Dyer, R., Johnson, R.L., and Martin, J.F. (1999). Function of Rieger syndrome gene in left-right asymmetry and craniofacial development. Nature *401*, 276-278.

Ma, H.Y., Xu, J., Eng, D., Gross, M.K., and Kioussi, C. (2013). Pitx2-mediated cardiac outflow tract remodeling. Developmental dynamics : an official publication of the American Association of Anatomists *242*, 456-468.

Maroto, M., Reshef, R., Munsterberg, A.E., Koester, S., Goulding, M., and Lassar, A.B. (1997). Ectopic Pax-3 activates MyoD and Myf-5 expression in embryonic mesoderm and neural tissue. Cell *89*, 139-148.

Messina, G., Biressi, S., Monteverde, S., Magli, A., Cassano, M., Perani, L., Roncaglia, E., Tagliafico, E., Starnes, L., Campbell, C.E.*, et al.* (2010). Nfix regulates fetal-specific transcription in developing skeletal muscle. Cell *140*, 554-566.

Ontell, M., Ontell, M.P., Sopper, M.M., Mallonga, R., Lyons, G., and Buckingham, M. (1993). Contractile protein gene expression in primary myotubes of embryonic mouse hindlimb muscles. Development *117*, 1435-1444.

Relaix, F., Polimeni, M., Rocancourt, D., Ponzetto, C., Schafer, B.W., and Buckingham, M. (2003). The transcriptional activator PAX3-FKHR rescues the defects of Pax3 mutant mice but induces a myogenic gain-of-function phenotype with ligand-independent activation of Met signaling in vivo. Genes & development *17*, 2950-2965.

Relaix, F., Rocancourt, D., Mansouri, A., and Buckingham, M. (2004). Divergent functions of murine Pax3 and Pax7 in limb muscle development. Genes Dev *18*, 1088-1105.

Relaix, F., Rocancourt, D., Mansouri, A., and Buckingham, M. (2005). A Pax3/Pax7-dependent population of skeletal muscle progenitor cells. Nature *435*, 948-953.

Rudnicki, M.A., Braun, T., Hinuma, S., and Jaenisch, R. (1992). Inactivation of MyoD in mice leads to up-regulation of the myogenic HLH gene Myf-5 and results in apparently normal muscle development. Cell *71*, 383-390.

Rudnicki, M.A., Schnegelsberg, P.N., Stead, R.H., Braun, T., Arnold, H.H., and Jaenisch, R. (1993). MyoD or Myf-5 is required for the formation of skeletal muscle. Cell *75*, 1351-1359.

Sassoon, D., Lyons, G., Wright, W.E., Lin, V., Lassar, A., Weintraub, H., and Buckingham, M. (1989). Expression of two myogenic regulatory factors myogenin and MyoD1 during mouse embryogenesis. Nature *341*, 303-307.

Schubert, F.R., Tremblay, P., Mansouri, A., Faisst, A.M., Kammandel, B., Lumsden, A., Gruss, P., and Dietrich, S. (2001). Early mesodermal phenotypes in splotch suggest a role for Pax3 in the formation of epithelial somites. Dev Dyn *222*, 506-521.

Seale, P., and Rudnicki, M.A. (2000). A new look at the origin, function, and "stem-cell" status of muscle satellite cells. Developmental biology *218*, 115-124.

Shih, H.P., Gross, M.K., and Kioussi, C. (2007a). Cranial muscle defects of Pitx2 mutants result from specification defects in the first branchial arch. Proceedings of the National Academy of Sciences of the United States of America *104*, 5907-5912.

Shih, H.P., Gross, M.K., and Kioussi, C. (2007b). Expression pattern of the homeodomain transcription factor Pitx2 during muscle development. Gene expression patterns : GEP *7*, 441-451.

Stockdale, F.E. (1992). Myogenic cell lineages. Developmental biology *154*, 284-298.

Tajbakhsh, S., Rocancourt, D., Cossu, G., and Buckingham, M. (1997). Redefining the genetic hierarchies controlling skeletal myogenesis: Pax-3 and Myf-5 act upstream of MyoD. Cell *89*, 127-138.

Weiss, S., Rossi, R., Pellegrino, M.A., Bottinelli, R., and Geeves, M.A. (2001). Differing ADP release rates from myosin heavy chain isoforms define the shortening velocity of skeletal muscle fibers. The Journal of biological chemistry *276*, 45902-45908.

Wigmore, P.M., and Evans, D.J. (2002). Molecular and cellular mechanisms involved in the generation of fiber diversity during myogenesis. International review of cytology *216*, 175-232.

Zhang, M., Koishi, K., and McLennan, I.S. (1998). Skeletal muscle fibre types: detection methods and embryonic determinants. Histology and histopathology *13*, 201-207.

Gene Networks During Cardiogenesis And Skeletal Myogenesis

Chapter 4

Conclusive Remarks and Future Directions

Hsiao-Yen Ma and Chrissa Kioussi

CONCUSIVE REMARKS

The muscle growth, assembly and maturation depend on proper myogenic cell migration, proliferation, differentiation and fusion. The timing of SSTFs expression determines distinct stage of myogenic cells, and it is critical for these series of cellular events. Pitx2 is not express in the first myogenic progenitors which expressed $Pax3^{+}$ and $Lbx1^{+}$. It express in these progenitor cells right after they have arrived in the forelimb. Pitx2 is essential in E/FMP transition phase and promote the EMP change to FMP (Chapter 3). In the Pitx2 null mice, although the myogenic event has been disrupted but it is still occurred. The timing of onset of Pitx2 expression suggests that Ptix2 may have late myogenic regulation function during fetal/neonatal muscle formation. In addition, all myoblasts are committed differentiated by expressing of Myf5. Myf5 mediated myogenesis get started from EMP in which Pitx2 has not been expressed yet. However, both EMB and FMB are affected in absence of Pitx2 (Fig 3.3, Fig 3.5). It indicates that Pitx2 functions in myoblasts specification by regulate muscle progenitor committed differentiation. EMF which differentiated from EMB was affected in absence of Pitx2. However, FMF which differentiated form FMB was not affected. It indicates that Pitx2 function may be compensated by Pitx3. It also suggests that Pitx2 may functions in regulating EMF rather than FMF. Embryonic muscle specific Pitx2 deletion mice ($Pitx2^{Pax3}$) exhibits uneven nuclei distribution and weaken muscle strength (Fig 3.8) implies Pitx2 may regulate EMB fusion and FMF assembly. Altogether, we believe Pitx2 may play a role in late muscle formation and maturation.

FUTURE DIRECTIONS

With these preliminary data and the available conditional knockout mouse model, we will further investigate the involvement of Pitx2 during forelimb muscle development in fetal/neonatal and adult stage. The Pax3, Pax7, Myf5 and MCK expression will be investigated in Pitx2^{Pax3} and Pitx2^{MCK} mice to determine Pitx2's cell autonomous effect and time of onset at E14.5, E16.5 and E18.5 embryos by using immunohistochemistry. The Pitx2 effects on morphology will be investigated on postnatal Pitx2^{Pax3} and Pitx2^{MCK} muscles by using HE staining, ATPase staining and SDH staining to determine the myofiber morphology and slow/fast muscle ratio. The immunohistochemistry on Pitx2^{Pax3} and Pitx2^{MCK} postnatal muscles will be used to investigate the molecular alteration by against MyHC isoforms. The motion and behavior will be observed on both conditional mice from birth to adulthood.

Disruption in any steps of myogenesis will result in some sort of myopathies. Completion of these studies will establish how Pitx2 regulates embryonic and fetal myoblasts to generate proper myofibers. By addressing the mechanism of myofiber formation and assembly, we will have a better understanding the function of Pitx2 during embryonic forelimb development. Our long term goal is to identify gene networks that are involved in embryonic and fetal myogenesis. The clarification of molecular and cellular mechanisms will provide fundamental view in developing strategies for treatment of myopathies.

BIBLIOGRAPHY

Abu-Issa, R., Smyth, G., Smoak, I., Yamamura, K., and Meyers, E.N. (2002). Fgf8 is required for pharyngeal arch and cardiovascular development in the mouse. Development *129*, 4613-4625.

Ai, D., Liu, W., Ma, L., Dong, F., Lu, M.F., Wang, D., Verzi, M.P., Cai, C., Gage, P.J., Evans, S.*, et al.* (2006). Pitx2 regulates cardiac left-right asymmetry by patterning second cardiac lineage-derived myocardium. Dev Biol *296*, 437-449.

Amendt, B.A., Sutherland, L.B., Semina, E.V., and Russo, A.F. (1998). The molecular basis of Rieger syndrome. Analysis of Pitx2 homeodomain protein activities. The Journal of biological chemistry *273*, 20066-20072.

Arima, Y., Miyagawa-Tomita, S., Maeda, K., Asai, R., Seya, D., Minoux, M., Rijli, F.M., Nishiyama, K., Kim, K.S., Uchijima, Y.*, et al.* (2012). Preotic neural crest cells contribute to coronary artery smooth muscle involving endothelin signalling. Nature communications *3*, 1267.

Bajard, L., Relaix, F., Lagha, M., Rocancourt, D., Daubas, P., and Buckingham, M.E. (2006). A novel genetic hierarchy functions during hypaxial myogenesis: Pax3 directly activates Myf5 in muscle progenitor cells in the limb. Genes & development *20*, 2450-2464.

Bertrand, N., Roux, M., Ryckebusch, L., Niederreither, K., Dolle, P., Moon, A., Capecchi, M., and Zaffran, S. (2011). Hox genes define distinct progenitor sub-domains within the second heart field. Developmental biology *353*, 266-274.

Birchmeier, C., and Brohmann, H. (2000). Genes that control the development of migrating muscle precursor cells. Curr Opin Cell Biol *12*, 725-730.

Biressi, S., Molinaro, M., and Cossu, G. (2007a). Cellular heterogeneity during vertebrate skeletal muscle development. Developmental biology *308*, 281-293.

Biressi, S., Tagliafico, E., Lamorte, G., Monteverde, S., Tenedini, E., Roncaglia, E., Ferrari, S., Cusella-De Angelis, M.G., Tajbakhsh, S., and Cossu, G. (2007b). Intrinsic phenotypic diversity of embryonic and fetal myoblasts is revealed by genome-wide gene expression analysis on purified cells. Developmental biology *304*, 633-651.

Biressi, S., Tagliafico, E., Lamorte, G., Monteverde, S., Tenedini, E., Roncaglia, E., Ferrari, S., Ferrari, S., Cusella-De Angelis, M.G., Tajbakhsh, S.*, et al.* (2007c). Intrinsic phenotypic diversity of embryonic and fetal myoblasts is

revealed by genome-wide gene expression analysis on purified cells. Developmental biology *304*, 633-651.

Bober, E., Franz, T., Arnold, H.H., Gruss, P., and Tremblay, P. (1994). Pax-3 is required for the development of limb muscles: a possible role for the migration of dermomyotomal muscle progenitor cells. Development *120*, 603-612.

Borycki, A.G., Brunk, B., Tajbakhsh, S., Buckingham, M., Chiang, C., and Emerson, C.P., Jr. (1999). Sonic hedgehog controls epaxial muscle determination through Myf5 activation. Development *126*, 4053-4063.

Bottinelli, R. (2001). Functional heterogeneity of mammalian single muscle fibres: do myosin isoforms tell the whole story? Pflugers Archiv : European journal of physiology *443*, 6-17.

Braun, T., Rudnicki, M.A., Arnold, H.H., and Jaenisch, R. (1992). Targeted inactivation of the muscle regulatory gene Myf-5 results in abnormal rib development and perinatal death. Cell *71*, 369-382.

Brown, C.B., Boyer, A.S., Runyan, R.B., and Barnett, J.V. (1996). Antibodies to the Type II TGFbeta receptor block cell activation and migration during atrioventricular cushion transformation in the heart. Dev Biol *174*, 248-257.

Bruneau, B.G., Nemer, G., Schmitt, J.P., Charron, F., Robitaille, L., Caron, S., Conner, D.A., Gessler, M., Nemer, M., Seidman, C.E.*, et al.* (2001). A murine model of Holt-Oram syndrome defines roles of the T-box transcription factor Tbx5 in cardiogenesis and disease. Cell *106*, 709-721.

Bruning, J.C., Michael, M.D., Winnay, J.N., Hayashi, T., Horsch, D., Accili, D., Goodyear, L.J., and Kahn, C.R. (1998). A muscle-specific insulin receptor knockout exhibits features of the metabolic syndrome of NIDDM without altering glucose tolerance. Molecular cell *2*, 559-569.

Buckingham, M., Meilhac, S., and Zaffran, S. (2005). Building the mammalian heart from two sources of myocardial cells. Nature reviews Genetics *6*, 826-835.

Burke, A.C., and Nowicki, J.L. (2003). A new view of patterning domains in the vertebrate mesoderm. Dev Cell *4*, 159-165.

Cai, C.L., Liang, X., Shi, Y., Chu, P.H., Pfaff, S.L., Chen, J., and Evans, S. (2003). Isl1 identifies a cardiac progenitor population that proliferates prior to differentiation and contributes a majority of cells to the heart. Developmental cell *5*, 877-889.

Campbell, A.L., Eng, D., Gross, M.K., and Kioussi, C. (2012a). Prediction of gene network models in limb muscle precursors. Gene *509*, 16-23.

Campbell, A.L., Shih, H.P., Xu, J., Gross, M.K., and Kioussi, C. (2012b). Regulation of motility of myogenic cells in filling limb muscle anlagen by Pitx2. PloS one *7*, e35822.

Campione, M., Ros, M.A., Icardo, J.M., Piedra, E., Christoffels, V.M., Schweickert, A., Blum, M., Franco, D., and Moorman, A.F. (2001). Pitx2 expression defines a left cardiac lineage of cells: evidence for atrial and ventricular molecular isomerism in the iv/iv mice. Developmental biology *231*, 252-264.

Cheng, L., Alvares, L.E., Ahmed, M.U., El-Hanfy, A.S., and Dietrich, S. (2004). The epaxial-hypaxial subdivision of the avian somite. Dev Biol *274*, 348-369.

Christ, B., Jacob, M., and Jacob, H.J. (1983). On the origin and development of the ventrolateral abdominal muscles in the avian embryo. An experimental and ultrastructural study. Anatomy and embryology *166*, 87-101.

Cornelison, D.D., and Wold, B.J. (1997). Single-cell analysis of regulatory gene expression in quiescent and activated mouse skeletal muscle satellite cells. Developmental biology *191*, 270-283.

Dietrich, S., Abou-Rebyeh, F., Brohmann, H., Bladt, F., Sonnenberg-Riethmacher, E., Yamaai, T., Lumsden, A., Brand-Saberi, B., and Birchmeier, C. (1999). The role of SF/HGF and c-Met in the development of skeletal muscle. Development *126*, 1621-1629.

Dixit, M., Ansseau, E., Tassin, A., Winokur, S., Shi, R., Qian, H., Sauvage, S., Matteotti, C., van Acker, A.M., Leo, O.*, et al.* (2007). DUX4, a candidate gene of facioscapulohumeral muscular dystrophy, encodes a transcriptional activator of PITX1. Proceedings of the National Academy of Sciences of the United States of America *104*, 18157-18162.

Dodou, E., Verzi, M.P., Anderson, J.P., Xu, S.M., and Black, B.L. (2004). Mef2c is a direct transcriptional target of ISL1 and GATA factors in the anterior heart field during mouse embryonic development. Development *131*, 3931-3942.

Duxson, M.J., Usson, Y., and Harris, A.J. (1989). The origin of secondary myotubes in mammalian skeletal muscles: ultrastructural studies. Development *107*, 743-750.

Echelard, Y., Vassileva, G., and McMahon, A.P. (1994). Cis-acting regulatory sequences governing Wnt-1 expression in the developing mouse CNS. Development *120*, 2213-2224.

Eng, D., Campbell, A., Hilton, T., Leid, M., Gross, M.K., and Kioussi, C. (2010). Prediction of regulatory networks in mouse abdominal wall. Gene *469*, 1-8.

Eng, D., and Dubovoy, A. (2012). High Left Ventricular Vent Return After Left and Right Ventricular Assist Device Placement in a Patient With a Mechanical Aortic Valve. J Cardiothorac Vasc Anesth.

Eng, D., Ma, H.Y., Xu, J., Shih, H.P., Gross, M.K., and Kiouss, C. (2012a). Loss of abdominal muscle in Pitx2 mutants associated with altered axial specification of lateral plate mesoderm. PLoS One *7*, e42228.

Eng, D., Ma, H.Y., Xu, J., Shih, H.P., Gross, M.K., and Kioussi, C. (2012b). Loss of abdominal muscle in Pitx2 mutants associated with altered axial specification of lateral plate mesoderm. PloS one *7*, e42228.

Engleka, K.A., Gitler, A.D., Zhang, M., Zhou, D.D., High, F.A., and Epstein, J.A. (2005). Insertion of Cre into the Pax3 locus creates a new allele of Splotch and identifies unexpected Pax3 derivatives. Developmental biology *280*, 396-406.

Engleka, K.A., Manderfield, L.J., Brust, R.D., Li, L., Cohen, A., Dymecki, S.M., and Epstein, J.A. (2012). Islet1 derivatives in the heart are of both neural crest and second heart field origin. Circulation research *110*, 922-926.

Epstein, J.A., Shapiro, D.N., Cheng, J., Lam, P.Y., and Maas, R.L. (1996). Pax3 modulates expression of the c-Met receptor during limb muscle development. Proceedings of the National Academy of Sciences of the United States of America *93*, 4213-4218.

Evans, S.M., Yelon, D., Conlon, F.L., and Kirby, M.L. (2010). Myocardial lineage development. Circulation research *107*, 1428-1444.

Franco, D., and Campione, M. (2003). The role of Pitx2 during cardiac development. Linking left-right signaling and congenital heart diseases. Trends Cardiovasc Med *13*, 157-163.

Frank, D.U., Fotheringham, L.K., Brewer, J.A., Muglia, L.J., Tristani-Firouzi, M., Capecchi, M.R., and Moon, A.M. (2002). An Fgf8 mouse mutant phenocopies human 22q11 deletion syndrome. Development *129*, 4591-4603.

Gage, P.J., Rhoades, W., Prucka, S.K., and Hjalt, T. (2005). Fate maps of neural crest and mesoderm in the mammalian eye. Invest Ophthalmol Vis Sci *46*, 4200-4208.

Gage, P.J., Suh, H., and Camper, S.A. (1999a). The bicoid-related Pitx gene family in development. Mammalian genome : official journal of the International Mammalian Genome Society *10*, 197-200.

Gage, P.J., Suh, H., and Camper, S.A. (1999b). Dosage requirement of Pitx2 for development of multiple organs. Development *126*, 4643-4651.

Galli, D., Dominguez, J.N., Zaffran, S., Munk, A., Brown, N.A., and Buckingham, M.E. (2008). Atrial myocardium derives from the posterior region of the second heart field, which acquires left-right identity as Pitx2c is expressed. Development *135*, 1157-1167.

Ganga, M., Espinoza, H.M., Cox, C.J., Morton, L., Hjalt, T.A., Lee, Y., and Amendt, B.A. (2003). PITX2 isoform-specific regulation of atrial natriuretic factor expression: synergism and repression with Nkx2.5. J Biol Chem *278*, 22437-22445.

Garg, V., Kathiriya, I.S., Barnes, R., Schluterman, M.K., King, I.N., Butler, C.A., Rothrock, C.R., Eapen, R.S., Hirayama-Yamada, K., Joo, K.*, et al.* (2003). GATA4 mutations cause human congenital heart defects and reveal an interaction with TBX5. Nature *424*, 443-447.

Gayraud-Morel, B., Chretien, F., Flamant, P., Gomes, D., Zammit, P.S., and Tajbakhsh, S. (2007). A role for the myogenic determination gene Myf5 in adult regenerative myogenesis. Developmental biology *312*, 13-28.

Goulding, M., Lumsden, A., and Paquette, A.J. (1994). Regulation of Pax-3 expression in the dermomyotome and its role in muscle development. Development *120*, 957-971.

Grifone, R., Demignon, J., Giordani, J., Niro, C., Souil, E., Bertin, F., Laclef, C., Xu, P.X., and Maire, P. (2007). Eya1 and Eya2 proteins are required for hypaxial somitic myogenesis in the mouse embryo. Developmental biology *302*, 602-616.

Grifone, R., Demignon, J., Houbron, C., Souil, E., Niro, C., Seller, M.J., Hamard, G., and Maire, P. (2005). Six1 and Six4 homeoproteins are required for Pax3 and Mrf expression during myogenesis in the mouse embryo. Development *132*, 2235-2249.

Gross, M.K., Dottori, M., and Goulding, M. (2002). Lbx1 specifies somatosensory association interneurons in the dorsal spinal cord. Neuron *34*, 535-549.

Gross, M.K., Moran-Rivard, L., Velasquez, T., Nakatsu, M.N., Jagla, K., and Goulding, M. (2000). Lbx1 is required for muscle precursor migration along a lateral pathway into the limb. Development *127*, 413-424.

Gunning, P., and Hardeman, E. (1991). Multiple mechanisms regulate muscle fiber diversity. FASEB journal : official publication of the Federation of American Societies for Experimental Biology *5*, 3064-3070.

Guo, C., Sun, Y., Zhou, B., Adam, R.M., Li, X., Pu, W.T., Morrow, B.E., Moon, A., and Li, X. (2011). A Tbx1-Six1/Eya1-Fgf8 genetic pathway controls mammalian cardiovascular and craniofacial morphogenesis. The Journal of clinical investigation *121*, 1585-1595.

Hamblet, N.S., Lijam, N., Ruiz-Lozano, P., Wang, J., Yang, Y., Luo, Z., Mei, L., Chien, K.R., Sussman, D.J., and Wynshaw-Boris, A. (2002). Dishevelled 2 is essential for cardiac outflow tract development, somite segmentation and neural tube closure. Development *129*, 5827-5838.

Harel, I., Maezawa, Y.,Avraham, R., Rinon, A., Ma, H., Cross, J. W., Leviatan, N., Hegesh, J. T., Roy, A., Jacob-Hirsch, J., Rechavi, G., Carvajhal, J., Tole, S., Kioussi, C., Quaggin, S.and Tzahor, E. (2012). Pharyngeal mesoderm regulatory network controls cardiac and head muscle morphogenesis. PNAS.

Harel I, M.Y., Avraham R, Rinon A, Ma HY, Cross J.W, Leviatan N, Hegesh J. T, Roy A, Jacob-Hirsch J, Rechavi G, Carvajal J, Tole S, Kioussi C, Quaggin S, and Tzahor E (2012). Pharyngeal mesoderm regulatory network controls cardiac and head muscle morphogenesis. Proceedings of the National Academy of Sciences. PNAS *in press*.

Harvey, R.P. (2002). Patterning the vertebrate heart. Nat Rev Genet *3*, 544-556.

Hasty, P., Bradley, A., Morris, J.H., Edmondson, D.G., Venuti, J.M., Olson, E.N., and Klein, W.H. (1993). Muscle deficiency and neonatal death in mice with a targeted mutation in the myogenin gene. Nature *364*, 501-506.

Hilton, T., Gross, M.K., and Kioussi, C. (2010). Pitx2-dependent occupancy by histone deacetylases is associated with T-box gene regulation in mammalian abdominal tissue. J Biol Chem *285*, 11129-11142.

Hinterberger, T.J., Sassoon, D.A., Rhodes, S.J., and Konieczny, S.F. (1991). Expression of the muscle regulatory factor MRF4 during somite and skeletal myofiber development. Developmental biology *147*, 144-156.

Hoffman, J.I., and Kaplan, S. (2002). The incidence of congenital heart disease. J Am Coll Cardiol *39*, 1890-1900.

Hu, T., Yamagishi, H., Maeda, J., McAnally, J., Yamagishi, C., and Srivastava, D. (2004). Tbx1 regulates fibroblast growth factors in the anterior heart field through a reinforcing autoregulatory loop involving forkhead transcription factors. Development *131*, 5491-5502.

Hurlstone, A.F., Haramis, A.P., Wienholds, E., Begthel, H., Korving, J., Van Eeden, F., Cuppen, E., Zivkovic, D., Plasterk, R.H., and Clevers, H. (2003). The Wnt/beta-catenin pathway regulates cardiac valve formation. Nature *425*, 633-637.

Hutcheson, D.A., Zhao, J., Merrell, A., Haldar, M., and Kardon, G. (2009). Embryonic and fetal limb myogenic cells are derived from developmentally distinct progenitors and have different requirements for beta-catenin. Genes & development *23*, 997-1013.

Ilagan, R., Abu-Issa, R., Brown, D., Yang, Y.P., Jiao, K., Schwartz, R.J., Klingensmith, J., and Meyers, E.N. (2006). Fgf8 is required for anterior heart field development. Development *133*, 2435-2445.

Jostes, B., Walther, C., and Gruss, P. (1990). The murine paired box gene, Pax7, is expressed specifically during the development of the nervous and muscular system. Mech Dev *33*, 27-37.

Joyner, A., and Wall, N. (2008). Immunohistochemistry of whole-mount mouse embryos. CSH Protoc *2008*, pdb prot4820.

Kassar-Duchossoy, L., Gayraud-Morel, B., Gomes, D., Rocancourt, D., Buckingham, M., Shinin, V., and Tajbakhsh, S. (2004). Mrf4 determines skeletal muscle identity in Myf5:Myod double-mutant mice. Nature *431*, 466-471.

Kassar-Duchossoy, L., Giacone, E., Gayraud-Morel, B., Jory, A., Gomes, D., and Tajbakhsh, S. (2005). Pax3/Pax7 mark a novel population of primitive myogenic cells during development. Genes & development *19*, 1426-1431.

Kelly, R.G. (2005). Molecular inroads into the anterior heart field. Trends Cardiovasc Med *15*, 51-56.

Kelly, R.G., Brown, N.A., and Buckingham, M.E. (2001). The arterial pole of the mouse heart forms from Fgf10-expressing cells in pharyngeal mesoderm. Dev Cell *1*, 435-440.

Kelly, R.G., and Papaioannou, V.E. (2007). Visualization of outflow tract development in the absence of Tbx1 using an FgF10 enhancer trap transgene. Dev Dyn *236*, 821-828.

Kioussi, C., Briata, P., Baek, S.H., Rose, D.W., Hamblet, N.S., Herman, T., Ohgi, K.A., Lin, C., Gleiberman, A., Wang, J.*, et al.* (2002). Identification of a Wnt/Dvl/beta-Catenin --> Pitx2 pathway mediating cell-type-specific proliferation during development. Cell *111*, 673-685.

Kirby, M. (2007). Cardiac Development (Oxford University Press, New York).

Kirby, M.L., Gale, T.F., and Stewart, D.E. (1983). Neural crest cells contribute to normal aorticopulmonary septation. Science *220*, 1059-1061.

Kirby, M.L., and Hutson, M.R. (2010). Factors controlling cardiac neural crest cell migration. Cell adhesion & migration *4*, 609-621.

Kitamura, K., Miura, H., Miyagawa-Tomita, S., Yanazawa, M., Katoh-Fukui, Y., Suzuki, R., Ohuchi, H., Suehiro, A., Motegi, Y., Nakahara, Y.*, et al.* (1999). Mouse Pitx2 deficiency leads to anomalies of the ventral body wall, heart, extra- and periocular mesoderm and right pulmonary isomerism. Development *126*, 5749-5758.

Krumlauf, R. (1994). Hox genes in vertebrate development. Cell *78*, 191-201.

Kume, T., Jiang, H., Topczewska, J.M., and Hogan, B.L. (2001). The murine winged helix transcription factors, Foxc1 and Foxc2, are both required for cardiovascular development and somitogenesis. Genes & development *15*, 2470-2482.

Kyrylkova, K., Kyryachenko, S., Kioussi, C., and Leid, M. (2012). Determination of gene expression patterns by in situ hybridization in sections. Methods Mol Biol *887*, 23-31.

L'Honore, A., Coulon, V., Marcil, A., Lebel, M., Lafrance-Vanasse, J., Gage, P., Camper, S., and Drouin, J. (2007). Sequential expression and redundancy of Pitx2 and Pitx3 genes during muscle development. Developmental biology *307*, 421-433.

L'Honore, A., Ouimette, J.F., Lavertu-Jolin, M., and Drouin, J. (2010). Pitx2 defines alternate pathways acting through MyoD during limb and somitic myogenesis. Development *137*, 3847-3856.

Lavine, K.J., and Ornitz, D.M. (2008). Fibroblast growth factors and Hedgehogs: at the heart of the epicardial signaling center. Trends in genetics : TIG *24*, 33-40.

Li, P., Pashmforoush, M., and Sucov, H.M. (2010). Retinoic acid regulates differentiation of the secondary heart field and TGFbeta-mediated outflow tract septation. Developmental cell *18*, 480-485.

Lin, C.R., Kioussi, C., O'Connell, S., Briata, P., Szeto, D., Liu, F., Izpisua-Belmonte, J.C., and Rosenfeld, M.G. (1999). Pitx2 regulates lung asymmetry, cardiac positioning and pituitary and tooth morphogenesis. Nature *401*, 279-282.

Lin, Q., Schwarz, J., Bucana, C., and Olson, E.N. (1997). Control of mouse cardiac morphogenesis and myogenesis by transcription factor MEF2C. Science *276*, 1404-1407.

Liu, C., Liu, W., Palie, J., Lu, M.F., Brown, N.A., and Martin, J.F. (2002). Pitx2c patterns anterior myocardium and aortic arch vessels and is required for local cell movement into atrioventricular cushions. Development *129*, 5081-5091.

Liu, W., Selever, J., Lu, M.F., and Martin, J.F. (2003). Genetic dissection of Pitx2 in craniofacial development uncovers new functions in branchial arch morphogenesis, late aspects of tooth morphogenesis and cell migration. Development *130*, 6375-6385.

Liu, W., Selever, J., Wang, D., Lu, M.F., Moses, K.A., Schwartz, R.J., and Martin, J.F. (2004). Bmp4 signaling is required for outflow-tract septation and branchial-arch artery remodeling. Proc Natl Acad Sci U S A *101*, 4489-4494.

Liu, Y., Cserjesi, P., Nifuji, A., Olson, E.N., and Noda, M. (1996). Sclerotome-related helix-loop-helix type transcription factor (scleraxis) mRNA is expressed in osteoblasts and its level is enhanced by type-beta transforming growth factor. The Journal of endocrinology *151*, 491-499.

Lopez-Sanchez, C., and Garcia-Martinez, V. (2011). Molecular determinants of cardiac specification. Cardiovascular research *91*, 185-195.

Lozano-Velasco, E., Chinchilla, A., Martinez-Fernandez, S., Hernandez-Torres, F., Navarro, F., Lyons, G.E., Franco, D., and Aranega, A.E. (2011a). Pitx2c

modulates cardiac-specific transcription factors networks in differentiating cardiomyocytes from murine embryonic stem cells. Cells, tissues, organs *194*, 349-362.

Lozano-Velasco, E., Contreras, A., Crist, C., Hernandez-Torres, F., Franco, D., and Aranega, A.E. (2011b). Pitx2c modulates Pax3+/Pax7+ cell populations and regulates Pax3 expression by repressing miR27 expression during myogenesis. Developmental biology *357*, 165-178.

Lu, M.F., Pressman, C., Dyer, R., Johnson, R.L., and Martin, J.F. (1999). Function of Rieger syndrome gene in left-right asymmetry and craniofacial development. Nature *401*, 276-278.

Lyons, I., Parsons, L.M., Hartley, L., Li, R., Andrews, J.E., Robb, L., and Harvey, R.P. (1995). Myogenic and morphogenetic defects in the heart tubes of murine embryos lacking the homeo box gene Nkx2-5. Genes & development *9*, 1654-1666.

Lyons, K.M., Pelton, R.W., and Hogan, B.L. (1990). Organogenesis and pattern formation in the mouse: RNA distribution patterns suggest a role for bone morphogenetic protein-2A (BMP-2A). Development *109*, 833-844.

Ma, H.Y., Xu, J., Eng, D., Gross, M.K., and Kioussi, C. (2013). Pitx2-mediated cardiac outflow tract remodeling. Developmental dynamics : an official publication of the American Association of Anatomists *242*, 456-468.

Ma, L., Lu, M.F., Schwartz, R.J., and Martin, J.F. (2005). Bmp2 is essential for cardiac cushion epithelial-mesenchymal transition and myocardial patterning. Development *132*, 5601-5611.

Makki, N., and Capecchi, M.R. (2010). Hoxa1 lineage tracing indicates a direct role for Hoxa1 in the development of the inner ear, the heart, and the third rhombomere. Developmental biology *341*, 499-509.

Mao, X., Fujiwara, Y., Chapdelaine, A., Yang, H., and Orkin, S.H. (2001). Activation of EGFP expression by Cre-mediated excision in a new ROSA26 reporter mouse strain. Blood *97*, 324-326.

Maroto, M., Reshef, R., Munsterberg, A.E., Koester, S., Goulding, M., and Lassar, A.B. (1997). Ectopic Pax-3 activates MyoD and Myf-5 expression in embryonic mesoderm and neural tissue. Cell *89*, 139-148.

McCulley, D.J., Kang, J.O., Martin, J.F., and Black, B.L. (2008). BMP4 is required in the anterior heart field and its derivatives for endocardial cushion

remodeling, outflow tract septation, and semilunar valve development. Dev Dyn *237*, 3200-3209.

McGinnis, W., Levine, M.S., Hafen, E., Kuroiwa, A., and Gehring, W.J. (1984). A conserved DNA sequence in homoeotic genes of the Drosophila Antennapedia and bithorax complexes. Nature *308*, 428-433.

Messina, G., Biressi, S., Monteverde, S., Magli, A., Cassano, M., Perani, L., Roncaglia, E., Tagliafico, E., Starnes, L., Campbell, C.E.*, et al.* (2010). Nfix regulates fetal-specific transcription in developing skeletal muscle. Cell *140*, 554-566.

Mjaatvedt, C.H., Nakaoka, T., Moreno-Rodriguez, R., Norris, R.A., Kern, M.J., Eisenberg, C.A., Turner, D., and Markwald, R.R. (2001). The outflow tract of the heart is recruited from a novel heart-forming field. Developmental biology *238*, 97-109.

Montarras, D., Chelly, J., Bober, E., Arnold, H., Ott, M.O., Gros, F., and Pinset, C. (1991). Developmental patterns in the expression of Myf5, MyoD, myogenin, and MRF4 during myogenesis. The New biologist *3*, 592-600.

Monzen, K., Shiojima, I., Hiroi, Y., Kudoh, S., Oka, T., Takimoto, E., Hayashi, D., Hosoda, T., Habara-Ohkubo, A., Nakaoka, T.*, et al.* (1999). Bone morphogenetic proteins induce cardiomyocyte differentiation through the mitogen-activated protein kinase kinase kinase TAK1 and cardiac transcription factors Csx/Nkx-2.5 and GATA-4. Mol Cell Biol *19*, 7096-7105.

Murphy, M., and Kardon, G. (2011). Origin of vertebrate limb muscle: the role of progenitor and myoblast populations. Curr Top Dev Biol *96*, 1-32.

Nabeshima, Y., Hanaoka, K., Hayasaka, M., Esumi, E., Li, S., Nonaka, I., and Nabeshima, Y. (1993). Myogenin gene disruption results in perinatal lethality because of severe muscle defect. Nature *364*, 532-535.

Nameroff, M., and Rhodes, L.D. (1989). Differential response among cells in the chick embryo myogenic lineage to photosensitization by Merocyanine 540. Journal of cellular physiology *141*, 475-482.

Niessen, K., and Karsan, A. (2008). Notch signaling in cardiac development. Circ Res *102*, 1169-1181.

Niro, C., Demignon, J., Vincent, S., Liu, Y., Giordani, J., Sgarioto, N., Favier, M., Guillet-Deniau, I., Blais, A., and Maire, P. (2010). Six1 and Six4 gene

expression is necessary to activate the fast-type muscle gene program in the mouse primary myotome. Developmental biology *338*, 168-182.

Nowotschin, S., Liao, J., Gage, P.J., Epstein, J.A., Campione, M., and Morrow, B.E. (2006). Tbx1 affects asymmetric cardiac morphogenesis by regulating Pitx2 in the secondary heart field. Development *133*, 1565-1573.

Oliver, G., Wehr, R., Jenkins, N.A., Copeland, N.G., Cheyette, B.N., Hartenstein, V., Zipursky, S.L., and Gruss, P. (1995). Homeobox genes and connective tissue patterning. Development *121*, 693-705.

Ontell, M., Ontell, M.P., Sopper, M.M., Mallonga, R., Lyons, G., and Buckingham, M. (1993). Contractile protein gene expression in primary myotubes of embryonic mouse hindlimb muscles. Development *117*, 1435-1444.

Oustanina, S., Hause, G., and Braun, T. (2004). Pax7 directs postnatal renewal and propagation of myogenic satellite cells but not their specification. The EMBO journal *23*, 3430-3439.

Pandey, S.N., Cabotage, J., Shi, R., Dixit, M., Sutherland, M., Liu, J., Muger, S., Harper, S.Q., Nagaraju, K., and Chen, Y.W. (2012). Conditional over-expression of PITX1 causes skeletal muscle dystrophy in mice. Biology open *1*, 629-639.

Park, E.J., Watanabe, Y., Smyth, G., Miyagawa-Tomita, S., Meyers, E., Klingensmith, J., Camenisch, T., Buckingham, M., and Moon, A.M. (2008). An FGF autocrine loop initiated in second heart field mesoderm regulates morphogenesis at the arterial pole of the heart. Development *135*, 3599-3610.

Perveen, R., Lloyd, I.C., Clayton-Smith, J., Churchill, A., van Heyningen, V., Hanson, I., Taylor, D., McKeown, C., Super, M., Kerr, B.*, et al.* (2000). Phenotypic variability and asymmetry of Rieger syndrome associated with PITX2 mutations. Invest Ophthalmol Vis Sci *41*, 2456-2460.

Prall, O.W., Menon, M.K., Solloway, M.J., Watanabe, Y., Zaffran, S., Bajolle, F., Biben, C., McBride, J.J., Robertson, B.R., Chaulet, H.*, et al.* (2007). An Nkx2-5/Bmp2/Smad1 negative feedback loop controls heart progenitor specification and proliferation. Cell *128*, 947-959.

Qiu, H.Y., Guo, C., Cheng, X.W., Huang, Y., Xiong, Z.Q., and Ding, Y.Q. (2008). Pitx3-CreER mice showing restricted Cre expression in developing ocular lens and skeletal muscles. Genesis *46*, 324-328.

Ray, H.J., and Niswander, L. (2012). Mechanisms of tissue fusion during development. Development *139*, 1701-1711.

Relaix, F., Polimeni, M., Rocancourt, D., Ponzetto, C., Schafer, B.W., and Buckingham, M. (2003). The transcriptional activator PAX3-FKHR rescues the defects of Pax3 mutant mice but induces a myogenic gain-of-function phenotype with ligand-independent activation of Met signaling in vivo. Genes & development *17*, 2950-2965.

Relaix, F., Rocancourt, D., Mansouri, A., and Buckingham, M. (2004). Divergent functions of murine Pax3 and Pax7 in limb muscle development. Genes & development *18*, 1088-1105.

Relaix, F., Rocancourt, D., Mansouri, A., and Buckingham, M. (2005). A Pax3/Pax7-dependent population of skeletal muscle progenitor cells. Nature *435*, 948-953.

Romano, L.A., and Runyan, R.B. (2000). Slug is an essential target of TGFbeta2 signaling in the developing chicken heart. Dev Biol *223*, 91-102.

Ross, J.J., Duxson, M.J., and Harris, A.J. (1987). Formation of primary and secondary myotubes in rat lumbrical muscles. Development *100*, 383-394.

Rudnicki, M.A., Braun, T., Hinuma, S., and Jaenisch, R. (1992). Inactivation of MyoD in mice leads to up-regulation of the myogenic HLH gene Myf-5 and results in apparently normal muscle development. Cell *71*, 383-390.

Rudnicki, M.A., Schnegelsberg, P.N., Stead, R.H., Braun, T., Arnold, H.H., and Jaenisch, R. (1993). MyoD or Myf-5 is required for the formation of skeletal muscle. Cell *75*, 1351-1359.

Sassoon, D., Lyons, G., Wright, W.E., Lin, V., Lassar, A., Weintraub, H., and Buckingham, M. (1989). Expression of two myogenic regulatory factors myogenin and MyoD1 during mouse embryogenesis. Nature *341*, 303-307.

Schnabel, R.B. (2011). Comparison of approaches to fine-map first-generation genome-wide association study results at chromosome 9p21. Circ Cardiovasc Genet *4*, 577-578.

Schubert, F.R., Tremblay, P., Mansouri, A., Faisst, A.M., Kammandel, B., Lumsden, A., Gruss, P., and Dietrich, S. (2001). Early mesodermal phenotypes in splotch suggest a role for Pax3 in the formation of epithelial somites. Dev Dyn *222*, 506-521.

Seale, P., and Rudnicki, M.A. (2000). A new look at the origin, function, and "stem-cell" status of muscle satellite cells. Developmental biology *218*, 115-124.

Semina, E.V., Ferrell, R.E., Mintz-Hittner, H.A., Bitoun, P., Alward, W.L., Reiter, R.S., Funkhauser, C., Daack-Hirsch, S., and Murray, J.C. (1998). A novel homeobox gene PITX3 is mutated in families with autosomal-dominant cataracts and ASMD. Nature genetics *19*, 167-170.

Semina, E.V., Reiter, R., Leysens, N.J., Alward, W.L., Small, K.W., Datson, N.A., Siegel-Bartelt, J., Bierke-Nelson, D., Bitoun, P., Zabel, B.U*., et al.* (1996). Cloning and characterization of a novel bicoid-related homeobox transcription factor gene, RIEG, involved in Rieger syndrome. Nature genetics *14*, 392-399.

Shih, H.P., Gross, M.K., and Kioussi, C. (2007a). Cranial muscle defects of Pitx2 mutants result from specification defects in the first branchial arch. Proceedings of the National Academy of Sciences of the United States of America *104*, 5907-5912.

Shih, H.P., Gross, M.K., and Kioussi, C. (2007b). Cranial muscle defects of Pitx2 mutants result from specification defects in the first branchial arch. Proc Natl Acad Sci U S A *104*, 5907-5912.

Shih, H.P., Gross, M.K., and Kioussi, C. (2007c). Expression pattern of the homeodomain transcription factor Pitx2 during muscle development. Gene expression patterns : GEP *7*, 441-451.

Smidt, M.P., Smits, S.M., and Burbach, J.P. (2004). Homeobox gene Pitx3 and its role in the development of dopamine neurons of the substantia nigra. Cell and tissue research *318*, 35-43.

Stockdale, F.E. (1992). Myogenic cell lineages. Developmental biology *154*, 284-298.

Sucov, H.M., Gu, Y., Thomas, S., Li, P., and Pashmforoush, M. (2009). Epicardial control of myocardial proliferation and morphogenesis. Pediatric cardiology *30*, 617-625.

Suga, H., Tschopp, P., Graziussi, D.F., Stierwald, M., Schmid, V., and Gehring, W.J. (2010). Flexibly deployed Pax genes in eye development at the early evolution of animals demonstrated by studies on a hydrozoan jellyfish. Proceedings of the National Academy of Sciences of the United States of America *107*, 14263-14268.

Tajbakhsh, S., Borello, U., Vivarelli, E., Kelly, R., Papkoff, J., Duprez, D., Buckingham, M., and Cossu, G. (1998). Differential activation of Myf5 and MyoD by different Wnts in explants of mouse paraxial mesoderm and the later activation of myogenesis in the absence of Myf5. Development *125*, 4155-4162.

Tajbakhsh, S., Rocancourt, D., Cossu, G., and Buckingham, M. (1997). Redefining the genetic hierarchies controlling skeletal myogenesis: Pax-3 and Myf-5 act upstream of MyoD. Cell *89*, 127-138.

Takeuchi, J.K., and Bruneau, B.G. (2009). Directed transdifferentiation of mouse mesoderm to heart tissue by defined factors. Nature *459*, 708-711.

Tanaka, M., Wechsler, S.B., Lee, I.W., Yamasaki, N., Lawitts, J.A., and Izumo, S. (1999). Complex modular cis-acting elements regulate expression of the cardiac specifying homeobox gene Csx/Nkx2.5. Development *126*, 1439-1450.

Tessari, A., Pietrobon, M., Notte, A., Cifelli, G., Gage, P.J., Schneider, M.D., Lembo, G., and Campione, M. (2008). Myocardial Pitx2 differentially regulates the left atrial identity and ventricular asymmetric remodeling programs. Circ Res *102*, 813-822.

Theveniau-Ruissy, M., Dandonneau, M., Mesbah, K., Ghez, O., Mattei, M.G., Miquerol, L., and Kelly, R.G. (2008). The del22q11.2 candidate gene Tbx1 controls regional outflow tract identity and coronary artery patterning. Circulation research *103*, 142-148.

Tirosh-Finkel, L., Elhanany, H., Rinon, A., and Tzahor, E. (2006). Mesoderm progenitor cells of common origin contribute to the head musculature and the cardiac outflow tract. Development *133*, 1943-1953.

Verzi, M.P., McCulley, D.J., De Val, S., Dodou, E., and Black, B.L. (2005). The right ventricle, outflow tract, and ventricular septum comprise a restricted expression domain within the secondary/anterior heart field. Dev Biol *287*, 134-145.

Vitelli, F., Morishima, M., Taddei, I., Lindsay, E.A., and Baldini, A. (2002). Tbx1 mutation causes multiple cardiovascular defects and disrupts neural crest and cranial nerve migratory pathways. Hum Mol Genet *11*, 915-922.

von Both, I., Silvestri, C., Erdemir, T., Lickert, H., Walls, J.R., Henkelman, R.M., Rossant, J., Harvey, R.P., Attisano, L., and Wrana, J.L. (2004). Foxh1 is essential for development of the anterior heart field. Developmental cell *7*, 331-345.

Waldo, K., Miyagawa-Tomita, S., Kumiski, D., and Kirby, M.L. (1998). Cardiac neural crest cells provide new insight into septation of the cardiac outflow tract: aortic sac to ventricular septal closure. Developmental biology *196*, 129-144.

Waldo, K.L., Hutson, M.R., Stadt, H.A., Zdanowicz, M., Zdanowicz, J., and Kirby, M.L. (2005). Cardiac neural crest is necessary for normal addition of the myocardium to the arterial pole from the secondary heart field. Dev Biol *281*, 66-77.

Waldo, K.L., Kumiski, D.H., Wallis, K.T., Stadt, H.A., Hutson, M.R., Platt, D.H., and Kirby, M.L. (2001). Conotruncal myocardium arises from a secondary heart field. Development *128*, 3179-3188.

Waldo, K.L., Lo, C.W., and Kirby, M.L. (1999). Connexin 43 expression reflects neural crest patterns during cardiovascular development. Dev Biol *208*, 307-323.

Watanabe, Y., Zaffran, S., Kuroiwa, A., Higuchi, H., Ogura, T., Harvey, R.P., Kelly, R.G., and Buckingham, M. (2012). Fibroblast growth factor 10 gene regulation in the second heart field by Tbx1, Nkx2-5, and Islet1 reveals a genetic switch for down-regulation in the myocardium. Proceedings of the National Academy of Sciences of the United States of America *109*, 18273-18280.

Webb, S., Qayyum, S.R., Anderson, R.H., Lamers, W.H., and Richardson, M.K. (2003). Septation and separation within the outflow tract of the developing heart. J Anat *202*, 327-342.

Weiss, S., Rossi, R., Pellegrino, M.A., Bottinelli, R., and Geeves, M.A. (2001). Differing ADP release rates from myosin heavy chain isoforms define the shortening velocity of skeletal muscle fibers. The Journal of biological chemistry *276*, 45902-45908.

Wigmore, P.M., and Evans, D.J. (2002). Molecular and cellular mechanisms involved in the generation of fiber diversity during myogenesis. International review of cytology *216*, 175-232.

Williams, B.A., and Ordahl, C.P. (1994). Pax-3 expression in segmental mesoderm marks early stages in myogenic cell specification. Development *120*, 785-796.

Wright, W.E., Sassoon, D.A., and Lin, V.K. (1989). Myogenin, a factor regulating myogenesis, has a domain homologous to MyoD. Cell *56*, 607-617.

Xu, H., Morishima, M., Wylie, J.N., Schwartz, R.J., Bruneau, B.G., Lindsay, E.A., and Baldini, A. (2004). Tbx1 has a dual role in the morphogenesis of the cardiac outflow tract. Development *131*, 3217-3227.

Yamagishi, H., Maeda, J., Hu, T., McAnally, J., Conway, S.J., Kume, T., Meyers, E.N., Yamagishi, C., and Srivastava, D. (2003). Tbx1 is regulated by tissue-specific forkhead proteins through a common Sonic hedgehog-responsive enhancer. Genes & development *17*, 269-281.

Yamagishi, H., Yamagishi, C., Nakagawa, O., Harvey, R.P., Olson, E.N., and Srivastava, D. (2001). The combinatorial activities of Nkx2.5 and dHAND are essential for cardiac ventricle formation. Developmental biology *239*, 190-203.

Yashiro, K., Shiratori, H., and Hamada, H. (2007). Haemodynamics determined by a genetic programme govern asymmetric development of the aortic arch. Nature *450*, 285-288.

Yusuf, F., and Brand-Saberi, B. (2006). The eventful somite: patterning, fate determination and cell division in the somite. Anatomy and embryology *211 Suppl 1*, 21-30.

Zhang, M., Koishi, K., and McLennan, I.S. (1998). Skeletal muscle fibre types: detection methods and embryonic determinants. Histology and histopathology *13*, 201-207.

Zhou, W., Lin, L., Majumdar, A., Li, X., Zhang, X., Liu, W., Etheridge, L., Shi, Y., Martin, J., Van de Ven, W.*, et al.* (2007). Modulation of morphogenesis by noncanonical Wnt signaling requires ATF/CREB family-mediated transcriptional activation of TGFbeta2. Nat Genet *39*, 1225-1234.